REPORT NO. PM-P-5
NOVEMBER 1973

RIDE ROUGHNESS TESTS
CLEVELAND TRANSIT SYSTEM
SEPTEMBER 1973

PRELIMINARY MEMORANDUM

THIS DOCUMENT CONTAINS PRELIMINARY INFORMATION SUBJECT TO CHANGE. IT IS CONSIDERED AN INTERNAL TSC WORKING PAPER WITH A SELECT DISTRIBUTION. IT IS NOT A FORMAL REFERABLE REPORT. DISTRIBUTION IS EFFECTED BY AND THE RESPONSIBILITY OF THE TSC PROGRAM MANAGER.

Prepared by: Lowell V. Babb

Approved by: George W. Neat
Assistant Program Manager
For Test and Evaluation
Urban Rail Supporting
Technology Program

Ronald J. Madigan
Program Manager
Urban Rail Supporting
Technology Program

U.S. DEPARTMENT OF TRANSPORTATION
TRANSPORTATION SYSTEMS CENTER
KENDALL SQUARE
CAMBRIDGE MA 02142

PREFACE

The Rail Programs Branch of the Urban Mass Transportation Administration (UMTA) Office of Research and Development is conducting programs directed towards the improvement of urban rail transportation systems. These research and development programs will result in improved prototype vehicle and component designs, improved ways and structures, and improved structural components.

The Transportation Systems Center (TSC) has been designated by UMTA as System Manager for the necessary technical support in these developmental areas. The UMTA-sponsored "Urban Rail Supporting Technology Program" at TSC has implemented a test program which has included tests on the New York City Transit Authority and the Massachusetts Bay Transportation Authority as well as on the Rail Transit Test Track at the High Speed Ground Test Center (HSGTC) in Pueblo, Colorado (1-6)*.

The Cleveland Transit System (CTS), under the sponsorship of UMTA, is the test site for an AC Propulsion test and evaluation project. The objective of this project is the evaluation of vehicles propelled by AC traction motors, during a 12-month test under actual revenue service operations. WABCO, Inc., Pittsburgh, Pennsylvania, designed the AC propulsion system installed on three CTS Airporter rapid transit cars. TRW, Inc., McLean, Virginia, is assisting in the collection and evaluation of data, and in implementing the UMTA-prepared project experimental design.

One phase of the test program is the measurement of ride roughness on an AC-propelled vehicle and a comparison with a corresponding measurement on a standard DC-propelled vehicle. TSC performed these ride roughness tests at UMTA's request. The tests were conducted during revenue rush-hour service on September 11, 18, and 19, 1973.

*Numbers in parentheses refer to references listed at the end of this report.

The ride roughness tests were coordinated by Frederick J. Rutyna in conjunction with his role as manager of the Applications Engineering Task of the Rail Technology Program. The logistics, scheduling and interface activities were coordinated by Gunars Spons. The test crew included Gunars Spons, Phillip Silva, and Lowell Babb.

The cooperation of CTS personnel, Bruce Werstak and Robert Bretz, and WABCO Project Manager, Robert Smith is gratefully acknowledged.

TABLE OF CONTENTS

LIST OF FIGURES

LIST OF FIGURES (CONTINUED)

LIST OF FIGURES (CONTINUED)

1. INTRODUCTION

The Cleveland Transit System (CTS) has undertaken an UMTA-sponsored program to evaluate the use of alternating current traction motors on rapid transit vehicles. WABCO, Inc., under contract to CTS, has retro-fitted three vehicles of the CTS fleet with 600 volt DC to AC inverters, AC traction motors and appropriate interfacing electronics to allow revenue operation on the CTS Windermere-Airport Line. Vehicle performance tests, detailed maintenance inspections, and passenger reaction surveys have been conducted by WABCO and TRW, Inc., on six controlled test vehicles. These vehicles represent both DC and AC propulsion systems, and various combinations of interior and exterior styling and cleaning requirements. Data from the tests will be evaluated and a final report issued by TRW. Completion of the 2.1 million dollar program is scheduled for April 1974.

The TSC effort in this program was the measurement of the ride roughness of one AC propelled vehicle and one conventional DC propelled vehicle. Measurements were made using a triaxial accelerometer placed on the car floor at two locations in the vehicle. Data were recorded on six round trip test runs during September, 1973. The data were processed at TSC and are included in Appendices A, B, and C of this report. System calibration is discussed in Appendix D. A technical paper by R.T. Bretz (7) describing the AC propulsion system is reprinted as Appendix E.

The CTS opened the Airport extension in 1968 and provided the first direct rapid transit link between an airport and a major city. The total route length is 19 miles and connects with the Shaker Heights Rapid Transit System as shown on the route map in Figure 1-1. The newest vehicles used on the Airport-Windermere Line were manufactured in 1968 and 1970 by Pullman-Standard. These vehicles are 70 feet in length and weigh approximately 64,700 pounds empty. The truck center length is 49 feet, 6 inches, with a wheel base of 6 feet, 6 inches. Wheel diameter on the Rockwell manufactured trucks is 28 inches.

The two vehicles used on the ride roughness test series are part of the fleet described above. Car 162 was used for the DC system tests while the AC system tests were conducted on car 154. Both cars had identical styling and cleaning requirements. Car 154 is shown in Figure 1-2.

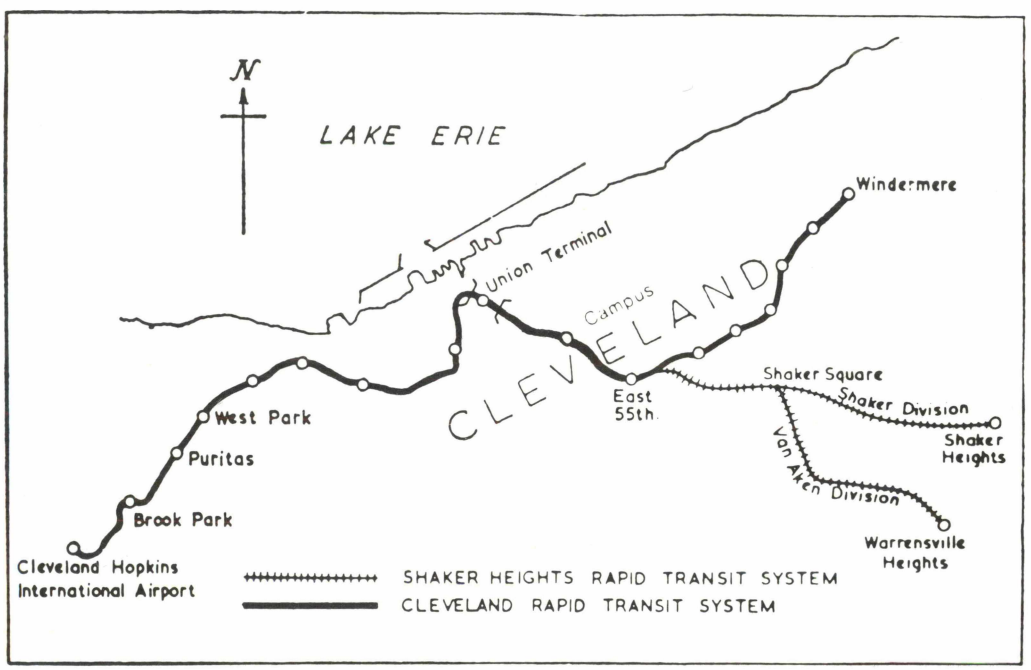

Figure 1-1 Route Map
Cleveland Transit System (8)

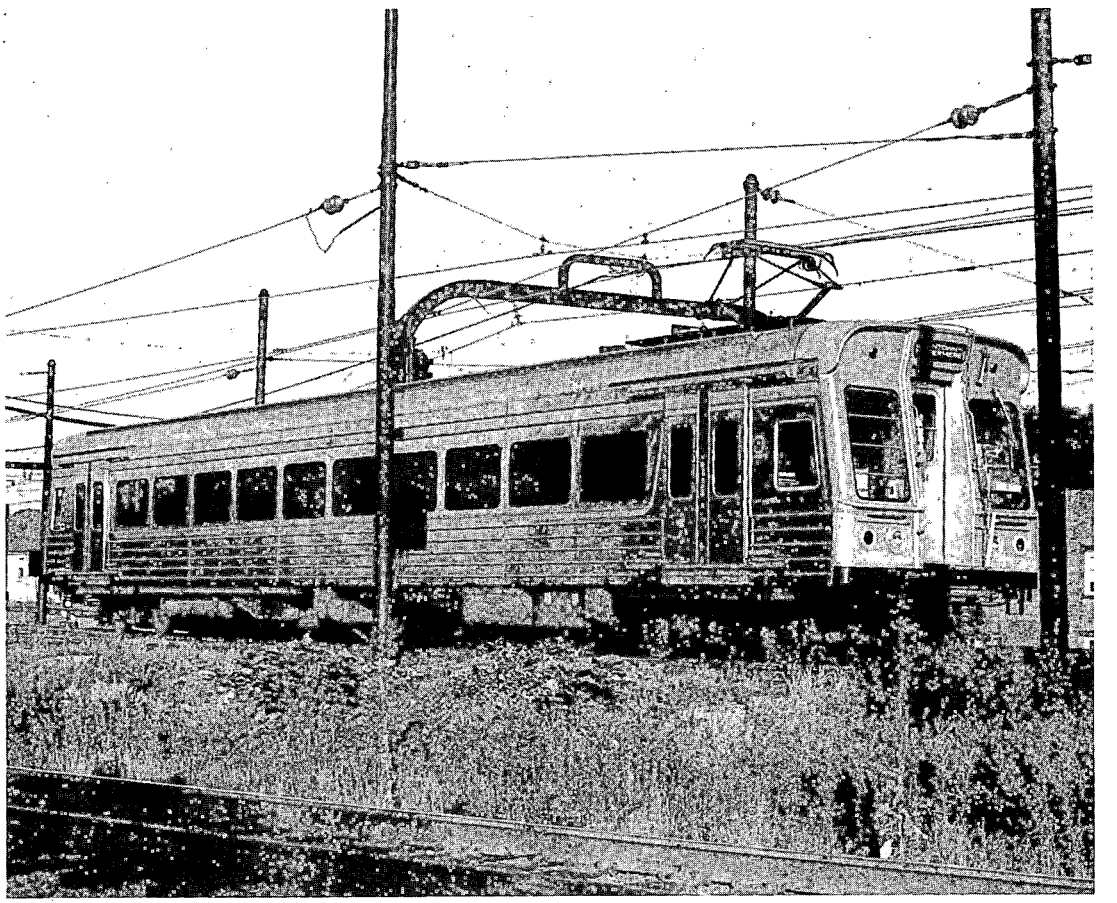

Figure 1-2 Car 154, AC-Propelled Vehicle
Cleveland Transit System

2. DISCUSSION

The test series was divided into three separate tests as listed in Figure 2-1. Each test is identified by two numbers: the sequence number and the procedure number. The first four digits of the sequence number (09-73-7XX) correspond to the test date, while the 7 in the last group denotes there have been six previous test series. Test procedures for ride roughness tests have been standardized and are identified by the test procedure number. These procedures and other pertinent information are described in the DOT/TSC document GSP 064, General Vehicle Test Plans for Urban Rapid Transit Cars (9).

The actual test runs began on September 11, 1973, and two round trips of data were recorded with the instrumentation aboard the AC vehicle. However, because of a malfunction with the vehicle control system during the braking cycle, these AC vehicle tests were repeated on September 19. The DC vehicle tests were performed on September 18 and 19. These latter AC and DC vehicle tests are reported in Appendices A and B, respectively, with representative data from the malfunctioning AC vehicle test included in Appendix C.

Test Series VII, Cleveland Transit System
September, 1973

Sequence Number	Procedure Number	Test Title
9-73-701	AC-R-5002-CTS	Ride Roughness
9-73-702	DC-R-5002-CTS	Ride Roughness
9-73-703	AC-R-5002-CTS	Ride Roughness

Figure 2-1 Test Run Summary, Test Series VII

On all six round trip test runs, the instrumented vehicle was the eastern car of a three-car train. On westbound runs to the Airport Station the test car trailed, while on return runs to Windermere the test car assumed the lead position. On the first test run for each vehicle, the ride roughness sensor was placed near the truck pivot at the coupled end of the car. Because of revenue passengers, the sensor was not placed directly over the truck pivot, but was displaced approximately 3'4" from the vehicle centerline. On the second test run, the sensor was moved mid-way between the two truck pivots and still laterally displaced. The remaining equipment was set-up at mid-car beneath two seats; the instrumentation inside the test vehicle is shown in Figures 2-2 and 2-3.

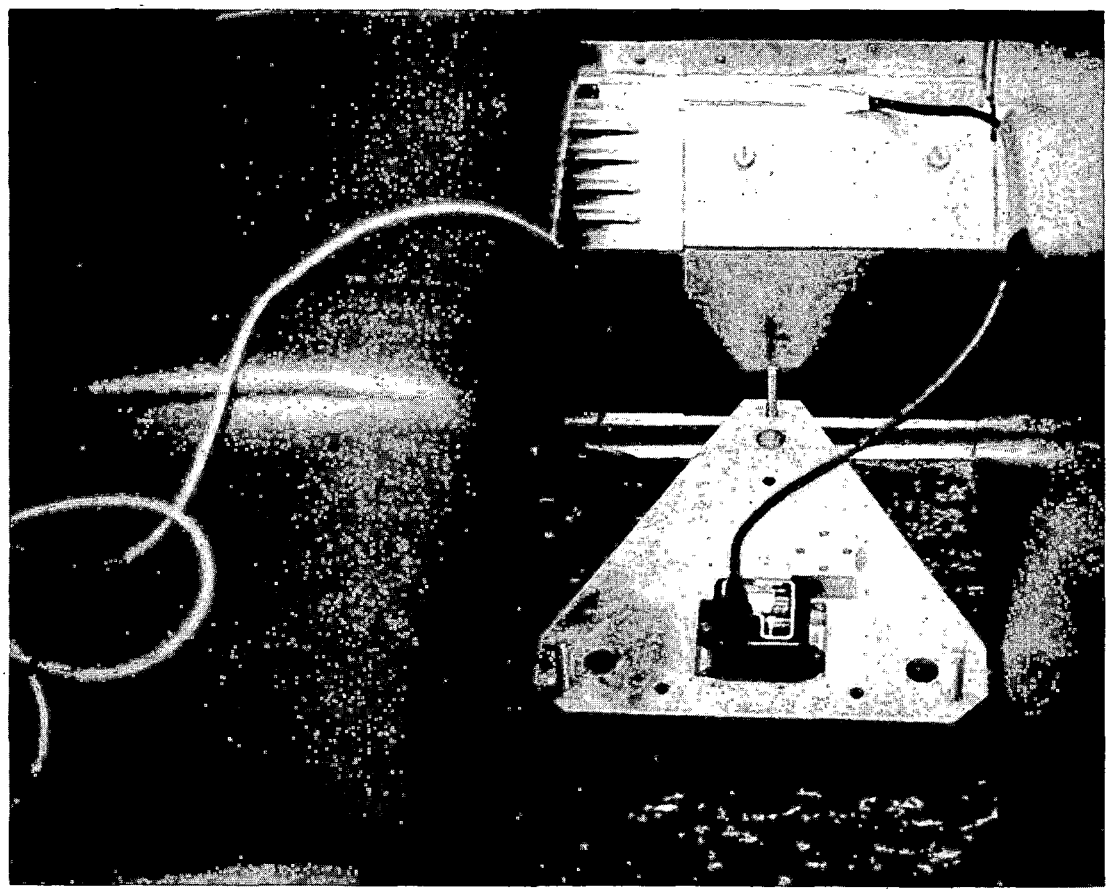

Figure 2-2 Ride Roughness Sensor Plate, Car 154

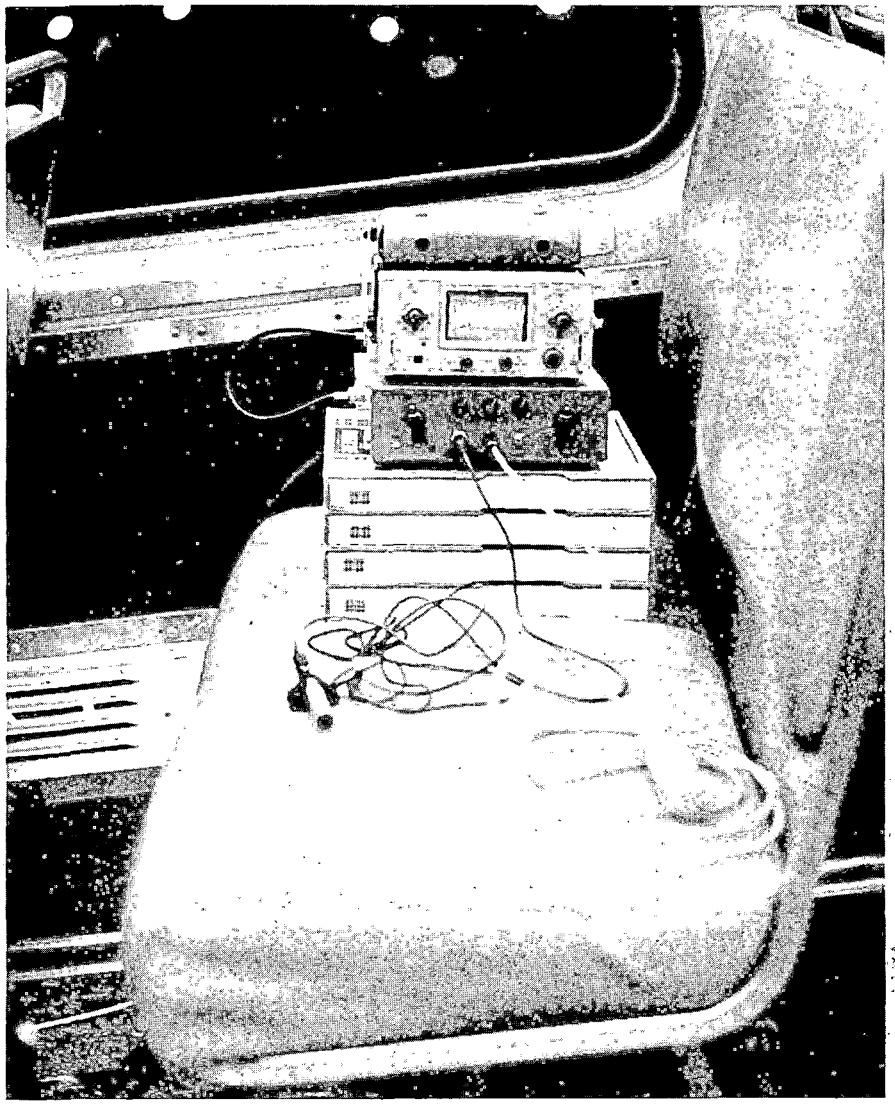

Figure 2-3 Ride Roughness Instrumentation System, Car 154

Three axes of unprocessed linear acceleration signals were recorded on magnetic tape, along with additional reference information to facilitate comparison of data from vehicles with the AC and DC propulsion systems. To obtain vehicle speed and distance data, a rotary shaft encoder was coupled to the vehicle axle with the output pulses recorded on the data tape. Vehicle location was determined from the recorded forward observer voice track and the test log. Raw data were monitored on a portable single channel oscilloscope to verify that the data were being recorded and to allow proper signal scaling.

The recorded data were analyzed at TSC using predominantly analog data processing equipment. The analyzed data are displayed in the form of distance-based stripcharts for the entire round trip test runs, time-based stripcharts of the deceleration/acceleration sequence at a single passenger station, and acceleration power spectral density plots from a quasi-constant speed portion of all test runs.

The distance-based stripcharts display the weighted, root-mean-square (RMS) value of the three acceleration signals. The weighting network is an electrical bandpass filter that approximates the human response to vibration in the 1 to 80 hz frequency range. This filtered signal is then processed by a true RMS analyzer with an exponential (RC) averaging time constant of three seconds. The vehicle speed was derived from the recorded shaft encoder pulses using a special-purpose processor calibrated to the wheel circumference. Pulses to drive the incremental chart recorder were also provided by this processor. Because ride roughness is strongly dependent upon the track perturbations, the distance-based charts greatly ease data comparisons between separate test runs.

The time-based charts display the weighted acceleration signals and their RMS values. For these charts, the RMS time constant was changed to one second to allow a faster response time.

Concluding the data analysis, acceleration power spectral density (PSD) analyses were done using a narrow band (200 line) real time spectrum analyzer. Frequency ranges of 0-20 hz and 0-100 hz

were analyzed. By viewing the distance-based stripcharts, a segment of track was selected in which both test vehicles maintained approximately the same constant speed on all test runs. Raw acceleration (unweighted) signals from this track segment were then used to produce the power spectral density plots. Vertical, lateral, and longitudinal PSD analyses were performed for each test run.

Representative samples of the processed data given in the appendices are included in this section of the report.

Four distance-based charts are shown in Figure 2-4. These charts display the ride roughness data from the AC and DC vehicles with both over-the-truck and mid-car sensor locations. The eastbound track segment includes Puritas, West Park, and Triskett Stations. The most obvious difference between the AC and DC vehicles is during acceleration away from a station. The DC vehicle speed controller is characterized by discrete positions (notches) instead of being continuously variable. As the controller is shifted to successive notches, large longitudinal accelerations are generated. The AC vehicle speed control is continuous and therefore avoids these acceleration transients. Similar transients occur as the wheels lock following deceleration, but these are characteristic of both vehicles.

The ride roughness weighting networks attenuate accelerations below a frequency of one hertz. Consequently, very low frequency components associated with vehicle decelerations and accelerations are not displayed. However, by observing the vehicle speed trace, it is apparent that the AC vehicle operated more smoothly on the test runs. In many cases, the AC speed was quickly brought to 55 mph and held constant until approaching the next station. The DC vehicle speed was slightly varying during most of the test runs.

The eastbound data between Puritas and Triskett Stations were analyzed to determine the average values of the ride roughness signals. The median signal levels of the data segments in which the vehicle speed exceeded 30 mph were found using a probability distribution analyzer. If a symmetrical probability density is assumed, the median values are equal to the mean values. These values are listed in Figure 2-5 for the three acceleration axes

TEST SEQUENCE: 9-73-701,2

DATE: SEPTEMBER 19, 1973

SITE: CLEVELAND TRANSIT SYSTEM

TIME: -

DIRECTION: Eastbound

VEHICLE: AC and DC

SENSOR LOCATION: Truck Pivot and Mid-car

SIGNAL PROCESSING: Accelerometer signals weighted (filtered) to approximate the human body response to vibration. The resulting signal is processed by a true root-mean-square (RMS) analyzer with a three second RC averaging time constant.

CHART ABSCISSA: Distance

NOTE 1. Ride roughness signals do not always reach zero when the vehicle stops. The movement of passengers and the vibrations of vehicle sub-systems may continue to excite the acceleration sensor.

NOTE 2. At the instant the vehicle wheels lock following deceleration, a large longitudinal acceleration transient is generated.

NOTE 3. The length of the event marks at stations is not significant. These marks were manually activated by the forward observer during the test run.

NOTE 4. The acceleration transient is caused by the DC vehicle notch control.

Figure 2-4 Ride Roughness Data

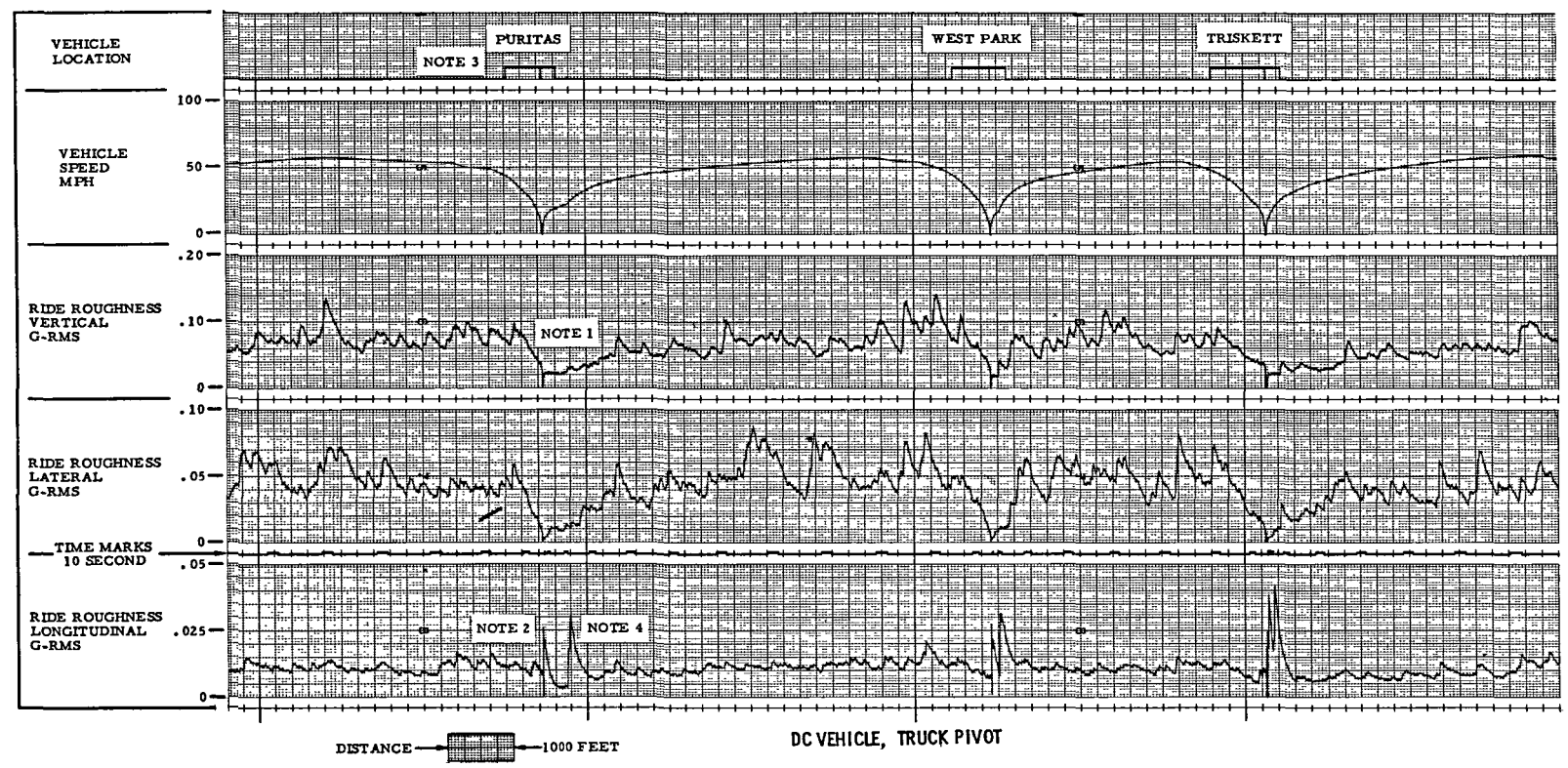

DC VEHICLE, TRUCK PIVOT

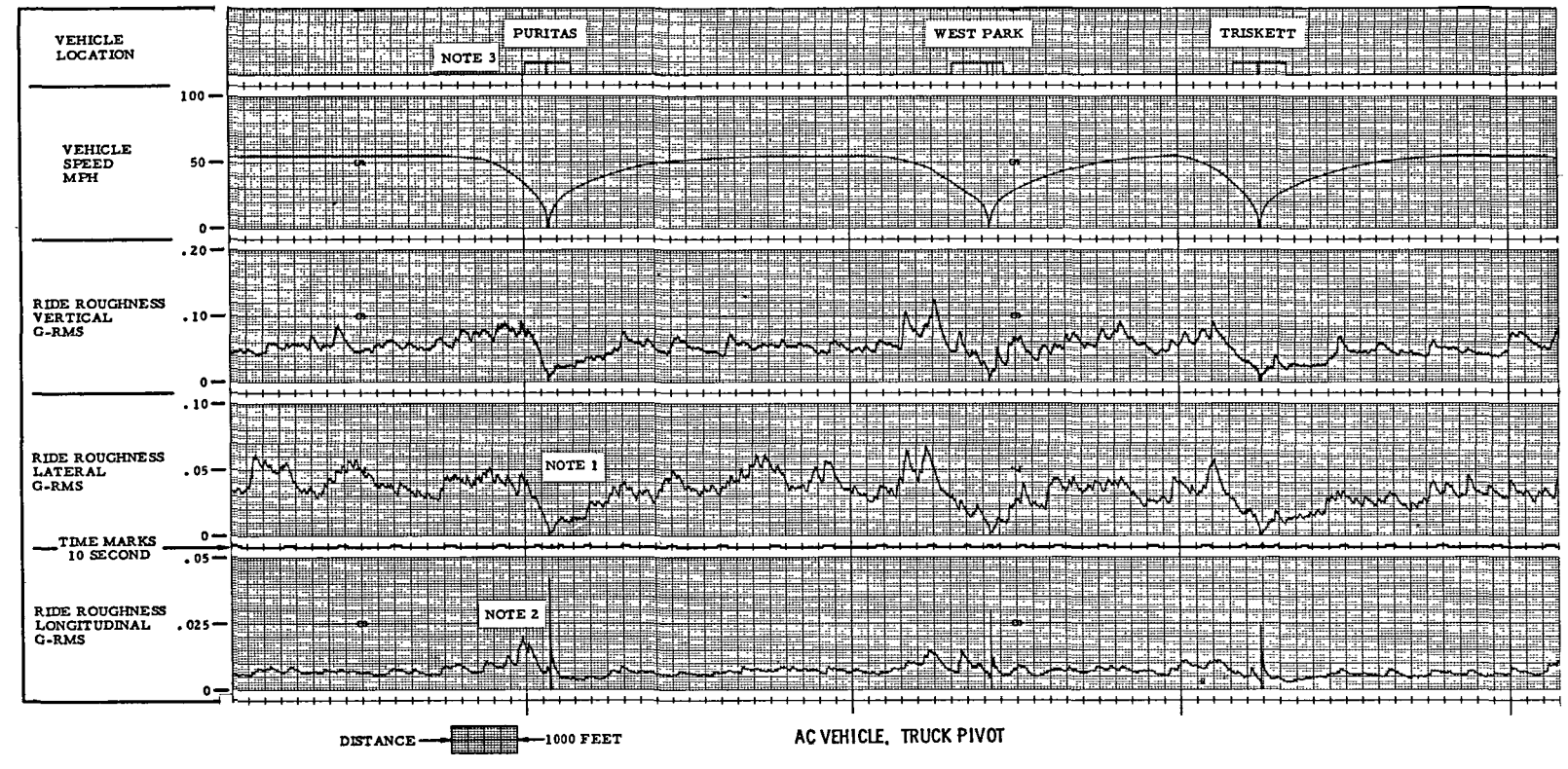

AC VEHICLE, TRUCK PIVOT

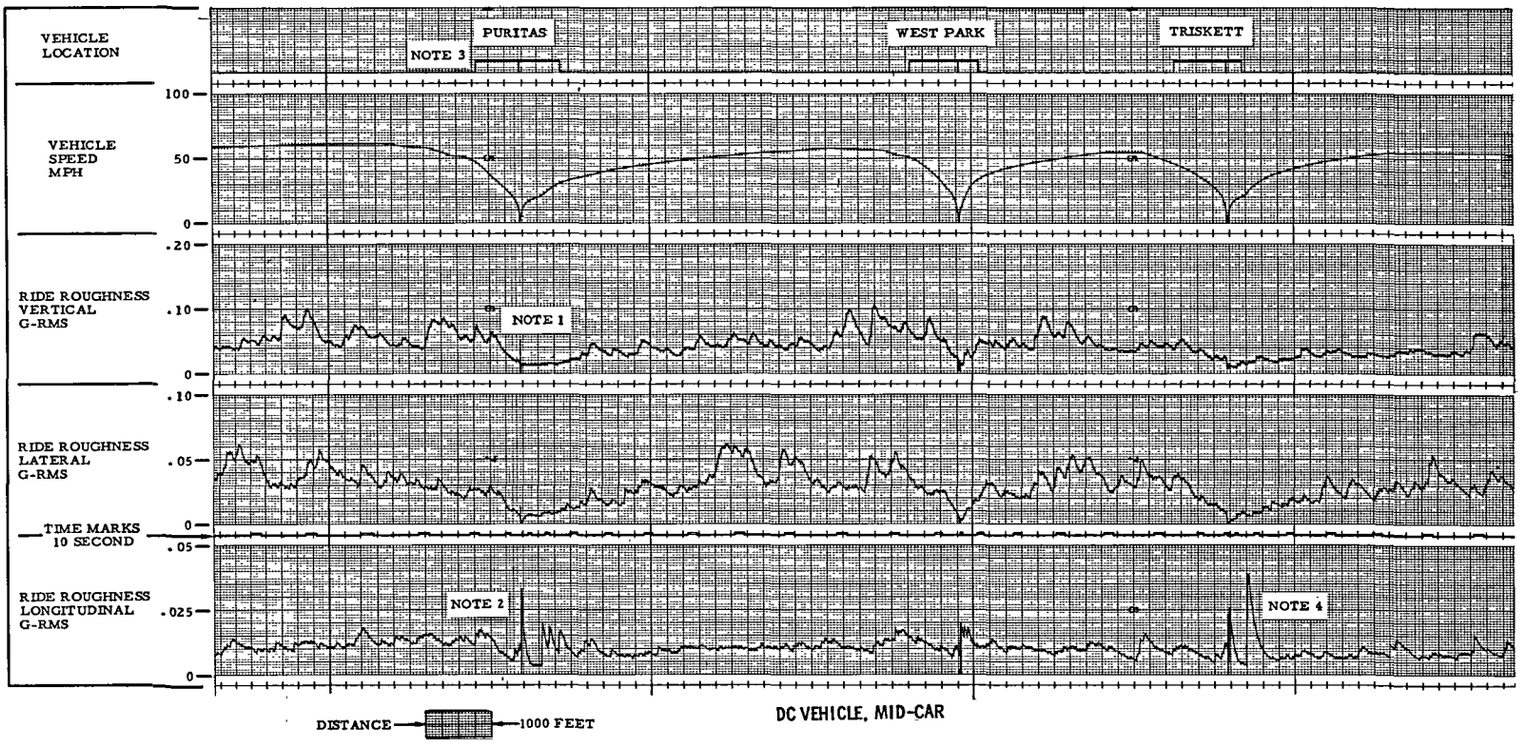

DC VEHICLE, MID-CAR

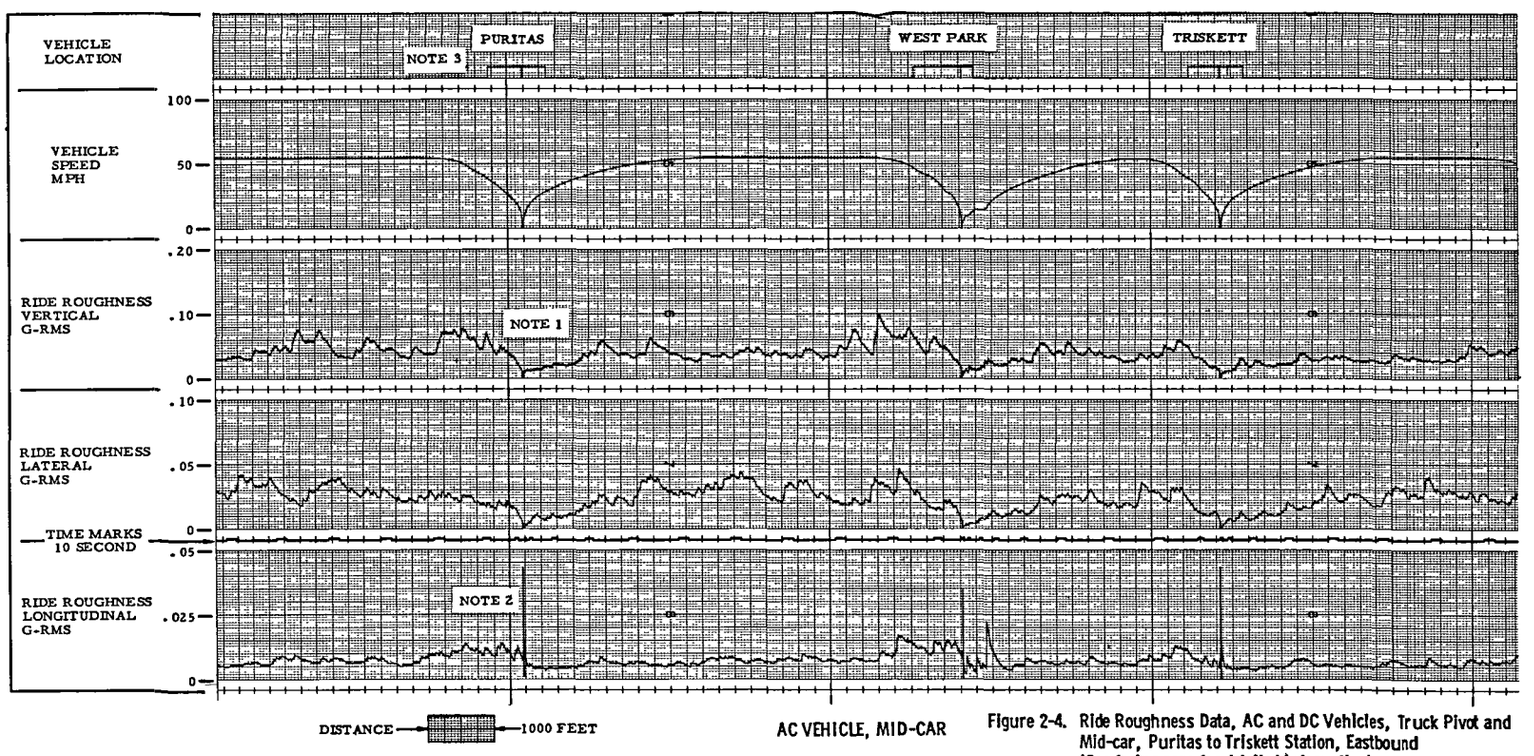

AC VEHICLE, MID-CAR

Figure 2-4. Ride Roughness Data, AC and DC Vehicles, Truck Pivot and Mid-car, Puritas to Triskett Station, Eastbound
(See facing page for detailed information)

with the sensor located at the truck pivot and at mid-car on both test vehicles.

AXIS	VEHICLE - SENSOR LOCATION			
	AC-TRK	AC-MID	DC-TRK	DC-MID
Vertical	.060	.040	.070	.050
Lateral	.036	.024	.048	.031
Longitudinal	.008	.008	.012	.011

Note 1. Difference in wheel wear between the AC vehicle and the DC vehicle could contribute to differences in vehicle ride roughness levels.

Note 2. The data base includes only track segments in which the the vehicle speed exceeded 30 mph.

Figure 2-5 Average Ride Roughness Levels, g-RMS, Puritas to Triskett Station, Eastbound

While the AC vehicle average values were generally 25 per cent less than the corresponding DC vehicle values, it is emphasized that this may have been caused by the increased wear evident on the wheels of the DC vehicle. While the AC vehicle wheels appeared nearly new, the DC wheels were more worn with a diameter change of nearly 0.25 inch between the center and outer edge of the wheels. This DC-vehicle wheel condition (Car 162) is evident in the photograph shown in Figure 2-6. Although this wheel has not exceeded CTS wheel wear limits, it could contribute to increased ride roughness. That the ride roughness is a strong function of track input can readily be seen from the Figure 2-4 charts. Most perturbations seen on one chart may be observed on all other charts. Also the vertical and lateral roughness values at mid-car are about 30 per cent less than the truck pivot values. This implies that significant pitch and yaw motions do occur.

Figure 2-6 Representative Wheel on the DC Test Vehicle, Car 162, Showing the Wheel Wear.

Figure 2-7 is a time-based chart of the AC and DC vehicle ride roughness as they accelerated eastbound from West Park Station. The sensor was located over the truck on both runs. The DC propulsion system notch control accelerations are also evident on this chart.

Samples of the longitudinal acceleration PSD plots are shown in Figure 2-8. While most of the plots were very similar, differences between the AC and DC vehicles do appear on the 0-20 hz plots of the longitudinal acceleration data. The power spectral density in the 2-9 hz frequency range on the AC vehicle data is approximately 80 per cent less than the corresponding data on the DC ve-

TEST SEQUENCE: 9-73-701,2

DATE: SEPTEMBER 19, 1973

SITE: CLEVELAND TRANSIT SYSTEM, West Park Station

TIME: -

DIRECTION: Eastbound

VEHICLE: AC and DC

SENSOR LOCATION: Truck Pivot

SIGNAL PROCESSING: Accelerometer signals weighted (filtered) to approximate the human body response to vibration. The resulting signal is processed by a true root-mean-square (RMS) analyzer with a three second RC averaging time constant.

CHART ABSCISSA: Time

NOTE 1. Ride roughness signals do not always reach zero when the vehicle stops. The movement of passengers and the vibrations of vehicle sub-systems may continue to excite the acceleration sensor.

NOTE 2. The bandwidth of the vertical ride roughness weighting filter is wider than the horizontal filter bandwidth.

NOTE 3. The acceleration transient is caused by the DC vehicle notch control.

Figure 2-7 Ride Roughness Data

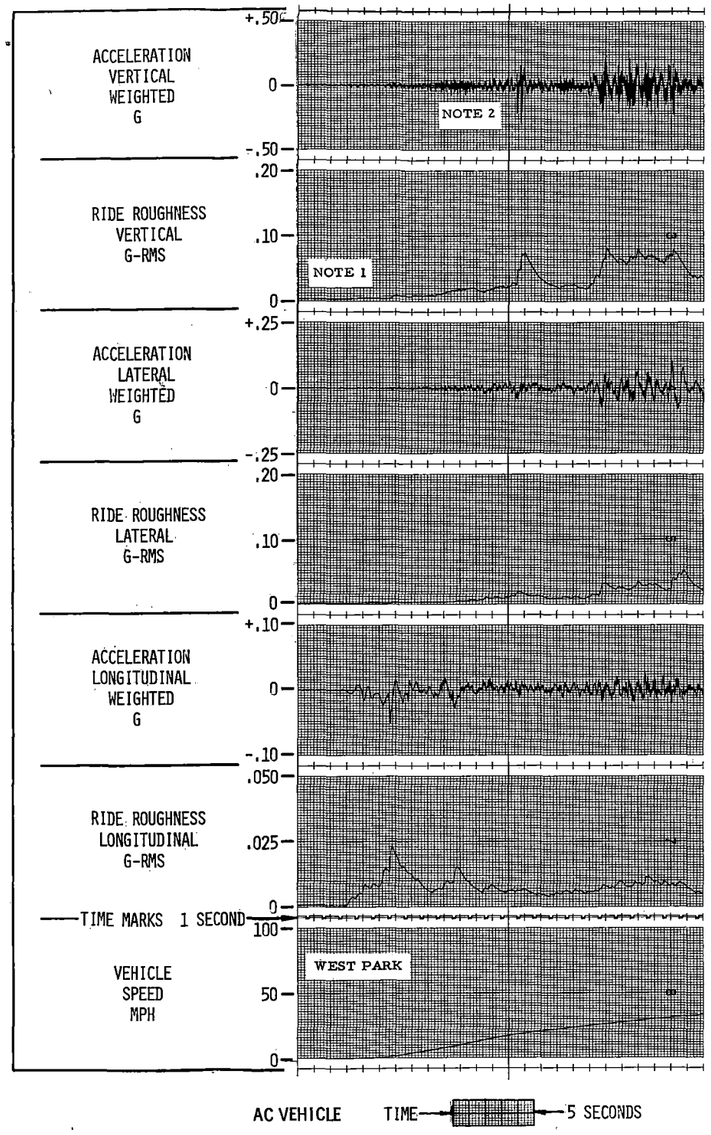

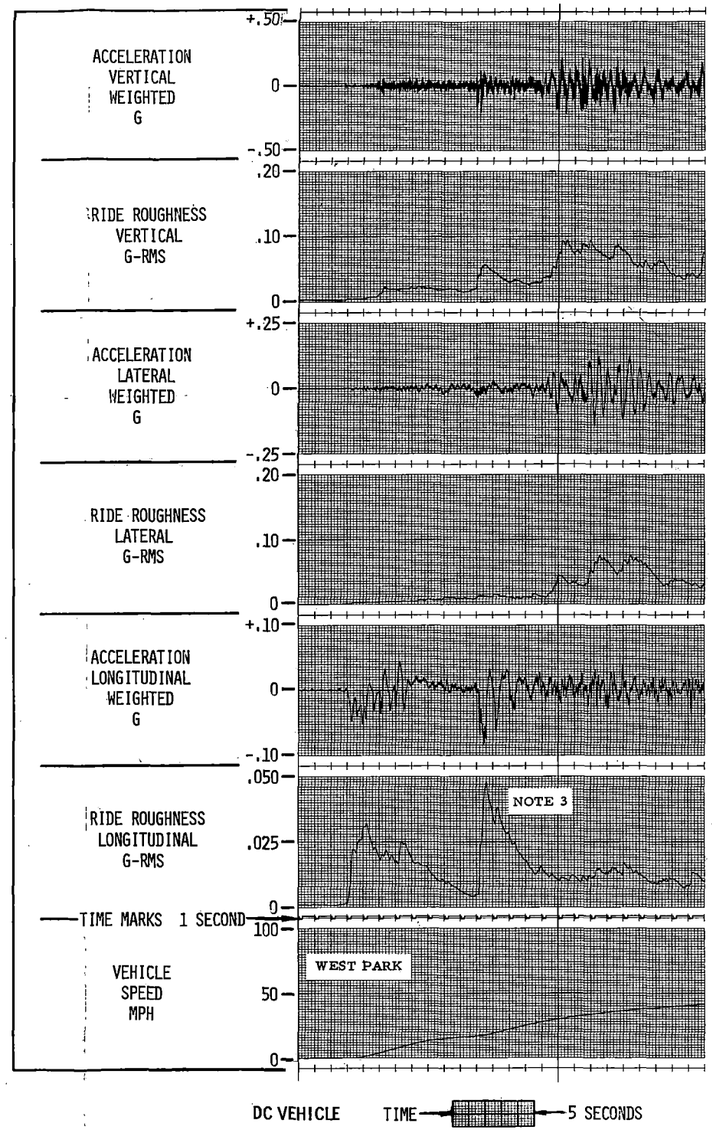

Figure 2-7. Ride Roughness Data, AC and DC Vehicles, Truck Pivot Vehicle Acceleration at West Park Station, Eastbound
(See facing page for detailed information)

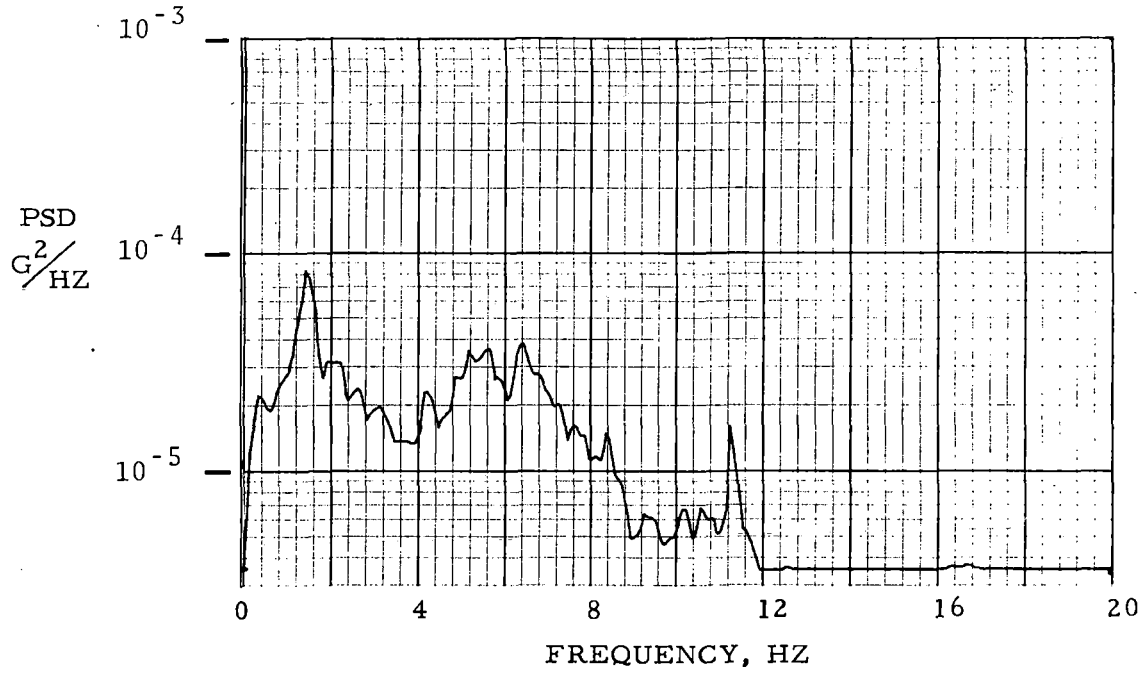

AC Vehicle, Mid-car

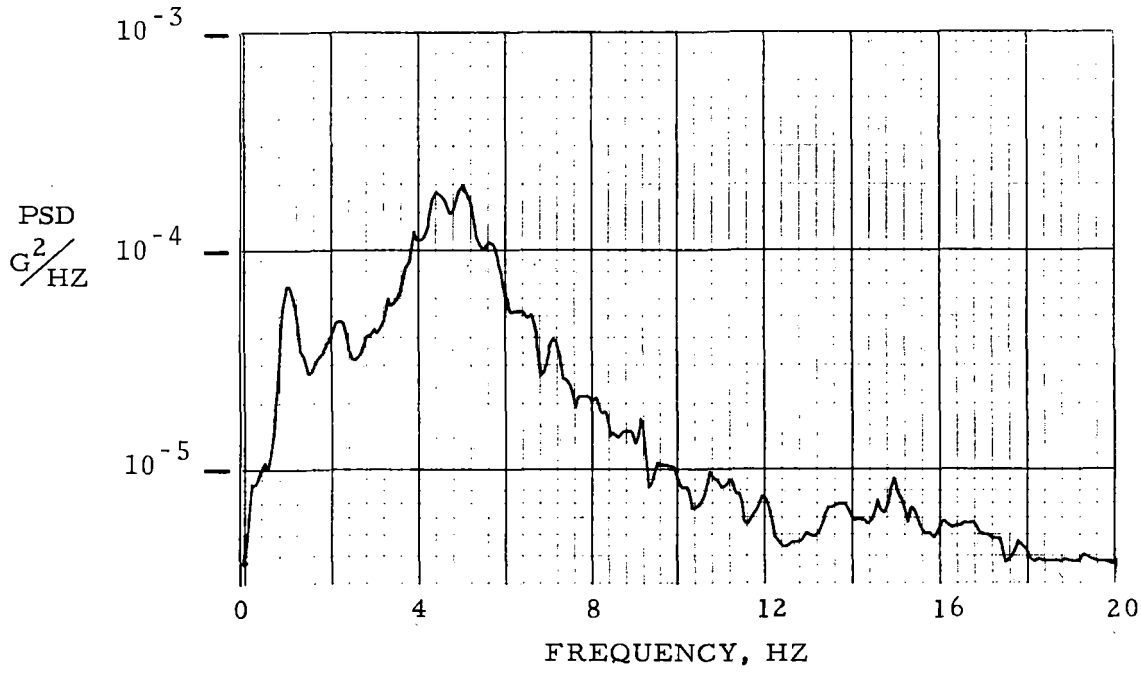

DC Vehicle, Mid-car

Figure 2-8 Acceleration Power Spectral Density, 0-20Hz Longitudinal, 55 MPH, AC and DC Vehicle, Mid-car, Brook Park to Puritas Station, Eastbound.

hicle. The data shown are from the mid-car sensor location, but the same observation can also be made on the truck pivot data in the Appendices.

3. CONCLUSIONS

The ride roughness levels experienced by the passenger on the CTS line are sufficiently low for both the AC vehicle and the DC vehicle to provide a comfortable ride according to standards published by the International Organization for Standardization (ISO).

The major differences between the AC and DC propelled vehicles are observed in the longitudinal axis data. Most obvious is the smooth acceleration transient during vehicle start-up. The continuously variable AC speed control allows for smoother accelerations than the conventional DC notch speed control. The AC vehicle was also capable of accelerating to a specific speed and maintaining that speed. DC vehicle speed control was less precise during the test runs. The longitudinal transients during vehicle acceleration can be readily compared in Figure 2-7. The power spectral density analyses of the constant speed section indicated that the longitudinal acceleration PSD levels in the 2-9 hz frequency range were nearly 80 per cent less for the AC vehicles.

The average ride roughness levels measured along the lateral and vertical axes were consistently lower for the AC vehicle than for the DC vehicle. While the improved ride of the AC vehicles may be attributed to factors other than the AC propulsion system, it can be concluded that there were no adverse ride roughness characteristics introduced by the AC conversion. The difference in the lateral and vertical ride roughness could be caused by the worn wheels on the DC test car as well as vibration coupling from the longitudinal axis.

Observation of the time-based charts and the PSD plots indicate that the predominate lateral ride roughness component is caused by kinematic hunting of the wheelsets. A periodic component at approximately 2 hz is noted on the lateral and vertical PSD plots which at the 55 mph test speed corresponds to a wave length of 40 feet. This value is typical of transit vehicle lateral hunting wavelengths. The human body response to lateral vibration peaks in the 1 to 2 hz

range and the lateral ride roughness values, therefore, are largely influenced by the hunting. This 2 hz component may represent rolling motion since the ride roughness sensor was displaced from the vehicle longitudinal centerline.

To compare the ride roughness of the test vehicles to internationally proposed standards, reference is given to Document ISO/TC 108, Guide for the Evaluation of Human Exposure to Whole-Body Vibration (10). This document was published by the International Organization for Standardization and applies particularly to transportation environments. The four physical factors that are considered in establishing the vibration limits are the intensity, frequency, direction, and duration of the vibration input. In the document, three human criteria are listed:

1. The preservation of working efficiency (Fatigue/Decreased Proficiency Boundary)
2. The preservation of health and safety (Exposure Limit)
3. The preservation of comfort (Reduced Comfort Boundary)

In terms of rapid transit commuters, the preservation of comfort is of maximum interest. Using the worst case weighted-RMS levels from Figure 2-5 (DC-TRK), the maximum exposure time can be found, consistent with the preservation of passenger comfort. For both vertical and lateral vibration inputs, the corresponding exposure time is approximately twenty minutes. During the test runs, a single one-way run required about forty minutes with approximately 50 per cent of that time spent with the vehicle exceeding 30 mph. It is concluded that a passenger riding the full 19 mile route length of the CTS line may do so in relative comfort.

APPENDIX A

RIDE ROUGHNESS TEST
AC VEHICLE

APPENDIX A
RIDE ROUGHNESS TEST, AC VEHICLE

Sequence No: 9-73-701

Procedure No: AC-R-5002-CTS

Objective:

To measure vibrations that would be experienced by a passenger standing near the truck pivot and at mid-car on an AC-propelled transit vehicle. The collected data are used to compare the ride characteristics of AC-propelled vehicles to those of conventional DC-propelled vehicles.

Status:

Ride roughness data were successfully recorded and processed. The data are presented in this appendix in the form of distance- and time-based stripcharts of the weighted RMS accelerations. Acceleration power spectral density plots are given for a representative section of track. The ride roughness levels at both sensor locations were sufficiently low to assure passengers a comfortable ride according to ISO standards.

Test Description:

Ride roughness tests were conducted on the test vehicle with the acceleration sensor placed at two separate locations on the car floor. A round trip run was made with the sensor near the truck pivot followed by a second round trip with the sensor placed mid-car. Because of the possible inconvenience to revenue passengers, the sensor was not placed along the longitudinal centerline. The sensor placements are shown in Figure A-1. The vehicle used for this test was car number 154, equipped with a DC-to-AC inverter and AC traction motors. On all test runs, the instrumented vehicle was the eastern car on a three-car train. The power system, reference information, and data collection, monitoring and processing are briefly described in the following paragraphs.

Prime power for the ride roughness test instrumentation was provided by a 28 volt gelled electrolyte battery. A battery of this type is readily recharged and does not require special handling during shipping. The voltages necessary for the signal conditioning equipment were furnished by DC-DC converters.

Speed and distance data were derived using a rotary shaft encoder mechanically coupled to a vehicle axle with a bi-directional flexible shaft. The mounting configuration is shown on vehicle 154 in Figure A-2. The 2048 pulses per revolution provided by the encoder were recorded on magnetic tape. A special purpose processor was used to determine the instantaneous speed of the vehicle during data playback. This processor consisted of programmable digital dividers and a duty cycle pulse integrator, both calibrated to correspond to the test vehicle wheel circumference. In addition, pulses to drive an incremental chart recorder were provided.

A manual event mark was entered on tape at each station. By correlating this signal with the voice track and log book, the vehicle location was deduced.

A 25 khz sinusoidal signal, linearly summed with the voice track, was included as standard operating procedure to facilitate digital data processing, should it be desired at a later date. This signal could be used to direct the sampling circuits during

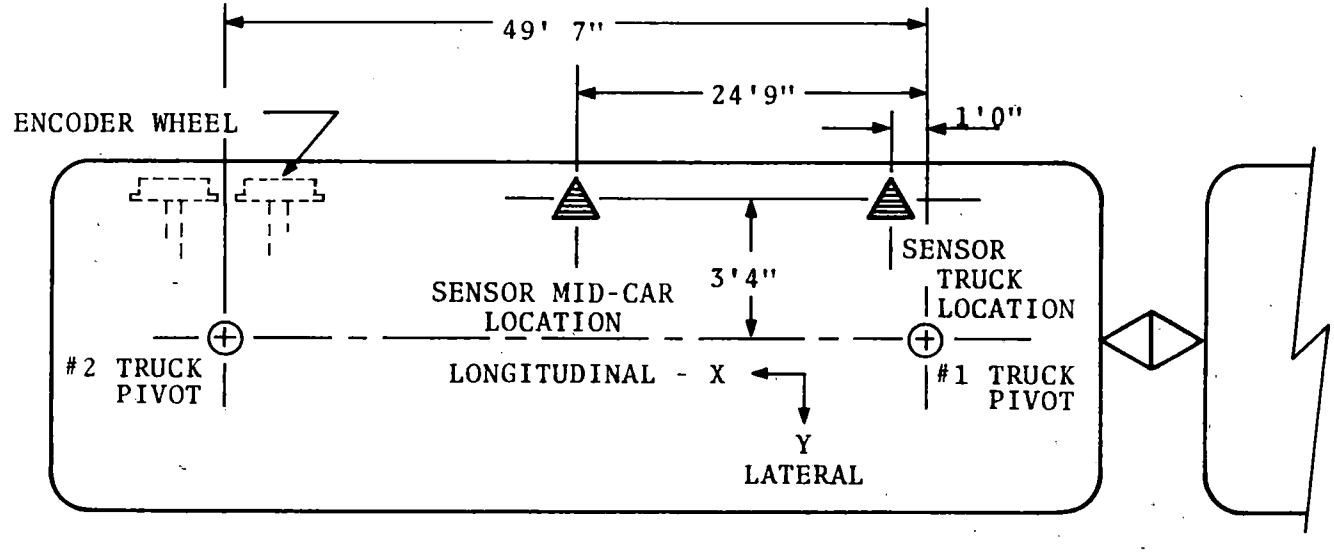

#1 End faces West (AIRPORT) in normal service.
#2 End faces East (WINDERMERE) in normal service.
The Pantograph is located at the #2 End.

Figure A-1 Sensor Placement, Ride Roughness Tests, CTS

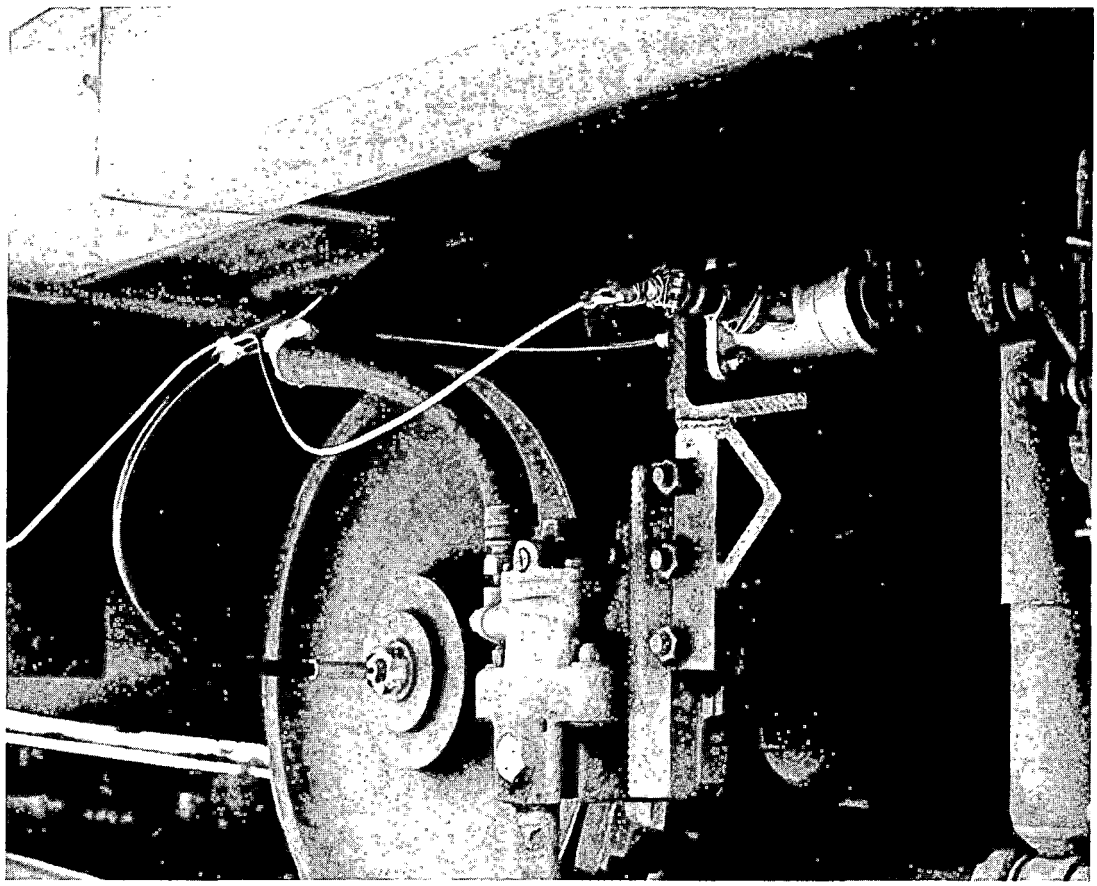

Figure A-2 Rotary Shaft Encoder Mounting, Car 154

the digitization process. However, analog processing was used to reduce the data for this report.

All data signals were recorded on magnetic tape for subsequent processing. The tape channel modes (FM or Direct) and the channel assignments are listed in Figure A-3.

To insure that all test data were correctly scaled and properly recorded, tape recorder input and output signals were monitored on a single channel battery powered oscilloscope. During a given test run, all signals were periodically monitored. The instrumentation mounted on the test vehicle is shown in block diagram form in Figure A-4.

Signal	Tape Track	Mode	Remarks
Reference (0 VDC)	1	FM	Tape Speed Comp.
Acceleration, RRH (X)	3	FM	Sensitivity Selectable
Acceleration, RRH (Y)	5	FM	(0.5, .75, 1.0 g F.S.)
Acceleration, RRV (Z)	7	FM	
Voice	4	Direct	Linearly Summed
Reference, 25KHz	4	Direct	Linearly Summed
Distance Pulses	2	Direct	0 to +2.0 Volts
Event Mark	6	FM	0 to +2.0 Volts

Figure A-3 Tape Track Assignments

Instrumentation:

The instrumentation utilized for both the data record mode and the playback/analysis mode is listed below. Brief specifications are included, but for detailed information, the reader is referred to the manufacturer.

A. Power Conditioning:

Battery - 30 volt, 12 amp-hour @ 3 amp
UDEC Model 30PB66-271-1, Waltham, MA

Battery Charger - 30 volt, UDEC Model CC271-1

DC-DC Converters - ±15, +5 VDC for instrumentation
MIL Electronics Md SD815, SS85,
Lowell, MA

B. Calibration and Control:

Calibration and Control Unit - The junction box for the system including:

(a) Signal Conditioning (Scaling)

(b) Accelerometer Calibration

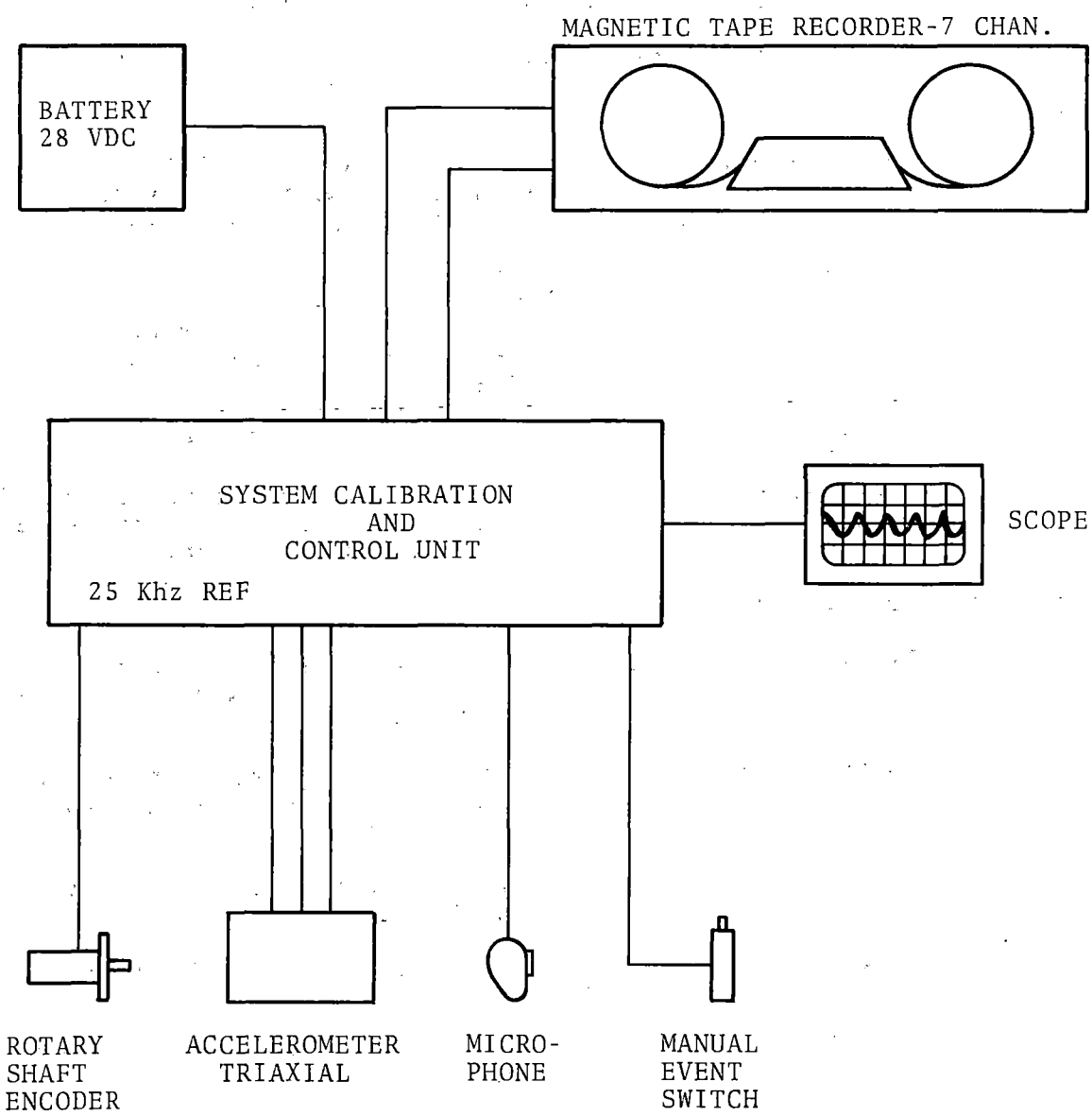

Figure A-4. Ride Roughness System Block Diagram
Data Record Mode

(c) Data Monitor Selector

(d) I/O for all transducers, power, etc.

(e) 25 khz Time Reference

C. Transducers:

Rotary Shaft Encoder	- Model T-2048-D-11-0-5-LED-5 Trump-Ross, North Billerica, Ma. 2048 Pulses per revolution
Accelerometer	- Model 5603-P2 Systron-Donner, Concord, Ca. +1G Full Scale, Linear Triaxial Servo Type, Natural Frequency >500 hz
Microphone	- Used to record voice track
Event Switch	- 2.0 VDC signal to be recorded and used to mark certain events such as signal numbers, stations.

D. Data Acquistion:

Magnetic Tape Recorder	- Model MTR 3200, Lockheed Electronics (Leach) Azusa, Ca. S/N 3200-5012, 7 1/2 ips
Channel 1,3,5,6,7	- FM Record/Reproduce, IRIG +40% deviation, Intermediate band, 0-2500 hz (-3db)
Channel 2,4	- Direct record/reproduce, 300-31,250 hz
Tape	- 1/2" on 8" dia. reel, 3" NAB HUB
Oscilloscope	- Type 323, Tektronix, Beavertown, Or.

E. Data Processing and Display:

Tape Speed Compensation Unit	- Differential amplifier system to reduce the effects of tape flutter (20 and 80 hz) components on the accelerometer channels. A signal/noise ratio of 40dB resulted.
Ride Roughness Filter	- Bandpass weighting networks to simulate human body response to vertical and horizontal vibra-

tions.

RMS Processor	- Model R310, Intronics, Newton, Ma. Converts the filtered accelerometer data to a root-mean-square signal, averaging time constant of three seconds or one second, operator selectable.
Speed and Distance Processor	- Converts the recorded output of the shaft encoder into an analog speed signal and furnishes pulses to drive the chart recorder.
Spectrum Analyzer	- Model SAI 51, Saicor, Hauppague, NY. Real time with digital integrator, 200 line
Chart Recorder	- Gould Brush 480 with incremental drive. Cleveland, Ohio DC-100 hz at 10 divisions.
X-Y Plotter	- HP Model 7000A Pasadena, Ca.
Probability Distribution Analyzer	- Model SAI 42, Saicor, Hauppague, NY. Provided median signal level of weighted RMS ride roughness signals.

Test Procedures:

The plan for the test series called for unweighted acceleration data to be recorded on magnetic tape. Three axes of acceleration were simultaneously recorded on each test run. In addition, reference information about vehicle speed and location was furnished. A pre-run checklist and detailed test documentation were included in the test log which was maintained during the complete test series.

To maximize the accuracy of the test data, detailed calibration procedures were initiated. These are described in Appendix D.

The actual procedures used during the test series are summarized below:

Pre-run

1. Install required equipment.
2. Photograph placement of sensors.
3. Calibrate all instrumentation.
4. Complete all log entries on documentation sheet and checklist.

Test Run

1. Turn on all equipment.
2. Operate all test vehicles at revenue speeds.
3. Use voice and event marks to document vehicle location with corresponding log entries.
4. At end of one-way run, calibrate tape, rewind, and document.
5. At end of test day, initiate prime battery and scope battery charging.

Data:

The block diagram for the data playback and analysis mode is shown in Figure A-5. The processed data in this test series are displayed as distance-based stripcharts of the round trip runs, a time-based stripchart of the deceleration/acceleration sequence at a passenger station, and acceleration power spectral density plots.

Signal routing is accomplished by the calibration and control unit acting in a totally passive mode. The three acceleration signals are then differentially summed with the recorded zero-volt reference signal in the tape speed compensation chassis. Since all four signals were recorded by the same head stack (channels 1,3,5,7), signal errors from tape speed variations are common to the four tracks. By substracting the reference signal from the data signals, a signal to noise ratio greater than 40 dB was achieved.

The compensated acceleration signals are next passed through a weighting network, or electrical filter. Different networks are used for vertical and horizontal data with the measured frequency response of each filter given in Figure A-6 and A-7. The filter characteristics approximate the human body response to vibration in in the 1 to 80 hz range. This response is defined in Guide for the Evaluation of Human Exposure to the Whole-Body Vibration (10), published by the International Organization for Standardization. The reference curves are also plotted in the above figures. Presentation of the filtered signal in this form is specified in the test procedure detailed in GSP-064 (9).

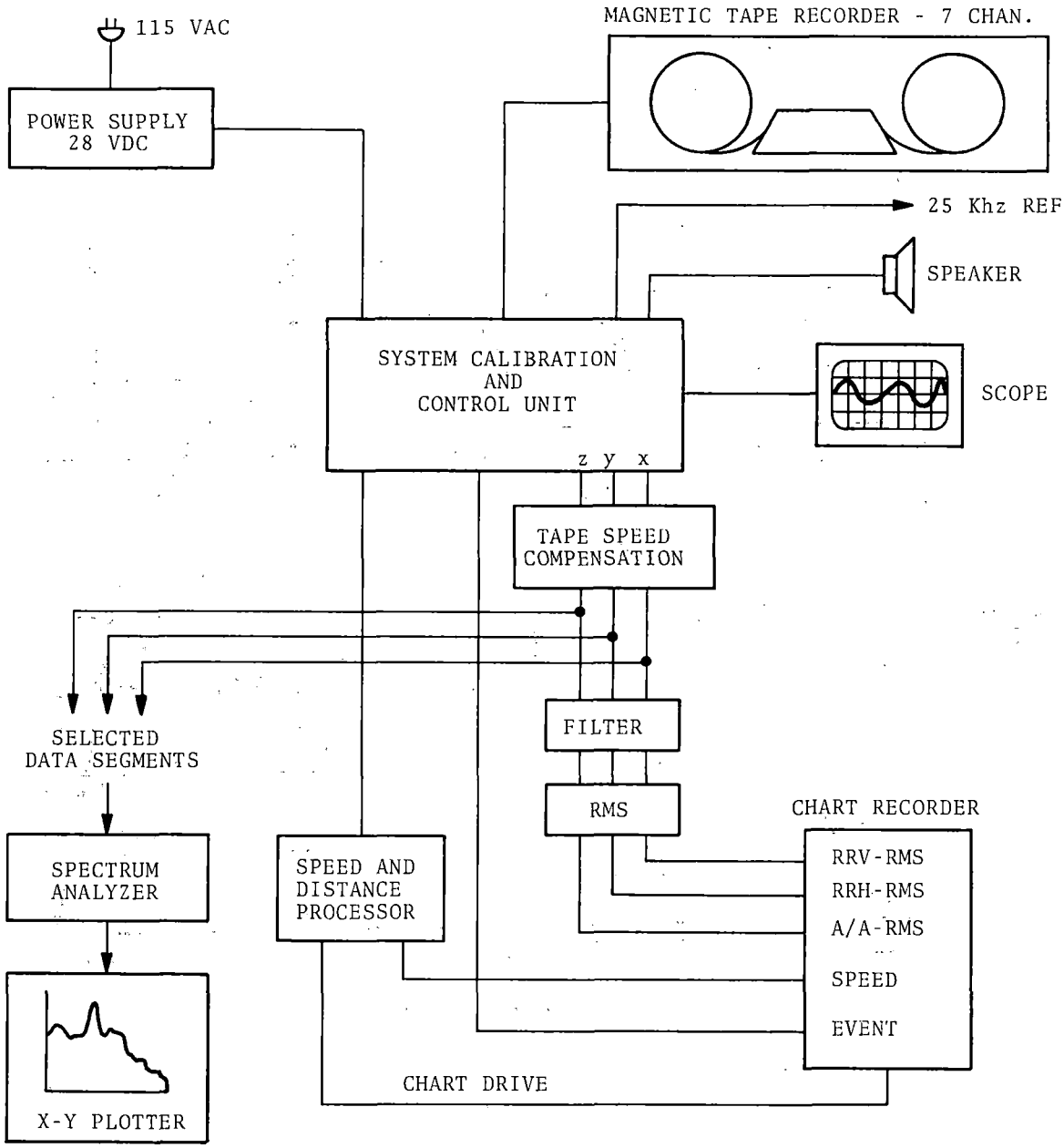

Figure A-5. Ride Roughness System Block Diagram
Data Play-Back and Analysis Mode

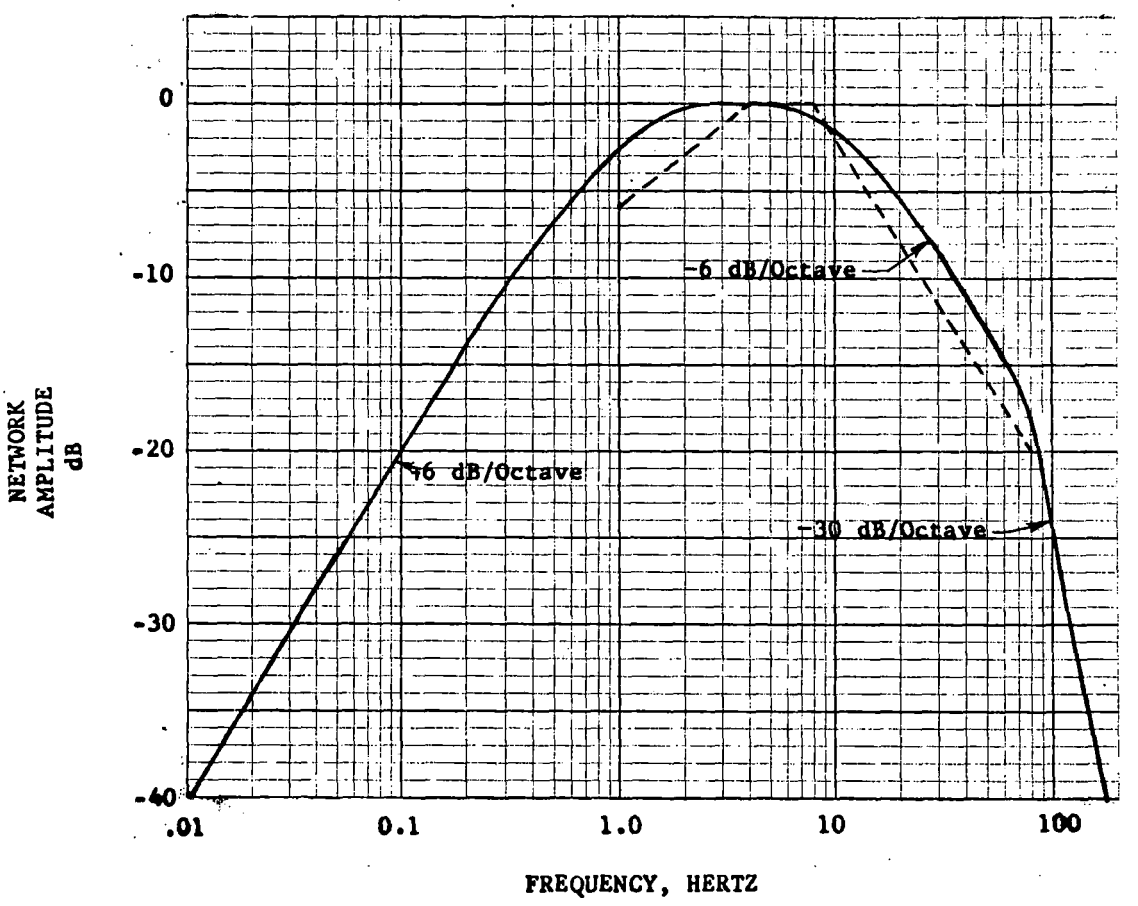

Figure A-6 Weighting Network Frequency Response, Ride Roughness Vertical Vibration, Recommended ISO Curve (dashed)

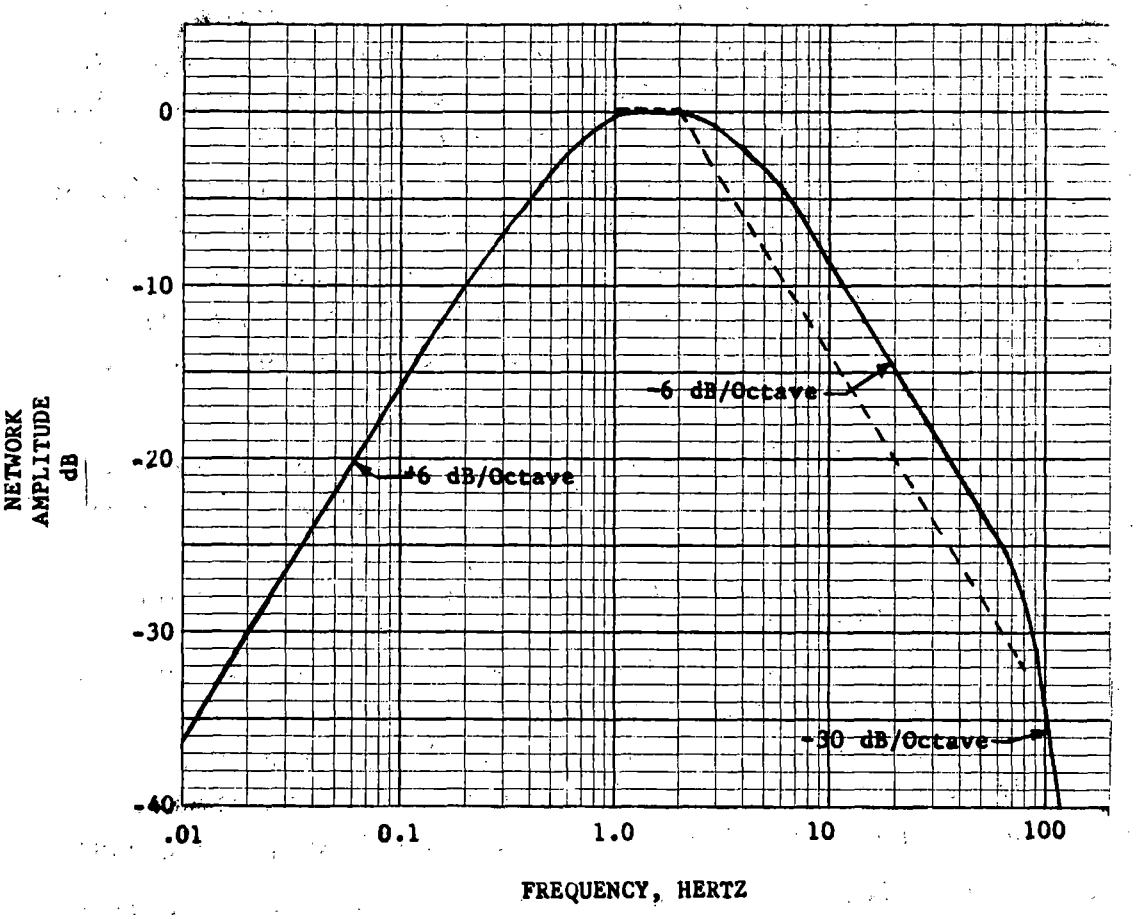

Figure A-7 Weighting Network Frequency Response, Ride Roughness Horizontal Vibration, Recommended ISO Curve (dashed)

A true root-mean-square (RMS) processor was used to determine the RMS value of the weighted signals. The averaging time constant was exponential (RC) in form and was set at one or three seconds depending on the desired data display. The resulting signal was displayed on the chart calibrated in g-rms units.

The recorded pulses from the axle-mounted shaft encoder were used to derive the instantaneous vehicle speed. A one-shot multivibrator circuit was triggered on the leading edge of the recorded pulses and a duty cycle pulse integrator processed this pulse train to yield an analog speed signal. The incremental chart recorder required eight pulses per foot of vehicle travel. Digital dividing circuits operating on the shaped recorded pulses provided the required signals to drive the recorder. Since the speed and distance signals are dependent upon the encoder wheel circumference, the pulse integrator and dividing circuits are programmable to allow system calibration.

The distance-based charts are plotted with an absicissa scale of 50 feet per minor division. The data signals shown on each of the figures are listed below.

1. Event marks corresponding to stations identified from the voice track and log book.
2. Vehicle speed as derived from the recorded encoder pulses.
3. Time marks at 10 second intervals.
4. Ride Roughness Acceleration, Vertical RMS, (weighted)
5. Ride Roughness Acceleration, Lateral RMS, (weighted)
6. Ride Roughness Acceleration, Longitudinal RMS, (weighted)

The RMS time constant was set at three seconds for these distance-based charts. Data from the AC vehicle with the sensor located near the truck pivot are shown in Figures A-8 and A-9. Mid-car sensor data are shown in Figures A-10 and A-11.

The time-based data chart in Figure A-12 is the deceleration/acceleration sequence at West Park Station. The data shown are from the sensor located near the truck pivot with the vehicle traveling eastbound. On these charts, the RMS averaging time constant was one second. To show the relationship between the three weighted

acceleration signals and their RMS signals, all six traces are displayed on the chart.

After all of the test data were displayed on the strip charts, a segment of track was selected through which all test vehicles ran at approximately the same constant speed. These data were the best approximation to a stationary process and their use maximized the statistical validity of the power spectral density (PSD) estimates. The unweighted data from this track segment were analyzed for both truck and mid-car sensor locations. Plots were generated for the vertical, lateral, and longitudinal acceleration PSD's in the 0-20hz and 0-100hz frequency range. Frequency resolution on the 200 line analyzer was 0.1hz and 0.5hz, respectively.

The track segment chosen was between Brook Park and Puritas Stations, eastbound. All test vehicles traversed this section at approximately 55 mph which resulted in 80 seconds of quasi-stationary data. With this time length of data, the statistical degrees of freedom were 16 for the 20 hertz PSD plots and 64 for the 100 hertz plots. As a result, the 95 per cent confidence levels for the PSD plots lie between +3.6 dB and -2.5 dB of the measured value for the 20 hertz plots and +1.7 dB and -1.4 dB for the 100 hertz plots.

The PSD plots are shown in Figures A-13 through A-18.

TEST SEQUENCE: 9-73-701

DATE: SEPTEMBER 19, 1973

SITE: CLEVELAND TRANSIT SYSTEM

TIME: 6:46 AM to 7:21 AM

DIRECTION: Westbound

VEHICLE: AC, No. 154

SENSOR LOCATION: Truck Pivot

SIGNAL PROCESSING: Accelerometer signals weighted (filtered) to approximate the human body response to vibration. The resulting signal is processed by a true root-mean-square (RMS) analyzer with a three second RC averaging time constant.

CHART ABSCISSA: Distance

NOTE 1. Ride roughness signals do not always reach zero when the vehicle stops. The movement of passengers and the vibrations of vehicle sub-systems may continue to excite the acceleration sensor.

NOTE 2. At the instant the vehicle wheels lock following deceleration, a large longitudinal acceleration transient is generated.

NOTE 3. The length of the event marks at stations is not significant. These marks were manually activated by the forward observer during the test run.

Figure A-8 Ride Roughness Data

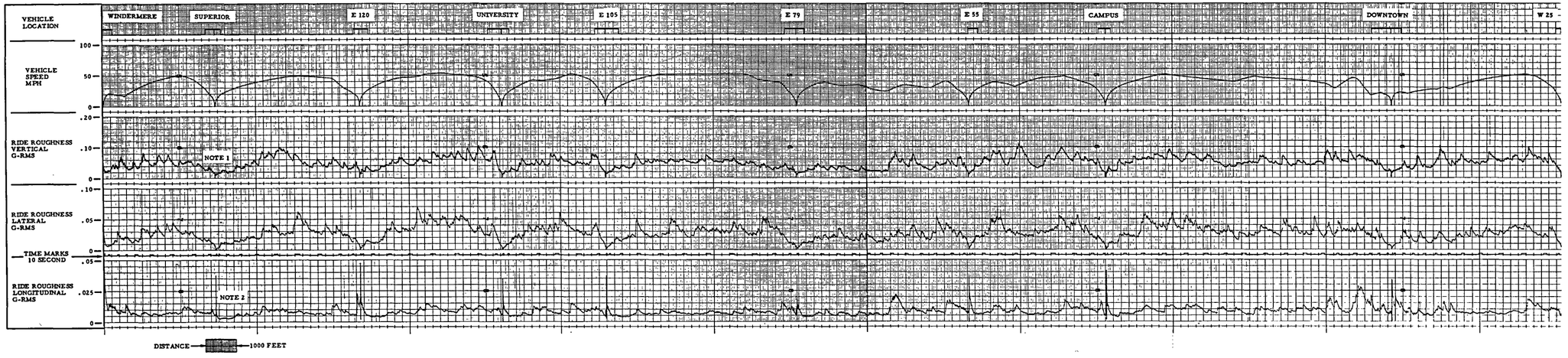

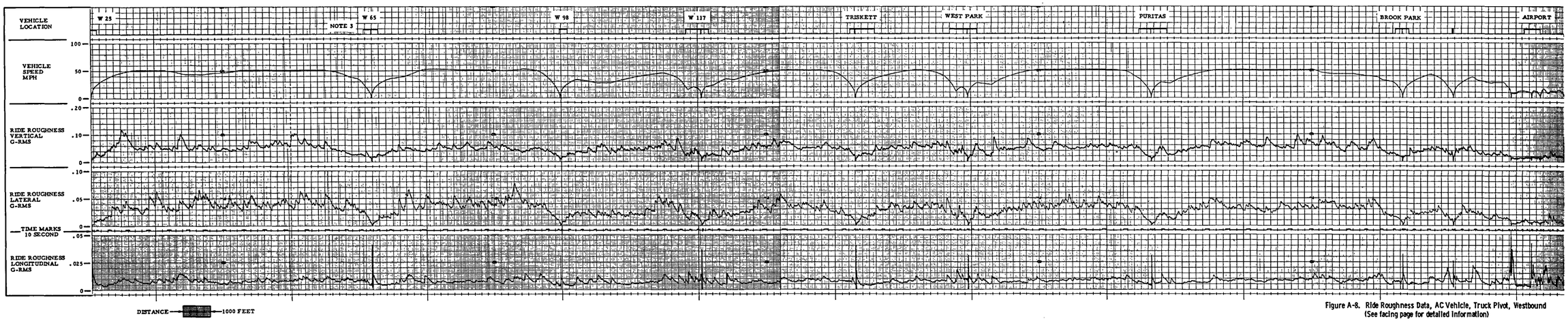

Figure A-8. Ride Roughness Data, AC Vehicle, Truck Pivot, Westbound
(See facing page for detailed information)

TEST SEQUENCE: 9-73-701

DATE: SEPTEMBER 19, 1973

SITE: CLEVELAND TRANSIT SYSTEM

TIME: 7:32 AM to 8:13 AM

DIRECTION: Eastbound

VEHICLE: AC, No. 154

SENSOR LOCATION: Truck Pivot

SIGNAL PROCESSING: Accelerometer signals weighted (filtered) to approximate the human body response to vibration. The resulting signal is processed by a true root-mean-square (RMS) analyzer with a three second RC averaging time constant.

CHART ABSCISSA: Distance

NOTE 1. Ride roughness signals do not always reach zero when the vehicle stops. The movement of passengers and the vibrations of vehicle sub-systems may continue to excite the acceleration sensor.

NOTE 2: At the instant the vehicle wheels lock following deceleration, a large longitudinal acceleration transient is generated.

NOTE 3: The length of the event marks at stations is not significant. These marks were manually activated by the forward observer during the test run.

NOTE 4: The data segment analyzed for the PSD plots is located between the dotted lines.

NOTE 5: The deceleration/acceleration sequence at West Park Station is also shown on a time-based chart in Figure A-12.

Figure A-9 Ride Roughness Data

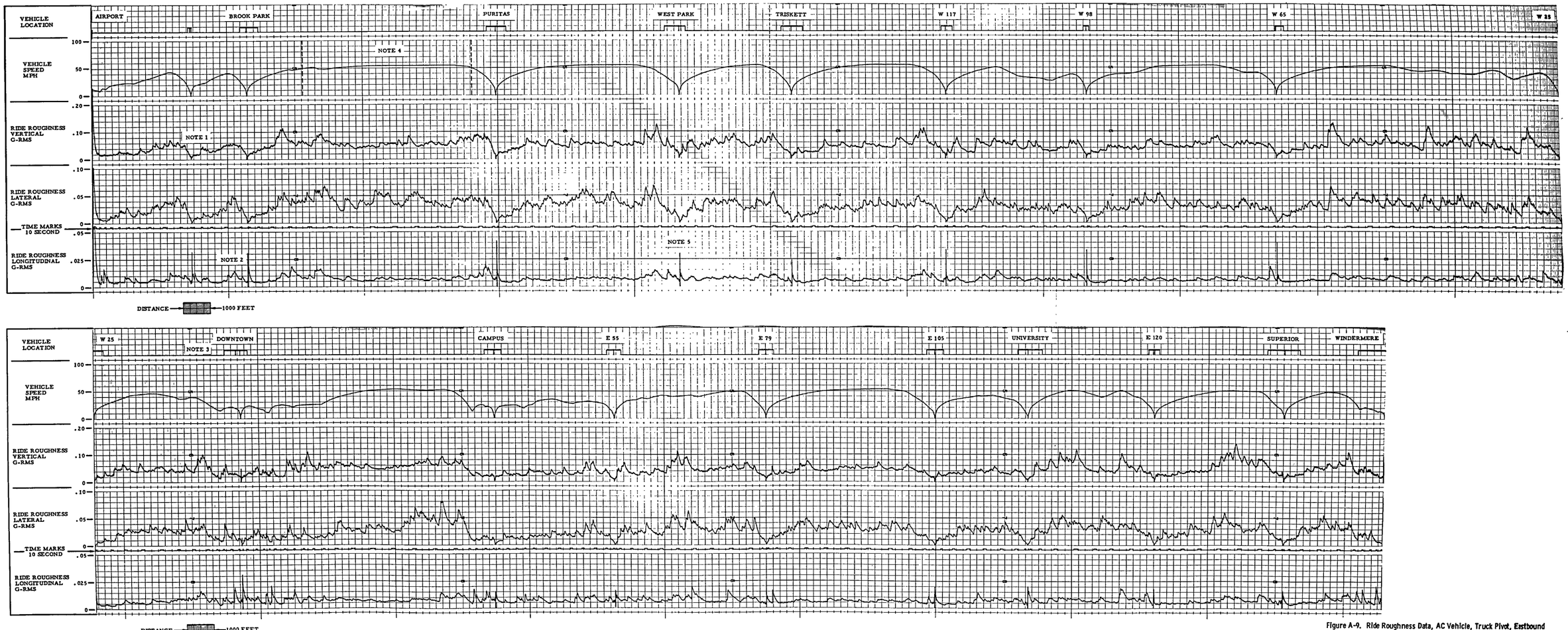

Figure A-9. Ride Roughness Data, AC Vehicle, Truck Pivot, Eastbound
(See facing page for detailed information)

TEST SEQUENCE: 9-73-701

DATE: SEPTEMBER 19, 1973

SITE: CLEVELAND TRANSIT SYSTEM

TIME: 8:22 AM to 9:00 AM

DIRECTION: Westbound

VEHICLE: AC, No. 154

SENSOR LOCATION: Mid-car

SIGNAL PROCESSING: Accelerometer signals weighted (filtered) to approximate the human body response to vibration. The resulting signal is processed by a true root-mean-square (RMS) analyzer with a three second RC averaging time constant.

CHART ABSCISSA: Distance

NOTE 1. Ride roughness signals do not always reach zero when the vehicle stops. The movement of passengers and the vibrations of vehicle sub-systems may continue to excite the acceleration sensor.

NOTE 2: At the instant the vehicle wheels lock following deceleration, a large longitudinal acceleration transient is generated.

NOTE 3: The length of the event marks at stations is not significant. These marks were manually activated by the forward observer during the test run.

Figure A-10 Ride Roughness Data

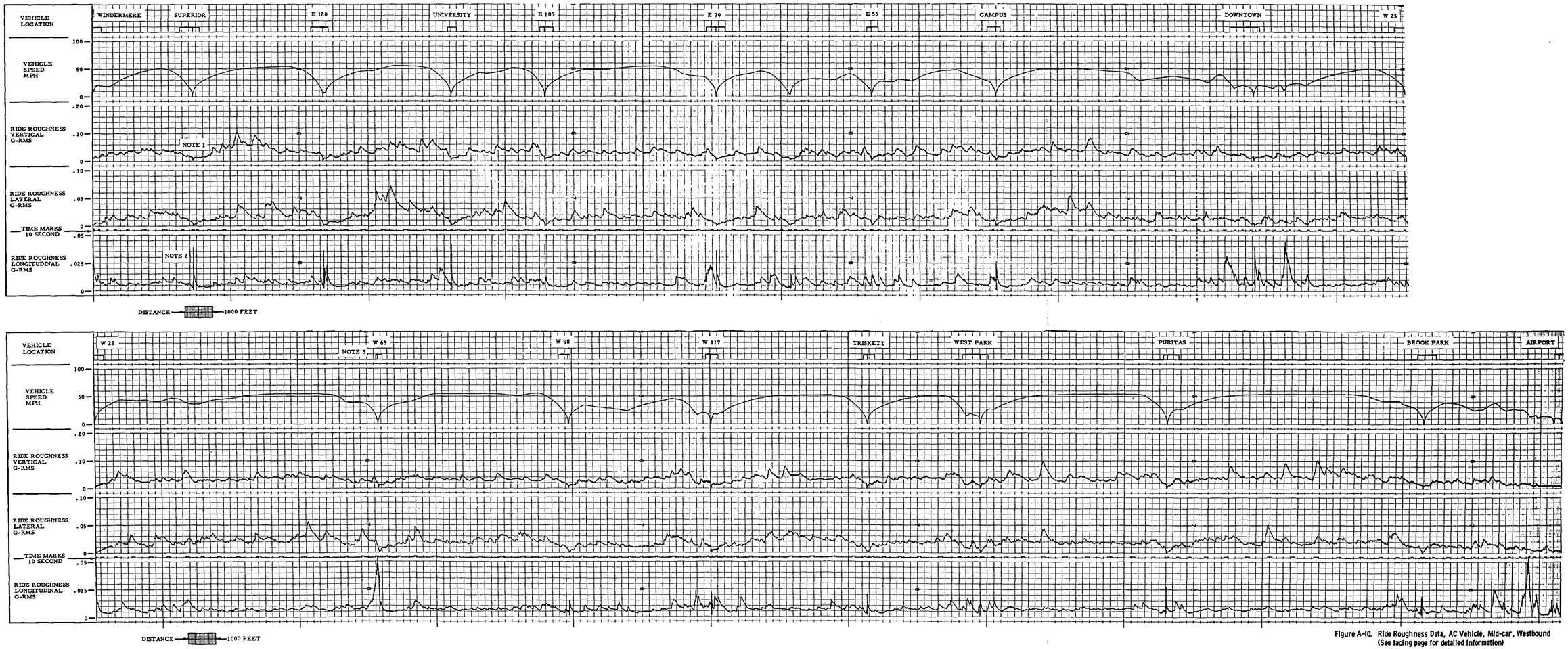

Figure A-10. Ride Roughness Data, AC Vehicle, Mid-car, Westbound
(See facing page for detailed information)

TEST SEQUENCE: 9-73-701

DATE: SEPTEMBER 19, 1973

SITE: CLEVELAND TRANSIT SYSTEM

TIME: 9:13 AM to 9:52 AM

DIRECTION: Eastbound

VEHICLE: AC, No. 154

SENSOR LOCATION: Mid-car

SIGNAL PROCESSING: Accelerometer signals weighted (filtered) to approximate the human body response to vibration. The resulting signal is processed by a true root-mean-square (RMS) analyzer with a three second RC averaging time constant.

CHART ABSCISSA: Distance

NOTE 1. Ride roughness signals do not always reach zero when the vehicle stops. The movement of passengers and the vibrations of vehicle sub-systems may continue to excite the acceleration sensor.

NOTE 2: At the instant the vehicle wheels lock following deceleration, a large longitudinal acceleration transient is generated.

NOTE 3: The length of the event marks at stations is not significant. These marks were manually activated by the forward observer during the test run.

NOTE 4: The data segment analyzed for the PSD plots is located between the dotted lines.

Figure A-11 Ride Roughness Data

Figure A-II. Ride Roughness Data, AC Vehicle, Mid-car, Eastbound
(See facing page for detailed information)

TEST SEQUENCE: 9-73-701

DATE: SEPTEMBER 19, 1973

SITE: CLEVELAND TRANSIT SYSTEM

TIME: 7:40 AM

DIRECTION: Eastbound

VEHICLE: AC, No. 154

SENSOR LOCATION: Truck Pivot

SIGNAL PROCESSING: Accelerometer signals weighted (filtered) to approximate the human body response to vibration. The resulting signal is processed by a true root-mean-square (RMS) analyzer with a one second RC averaging time constant.

CHART ABSCISSA: Time

NOTE 1. Ride roughness signals do not always reach zero when the vehicle stops. The movement of passengers and the vibrations of vehicle sub-systems may continue to excite the acceleration sensor.

NOTE 2: At the instant the vehicle wheels lock following deceleration, a large longitudinal acceleration transient is generated.

NOTE 3: The bandwidth of the vertical ride roughness weighting filter is wider than the horizontal filter bandwidth. The resulting vertical signal trace displays higher frequency components.

NOTE 4: The acceleration components (approximately 0.08g in magnitude) caused by the normal braking and accelerating of the vehicle are lower in frequency than the low frequency cut-off of the horizontal ride roughness filter. These components, therefore, are attenuated by the filter and do not appear on the data plot.

Figure A-12 Ride Roughenss Data

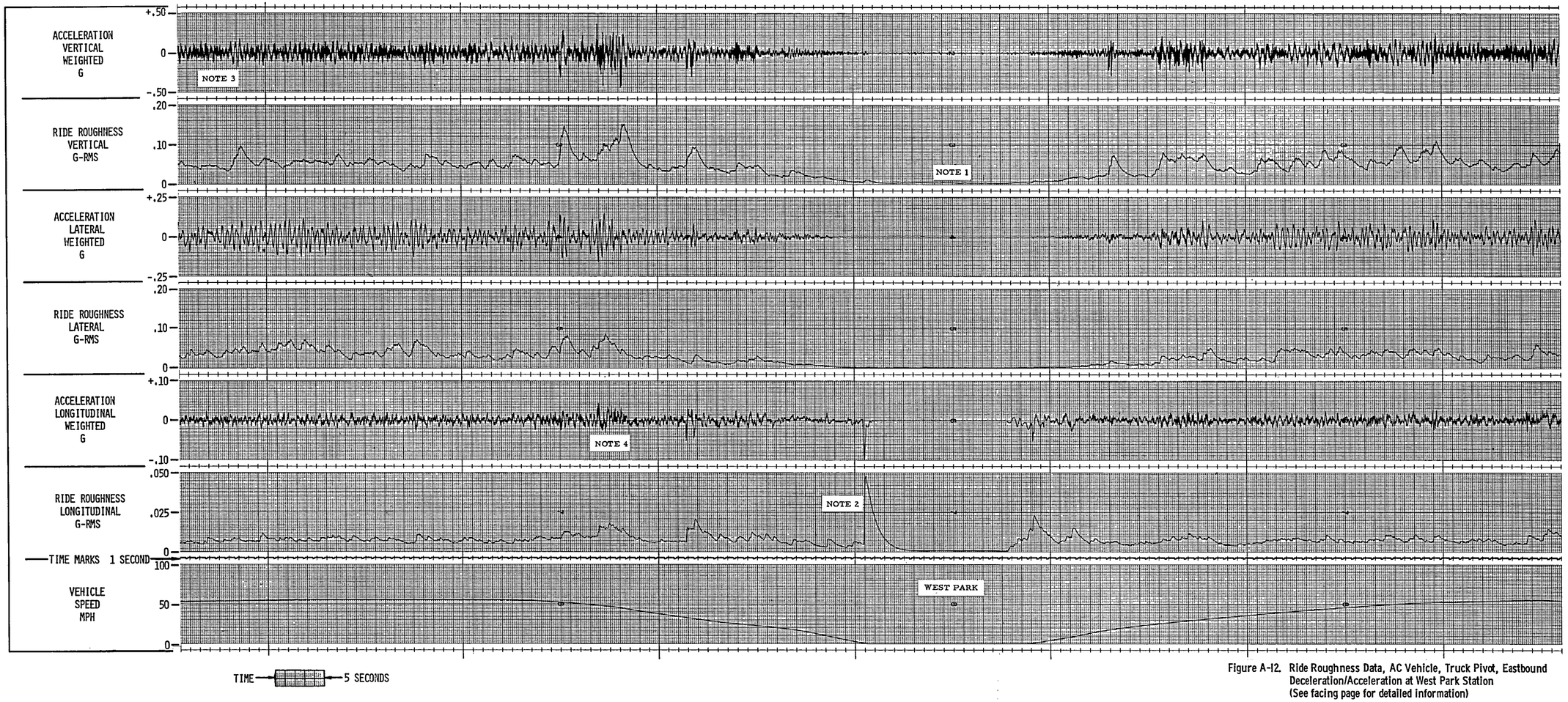

Figure A-12. Ride Roughness Data, AC Vehicle, Truck Pivot, Eastbound Deceleration/Acceleration at West Park Station
(See facing page for detailed information)

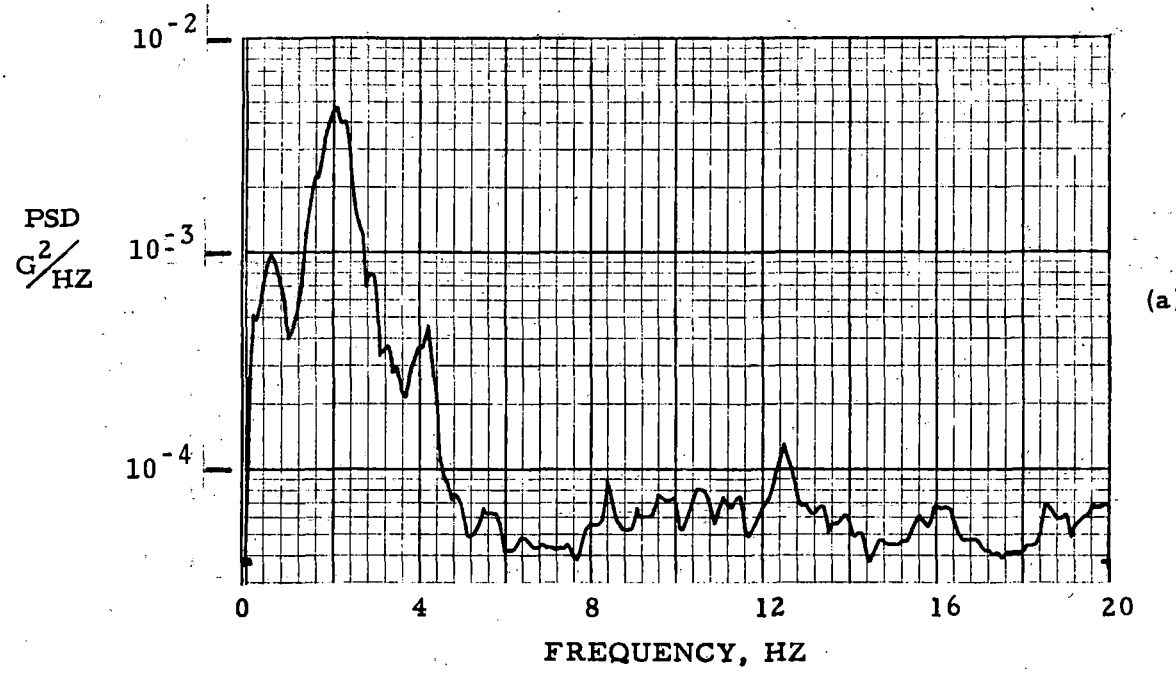

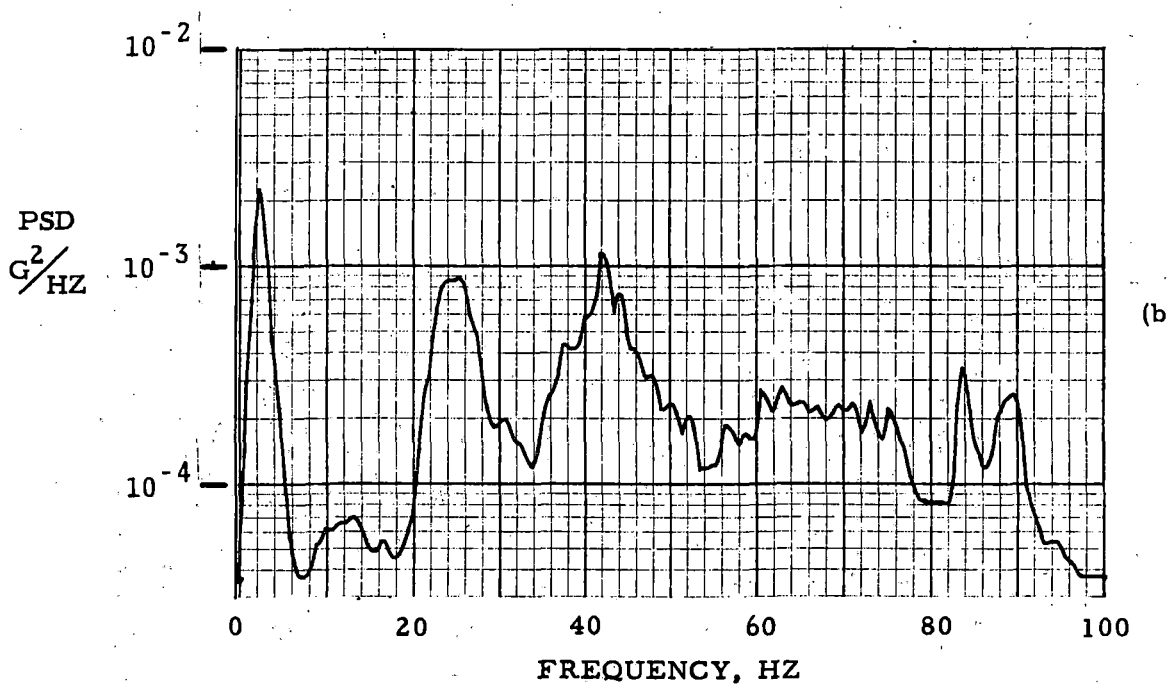

Figure A-13 Acceleration Power Spectral Density, Vertical, 55 MPH, AC Vehicle, Truck Pivot, Brook Park to Puritas Station, Eastbound

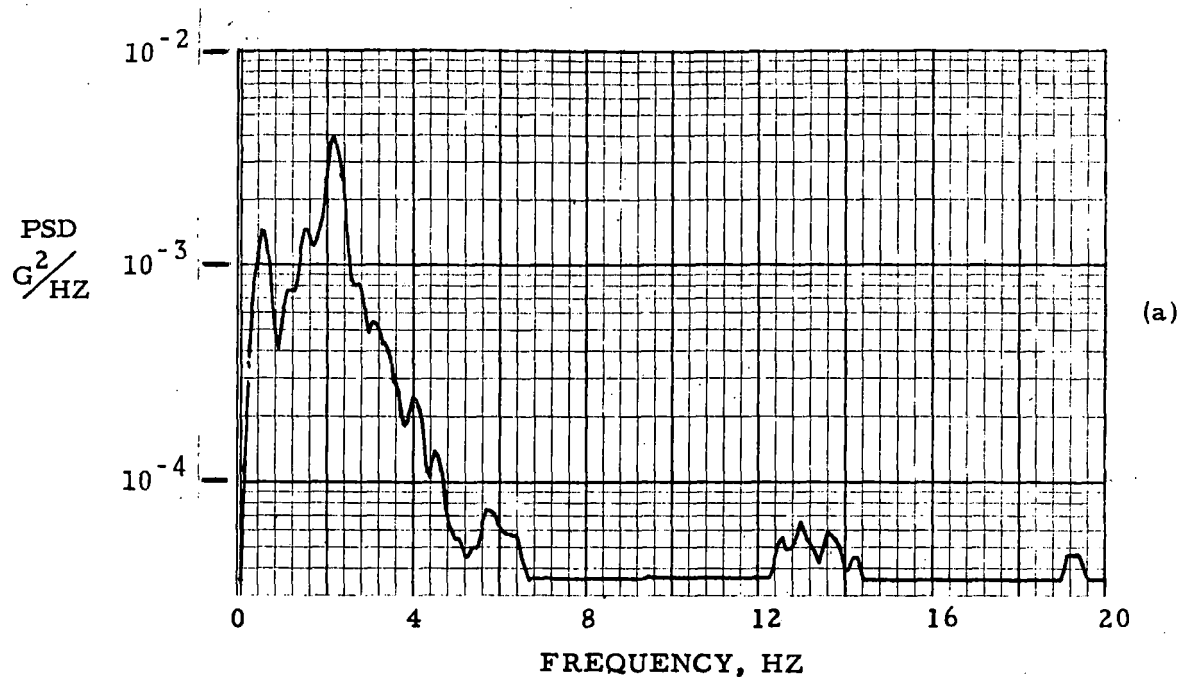

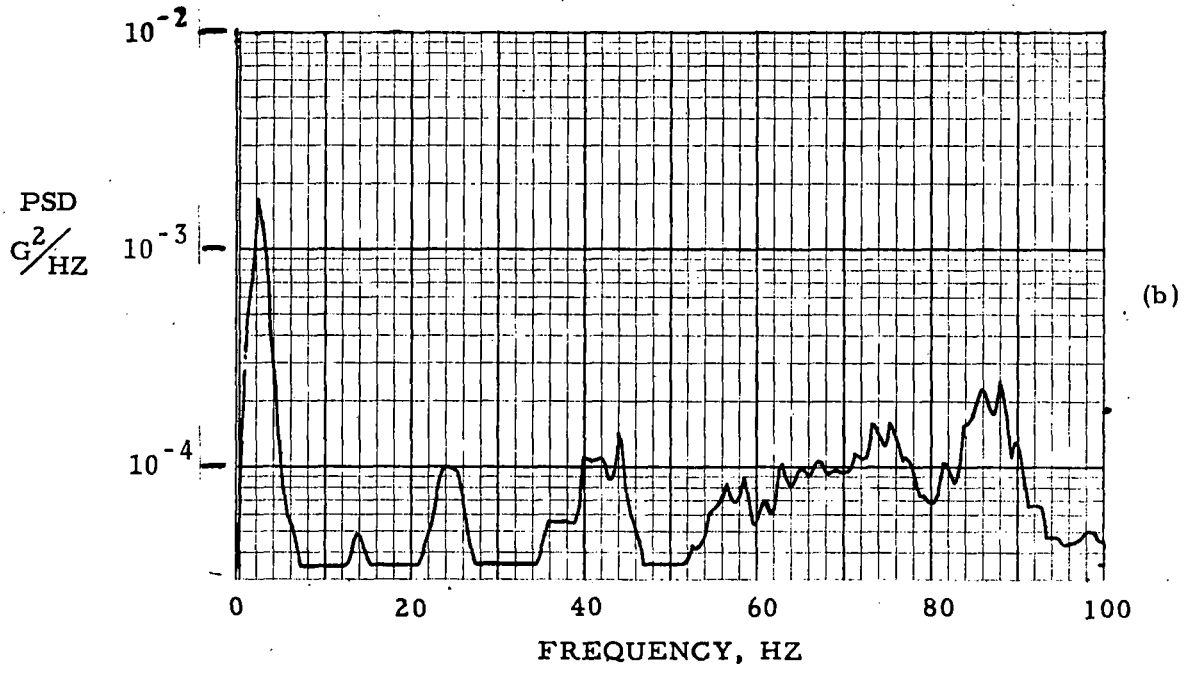

Figure A-14 Acceleration Power Spectral Density, Lateral, 55 MPH, AC Vehicle, Truck Pivot, Brook Park to Puritas Station, Eastbound

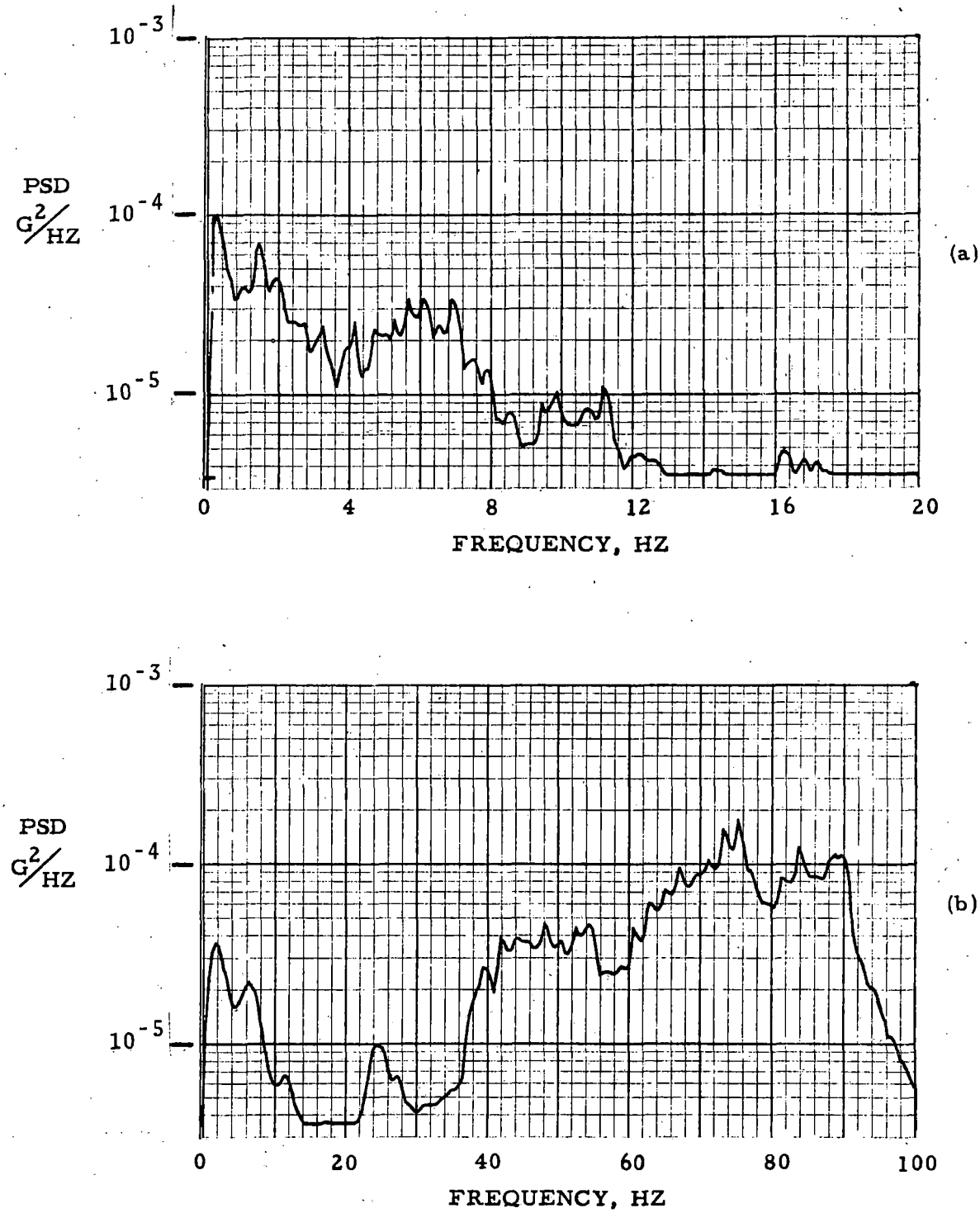

Figure A-15 Acceleration Power Spectral Density, Longitudinal, 55 MPH, AC Vehicle, Truck Pivot, Brook Park to Puritas Station, Eastbound

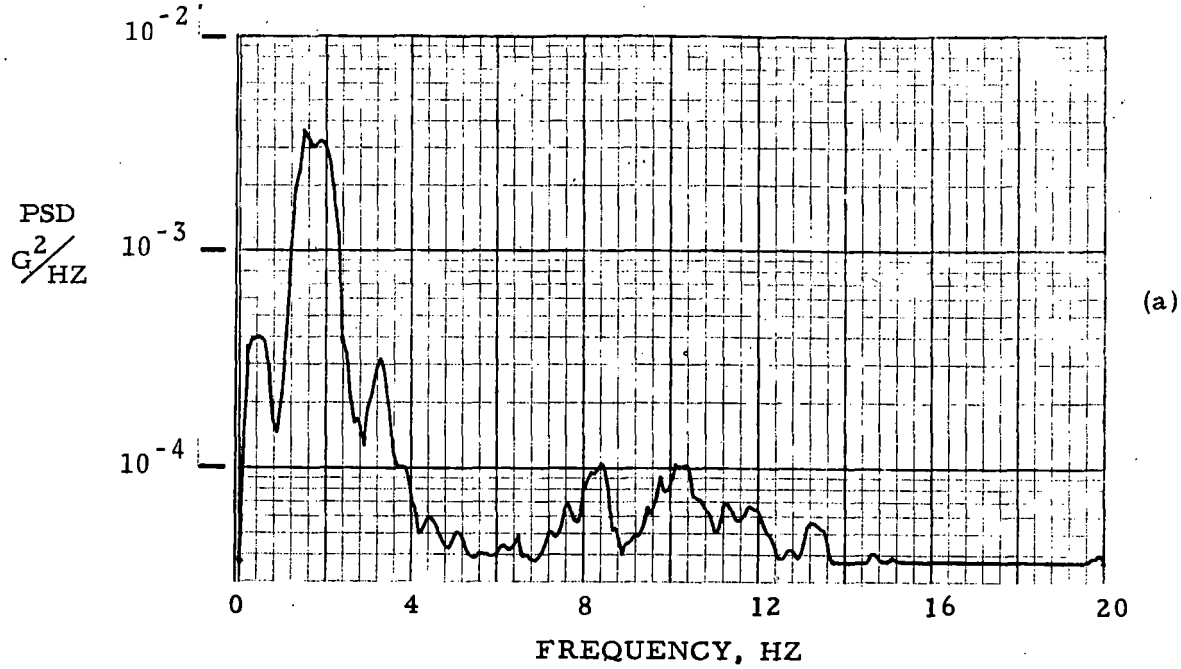

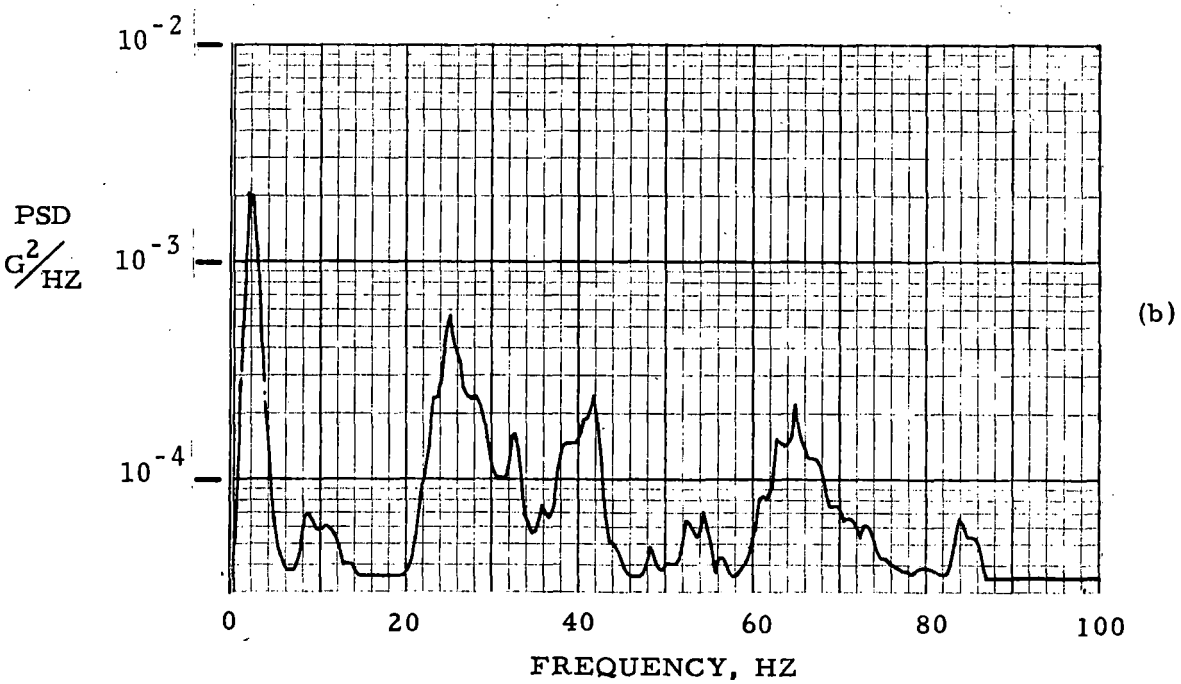

Figure A-16 Acceleration Power Spectral Density, Vertical, 55 MPH, AC Vehicle, Mid-Car, Brook Park to Puritas Station, Eastbound

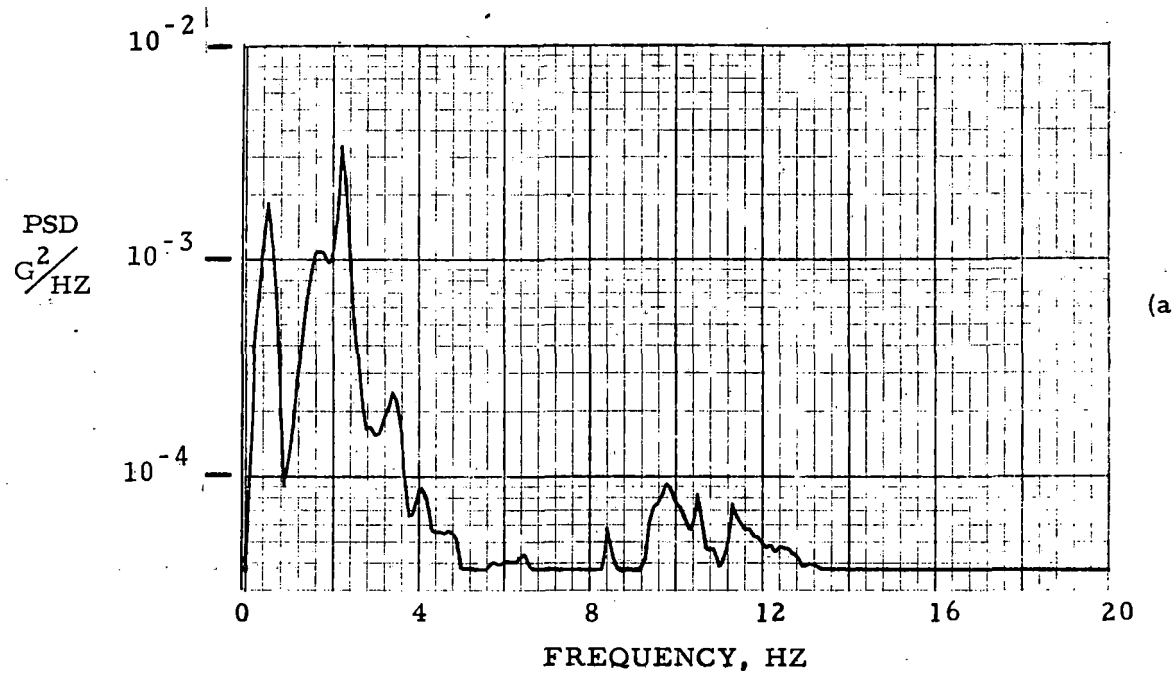

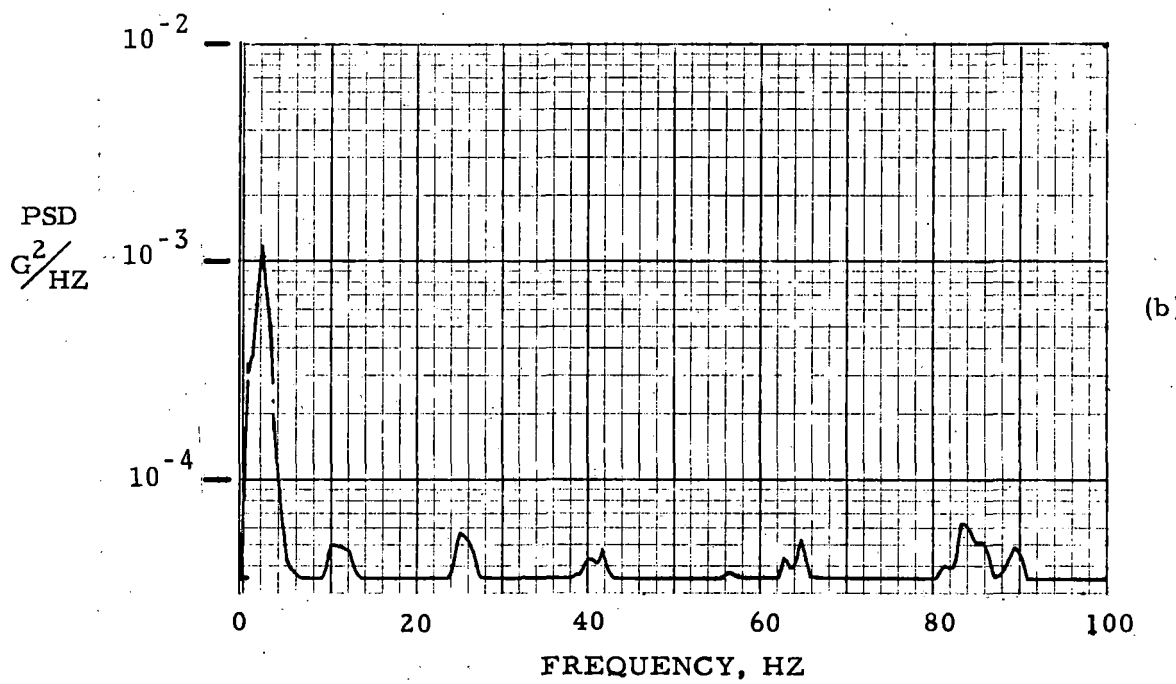

Figure A-17 Acceleration Power Spectral Density, Lateral, 55 MPH, AC Vehicle, Mid-Car, Brook Park to Puritas Station, Eastbound

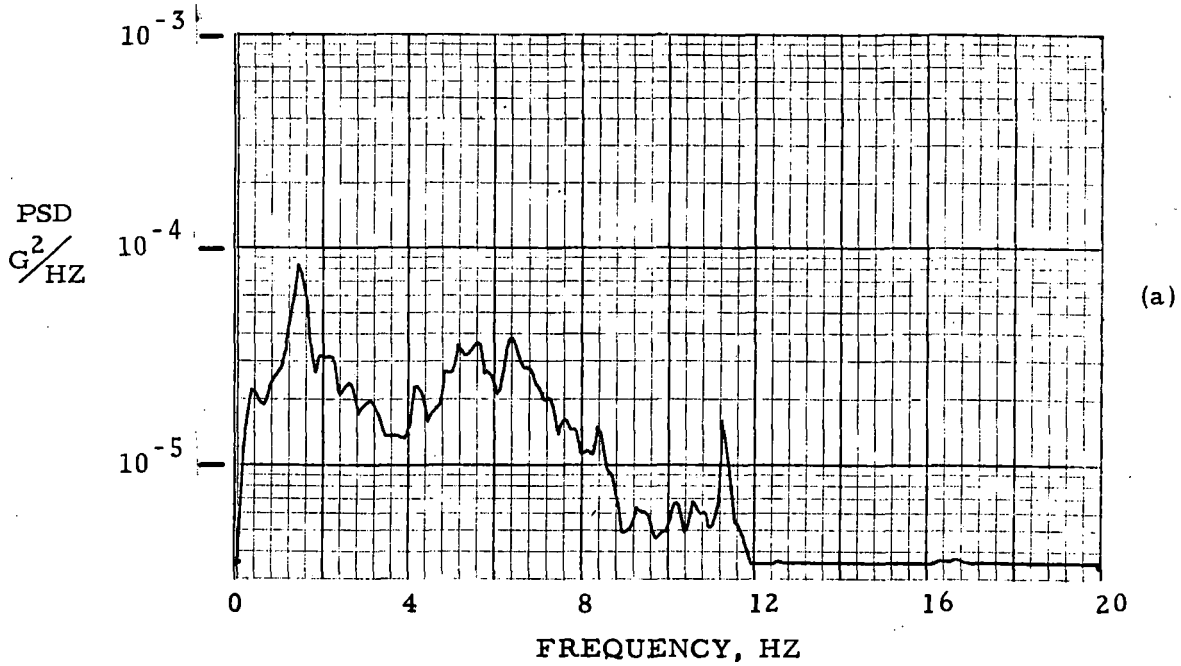

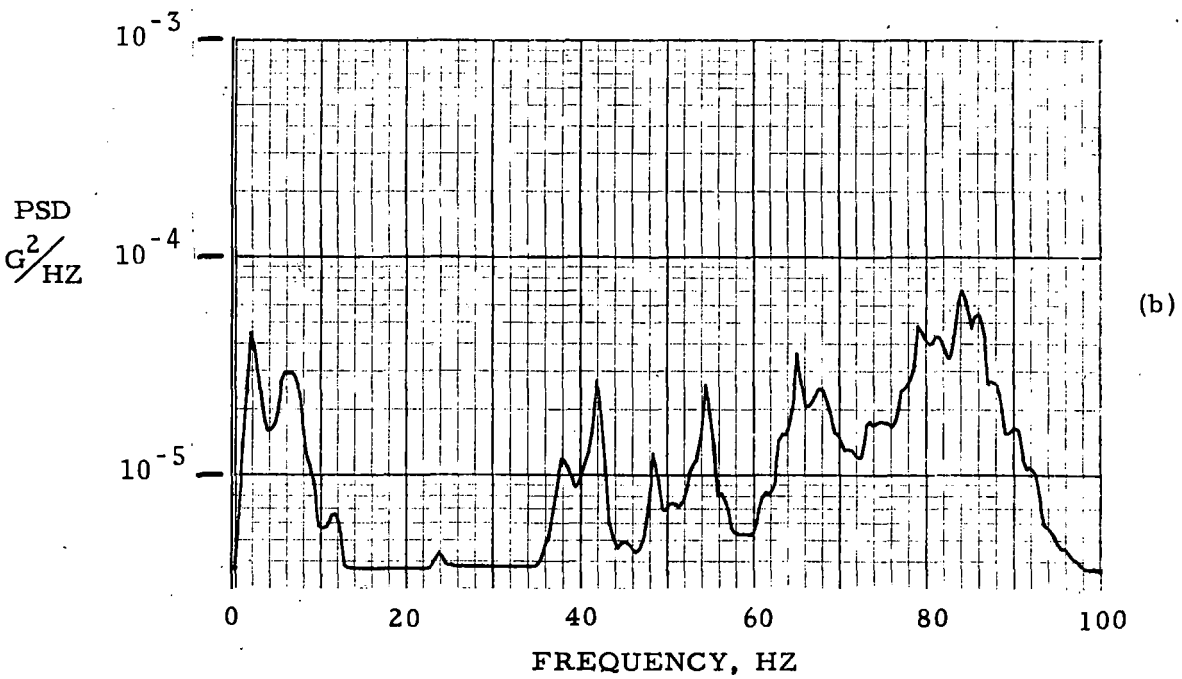

Figure A-18 Acceleration Power Spectral Density, Longitudinal, 55 MPH, AC Vehicle, Mid-Car, Brook Park to Puritas Station, Eastbound

APPENDIX B

RIDE ROUGHNESS TEST

DC VEHICLE

APPENDIX B

RIDE ROUGHNESS TEST, DC VEHICLE

Sequence No: 9-73-702

Procedure No: DC-R-5002-CTS

Objective:

To measure vibrations that would be experienced by a passenger near the truck and at mid-car on a DC-propelled transit vehicle. The collected data are used to compare the ride characteristics of AC-propelled vehicles to those of conventional DC-propelled vehicles.

Status:

Ride roughness data were successfully recorded and processed. The data are presented in this appendix in the form of distance- and time-based stripcharts of the weighted RMS acceleration. Acceleration power spectral density plots are given for a representative section of track. The ride roughness levels at both sensor locations were sufficiently low to assure passengers a comfortable ride according to ISO standards.

Test Description:

The test configuration, instrumentation, and procedures used on this DC test vehicle were indentical to those described in Appendix A. Car 162 was outfitted with the instrumentation and two round trip test runs were completed on Tuesday and Wednesday, September 18 and 19, 1973.

Data:

The processed data in this appendix are identical in form to the data in Appendix A. Distance-based stripcharts of the two round trip test runs are shown in Figures B-1 through B-4. Figure B-5 displays the deceleration/acceleration sequence at West Park Station eastbound. The acceleration power spectral density plots are given in Figures B-6 through B-11.

TEST SEQUENCE: 9-73-702

DATE: SEPTEMBER 18, 1973

SITE: CLEVELAND TRANSIT SYSTEM

TIME: 6:45 AM to 7:27 AM

DIRECTION: Westbound

VEHICLE: DC, No. 162

SENSOR LOCATION: Truck Pivot

SIGNAL PROCESSING: Accelerometer signals weighted (filtered) to approximate the human body response to vibration. The resulting signal is processed by a true root-mean-square (RMS) analyzer with a three second RC averaging time constant.

CHART ABSCISSA: Distance

NOTE 1. Ride roughness signals do not always reach zero when the vehicle stops. The movement of passengers and the vibrations of vehicle sub-systems may continue to excite the acceleration sensor.

NOTE 2: At the instant the vehicle wheels lock following deceleration, a large longitudinal acceleration transient is generated.

NOTE 3: The length of the event marks at stations is not significant. These marks were manually activated by the forward observer during the test run.

Figure B-1 Ride Roughness Data

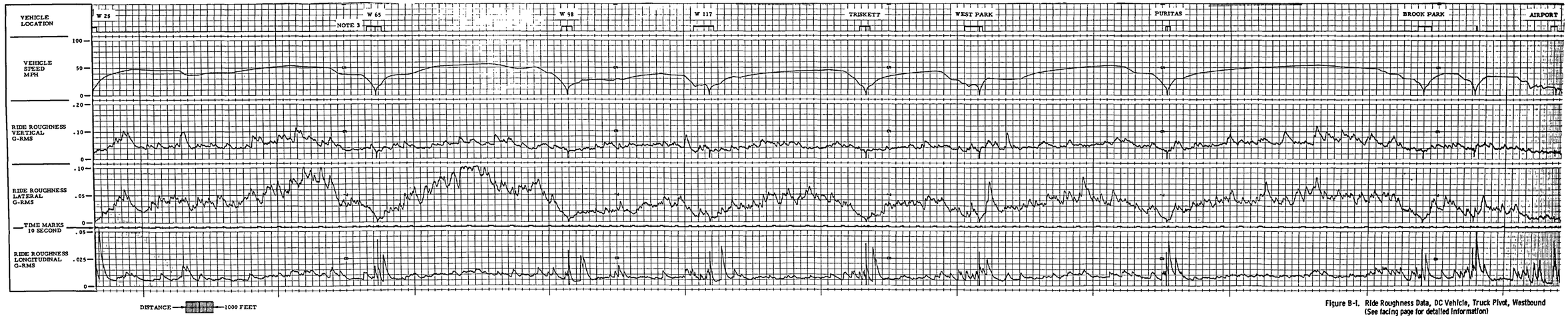

Figure B-1. Ride Roughness Data, DC Vehicle, Truck Pivot, Westbound
(See facing page for detailed information)

TEST SEQUENCE: 9-73-702

DATE: SEPTEMBER 19, 1973

SITE: CLEVELAND TRANSIT SYSTEM

TIME: 3:58 PM to 4:34 PM

DIRECTION: Eastbound

VEHICLE: DC, No. 162

SENSOR LOCATION: Truck Pivot

SIGNAL PROCESSING: Accelerometer signals weighted (filtered) to approximate the human body response to vibration. The resulting signal is processed by a true root-mean-square (RMS) analyzer with a three second RC averaging time constant.

CHART ABSCISSA: Distance

NOTE 1. Ride roughness signals do not always reach zero when the vehicle stops. The movement of passengers and the vibrations of vehicle sub-systems may continue to excite the acceleration sensor.

NOTE 2: At the instant the vehicle wheels lock following deceleration, a large longitudinal acceleration transient is generated.

NOTE 3: The length of the event marks at stations is not significant. These marks were manually activated by the forward observer during the test run.

NOTE 4: The data segment analyzed for the PSD plots is located between the dotted lines.

NOTE 5: Data recording on this run was not begun until leaving Brook Park Station. Revenue service schedule constraints did not allow adequate time.

NOTE 6: The deceleration/acceleration sequence at West Park Station is also shown on a time-based chart in Figure B-5.

Figure B-2 Ride Roughness Data

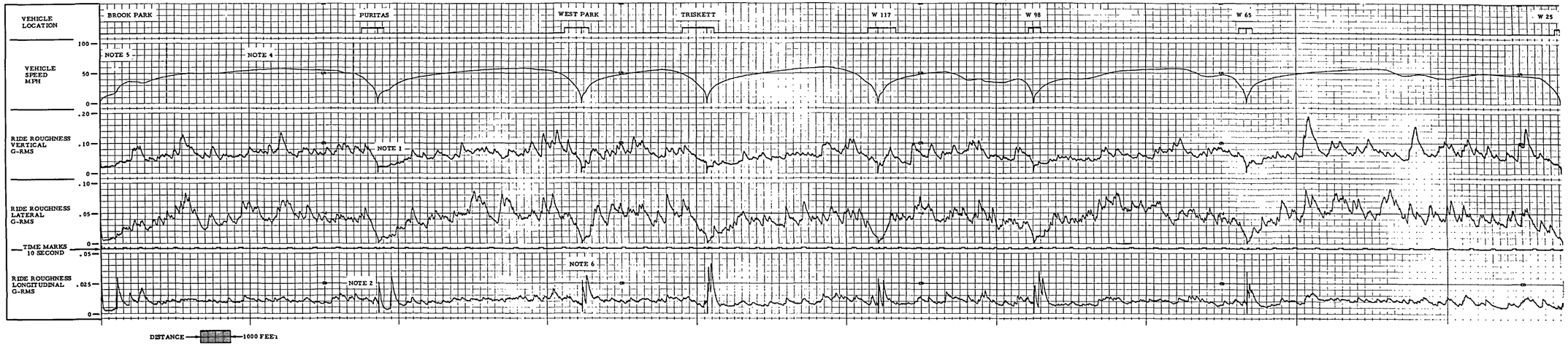

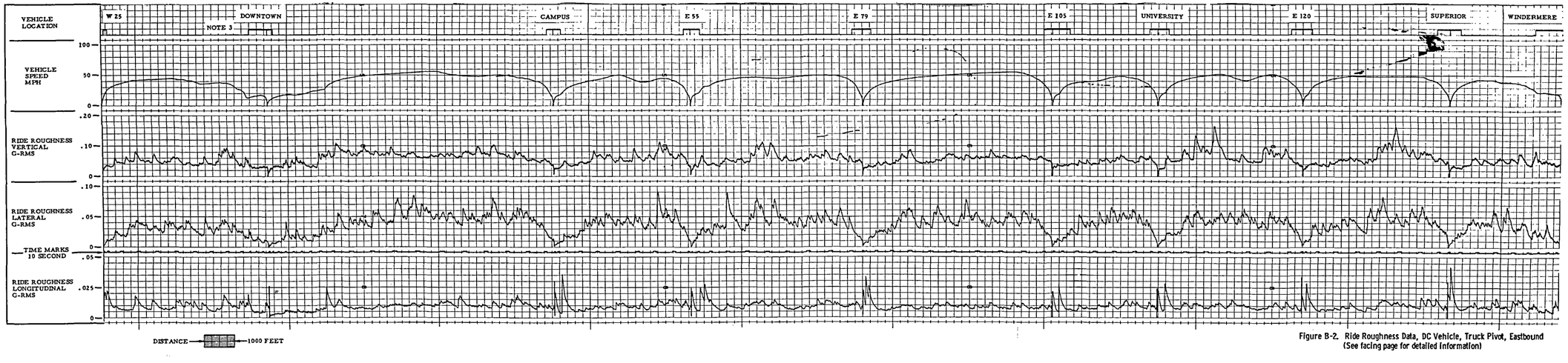

Figure B-2. Ride Roughness Data, DC Vehicle, Truck Pivot, Eastbound
(See facing page for detailed information)

TEST SEQUENCE: 9-73-702

DATE: SEPTEMBER 19, 1973

SITE: CLEVELAND TRANSIT SYSTEM

TIME: 4:41 PM to 5:32 PM

DIRECTION: Westbound

VEHICLE: DC, No. 162

SENSOR LOCATION: Mid-car

SIGNAL PROCESSING: Accelerometer signals weighted (filtered) to approximate the human body response to vibration. The resulting signal is processed by a true root-mean-square (RMS) analyzer with a three second RC averaging time constant.

CHART ABSCISSA: Distance

NOTE 1. Ride roughness signals do not always reach zero when the vehicle stops. The movement of passengers and the vibrations of vehicle sub-systems may continue to excite the acceleration sensor.

NOTE 2: At the instant the vehicle wheels lock following deceleration, a large longitudinal acceleration transient is generated.

NOTE 3: The length of the event marks at stations is not significant. These marks were manually activated by the forward observer during the test run.

NOTE 4: The ride roughness sensor cable was not connected at the start of this run.

Figure B-3 Ride Roughness Data

Figure B-3. Ride Roughness Data, DC Vehicle, Mid-car, Westbound
(See facing page for detailed information)

TEST SEQUENCE: 9-73-702

DATE: SEPTEMBER 19, 1973

SITE: CLEVELAND TRANSIT SYSTEM

TIME: 5:30 PM to 6:08 PM

DIRECTION: Eastbound

VEHICLE: DC, No. 162

SENSOR LOCATION: Mid-car

SIGNAL PROCESSING: Accelerometer signals weighted (filtered) to approximate the human body response to vibration. The resulting signal is processed by a true root-mean-square (RMS) analyzer with a three second RC averaging time constant.

CHART ABSCISSA: Distance

NOTE 1. Ride roughness signals do not always reach zero when the vehicle stops. The movement of passengers and the vibrations of vehicle sub-systems may continue to excite the acceleration sensor.

NOTE 2: At the instant the vehicle wheels lock following deceleration, a large longitudinal acceleration transient is generated.

NOTE 3: The length of the event marks at stations is not significant. These marks were manually activated by the forward observer during the test run.

NOTE 4: The data segment analyzed for the PSD plots is located between the dotted lines.

NOTE 5: This signal drop-out was caused by degraded recorder frequency response. This was the last data run and the battery power source was nearing failure.

Figure B-4 Ride Roughness Data

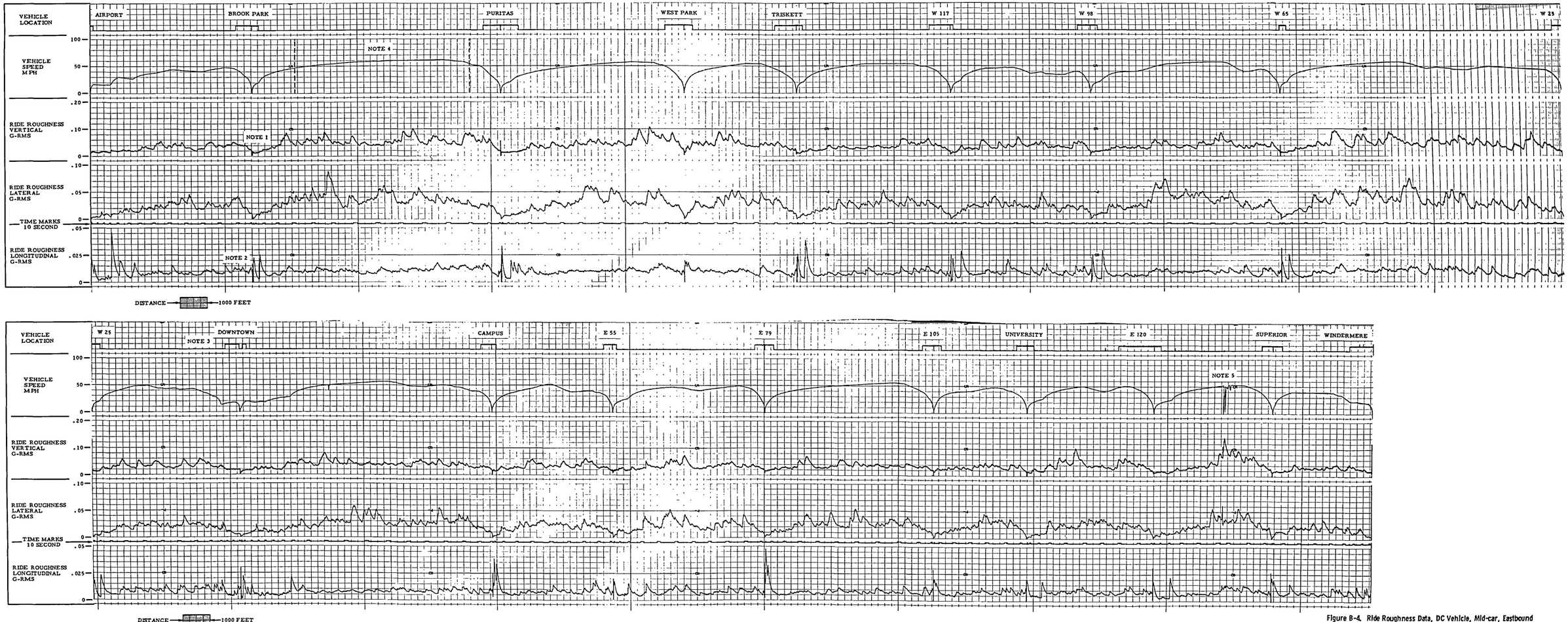

Figure B-4. Ride Roughness Data, DC Vehicle, Mid-car, Eastbound
(See facing page for detailed information)

TEST SEQUENCE: 9-73-702

DATE: SEPTEMBER 19, 1973

SITE: CLEVELAND TRANSIT SYSTEM

TIME: 4:03 PM

DIRECTION: Eastbound

VEHICLE: DC, No. 162

SENSOR LOCATION: Truck Pivot

SIGNAL PROCESSING: Accelerometer signals weighted (filtered) to approximate the human body response to vibration. The resulting signal is processed by a true root-mean-square (RMS) analyzer with a one second RC averaging time constant.

CHART ABSCISSA: Time

NOTE 1. Ride roughness signals do not always reach zero when the vehicle stops. The movement of passengers and the vibrations of vehicle sub-systems may continue to excite the acceleration sensor.

NOTE 2: At the instant the vehicle wheels lock following deceleration, a large longitudinal acceleration transient is generated.

NOTE 3: The bandwidth of the vertical ride roughness weighting filter is wider than the horizontal filter bandwidth.

NOTE 4: The acceleration components (approximately 0.08g in magnitude) caused by normal braking and accelerating of the vehicle are lower in frequency than the low frequency cut-off of weighting filters. These components, therefore, are attenuated by the filter and do not appear on the data plot.

Figure B-5 Ride Roughness Data

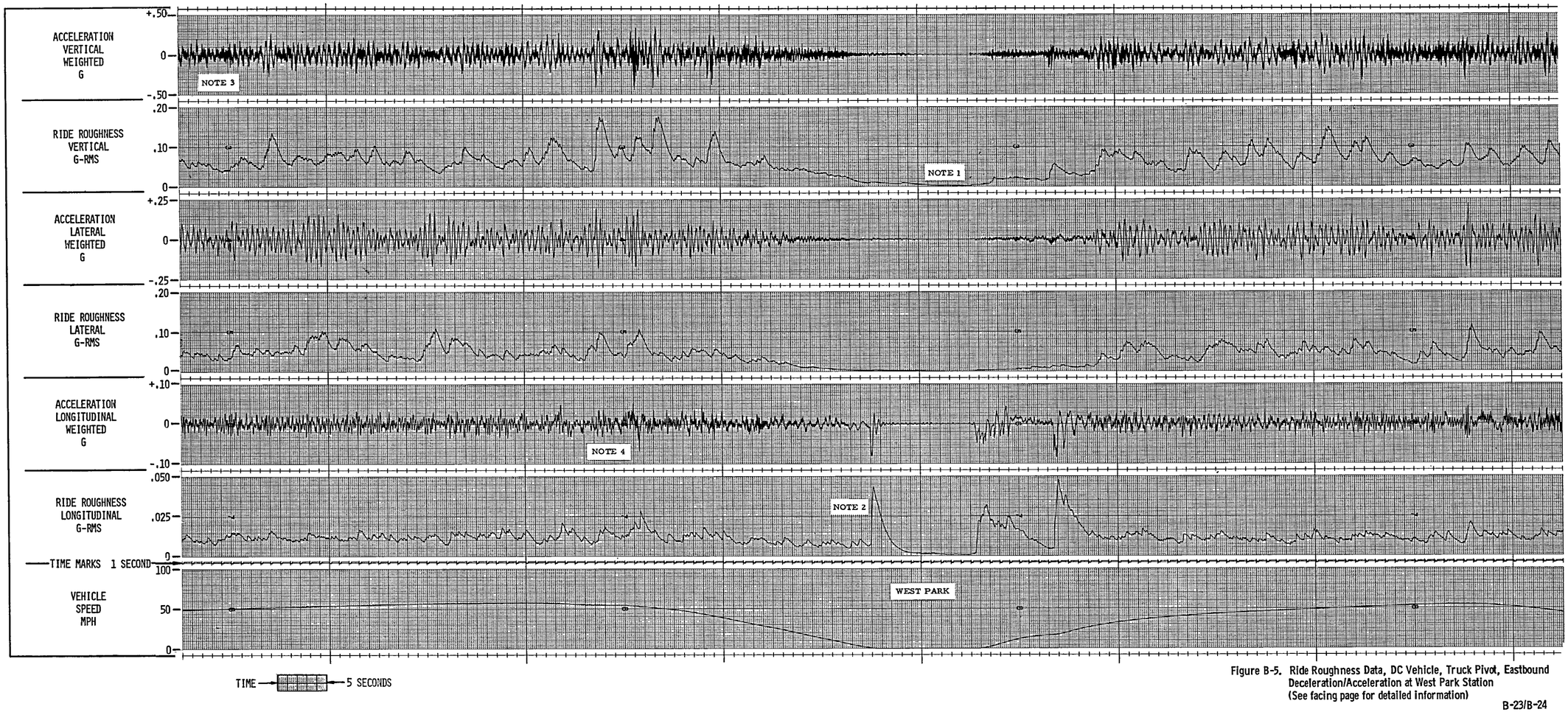

Figure B-5. Ride Roughness Data, DC Vehicle, Truck Pivot, Eastbound Deceleration/Acceleration at West Park Station
(See facing page for detailed information)

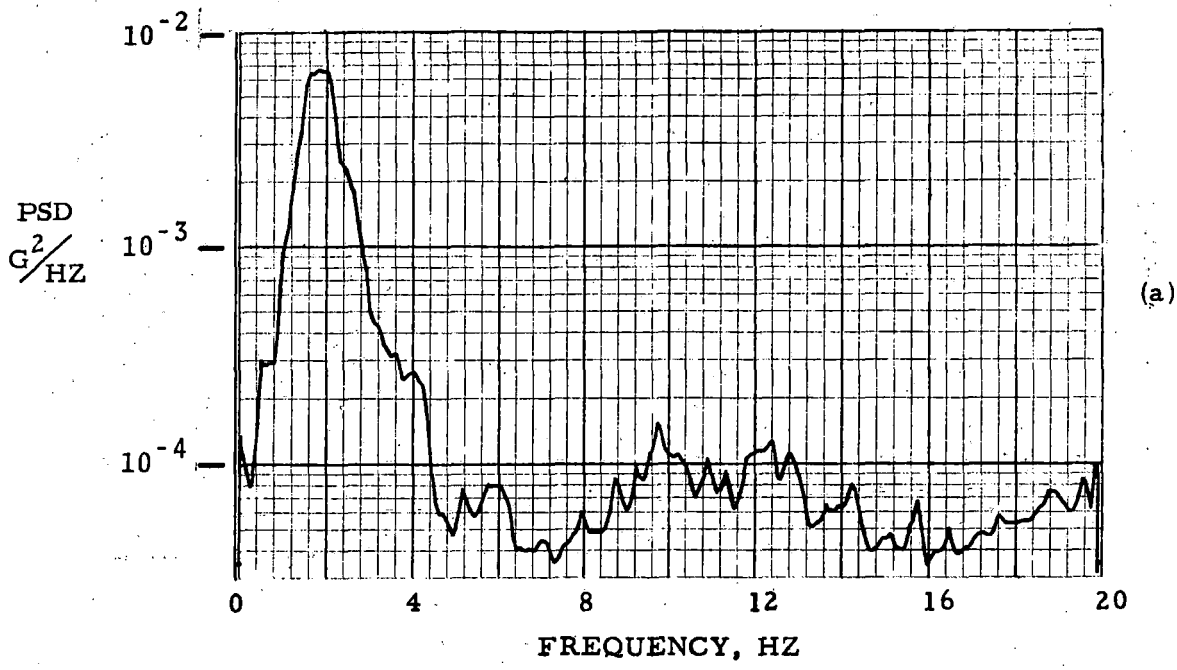

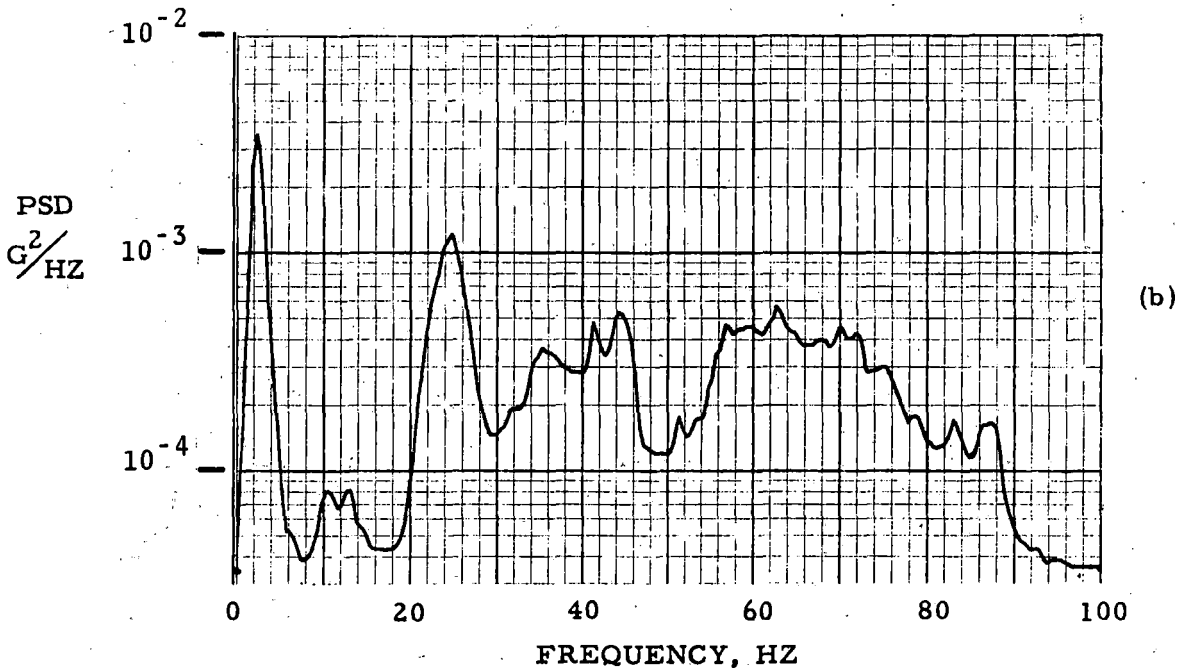

Figure B-6 Acceleration Power Spectral Density, Vertical, 55 MPH, DC Vehicle, Truck Pivot, Brook Park to Puritas Station, Eastbound

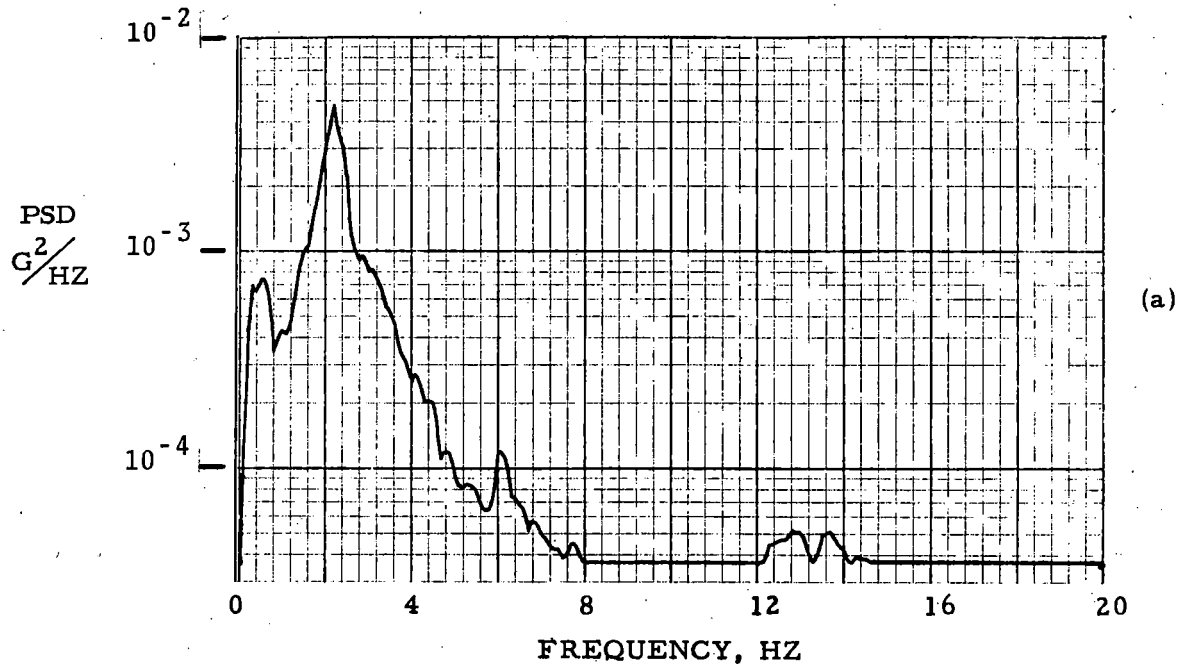

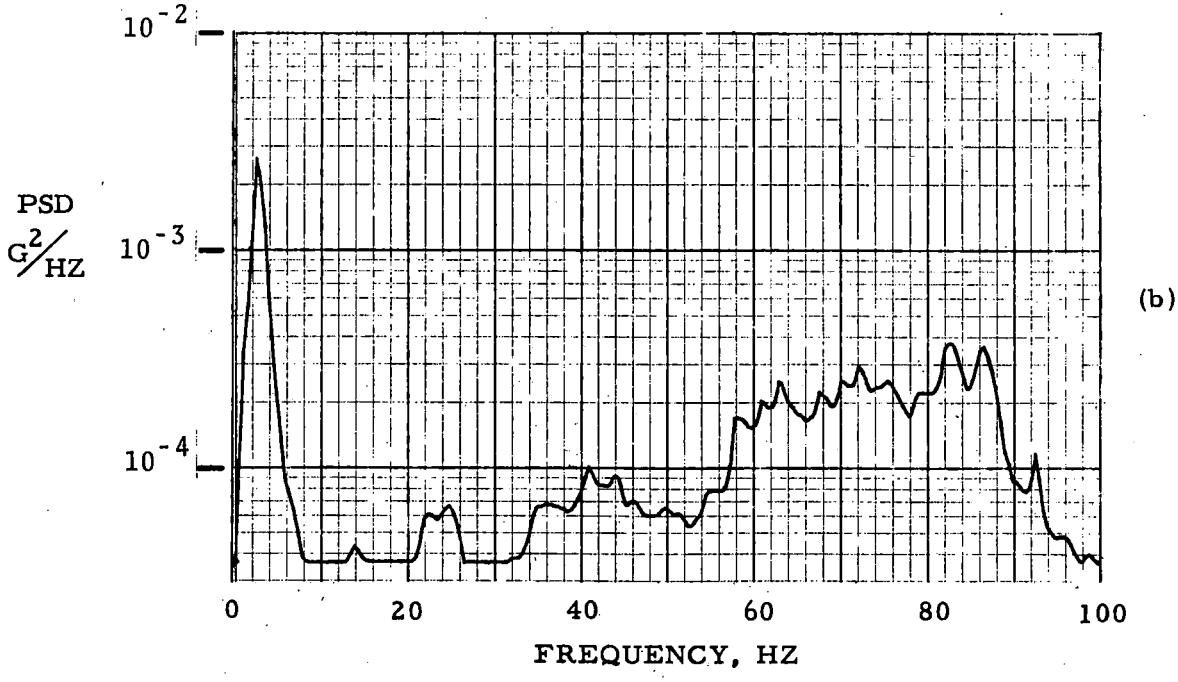

Figure B-7 Acceleration Power Spectral Density, Lateral, 55 MPH, DC Vehicle, Truck Pivot, Brook Park to Puritas Station Eastbound

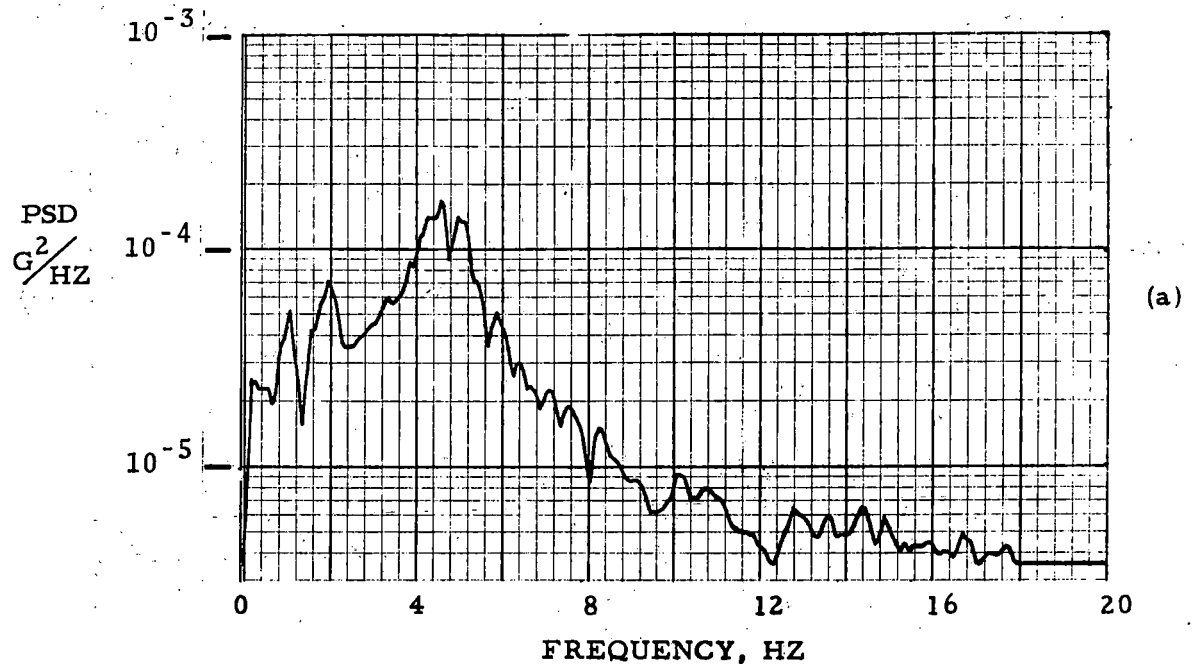

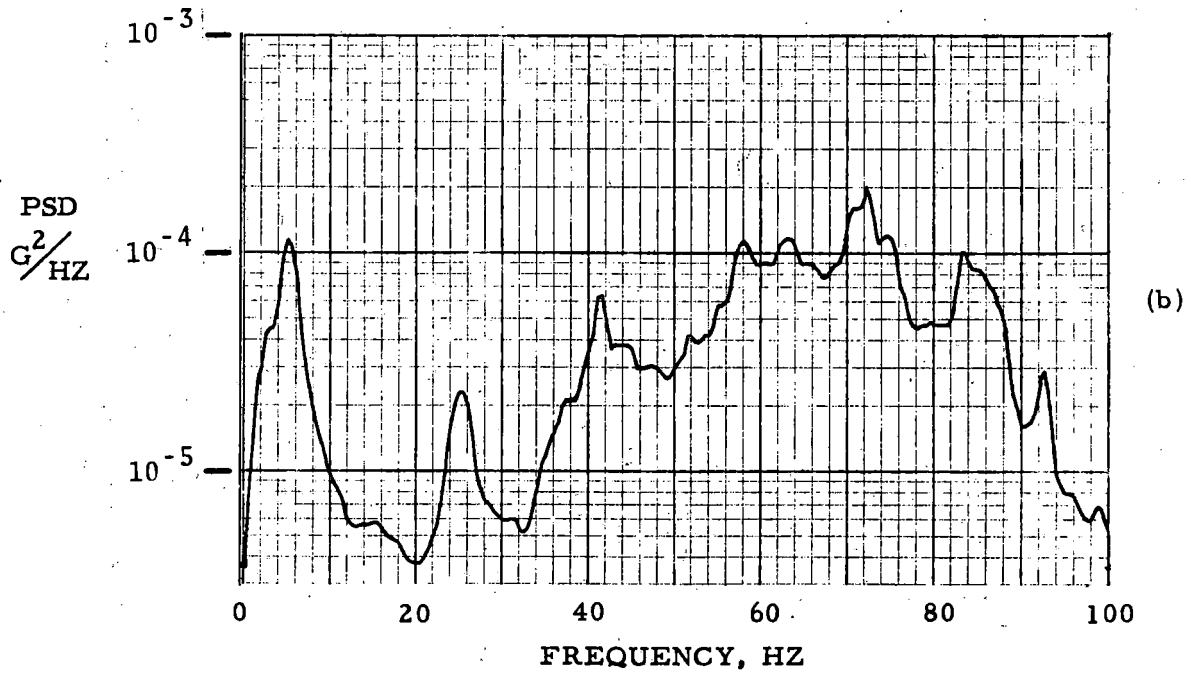

Figure B-8 Acceleration Power Spectral Density, Longitudinal, 55 MPH, DC Vehicle, Truck Pivot, Brook Park to Puritas Station, Eastbound

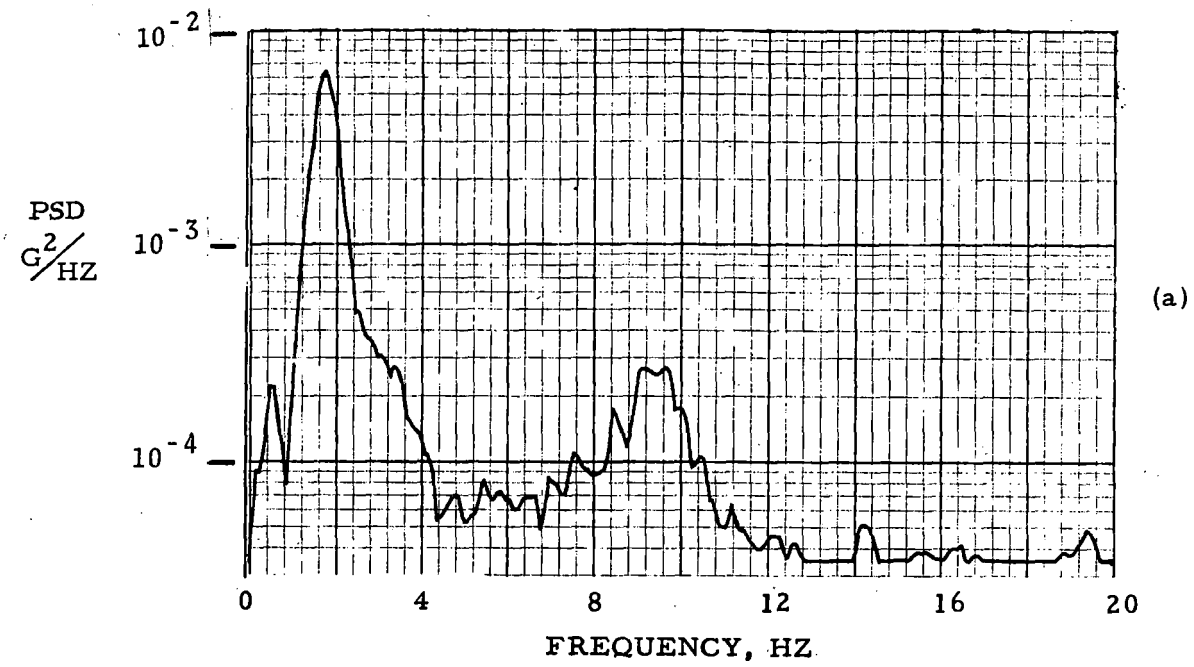

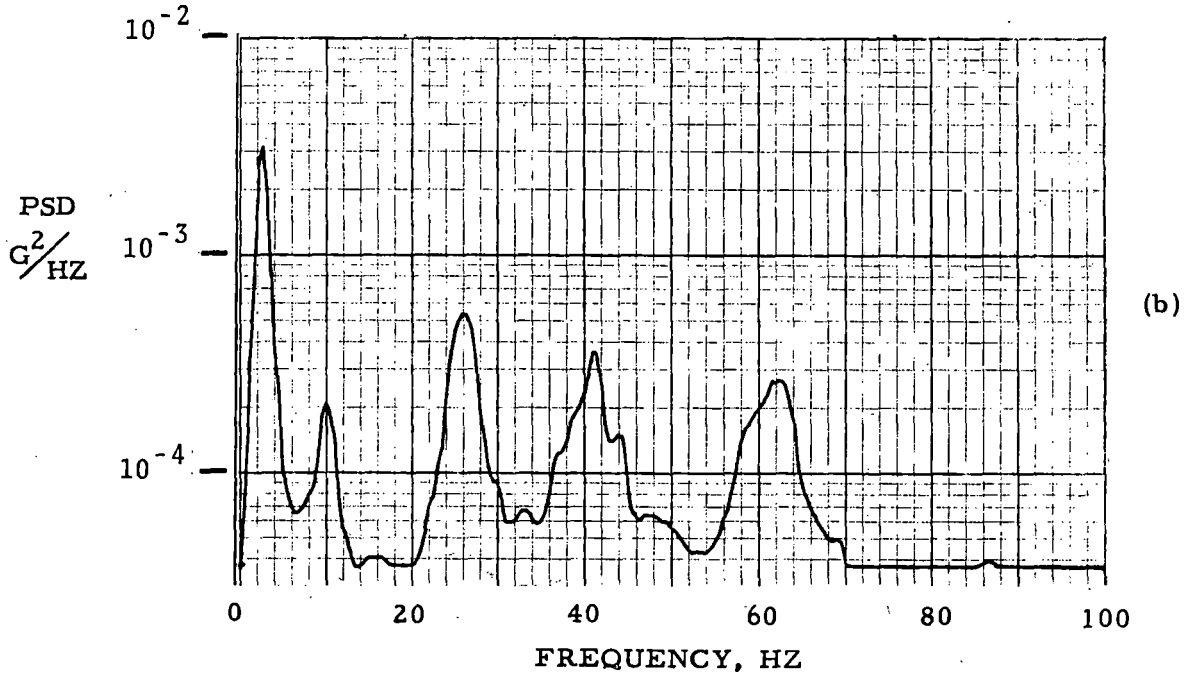

Figure B-9 Acceleration Power Spectral Density, Vertical, 55 MPH, DC Vehicle, Mid-car, Brook Park to Puritas Station, Eastbound

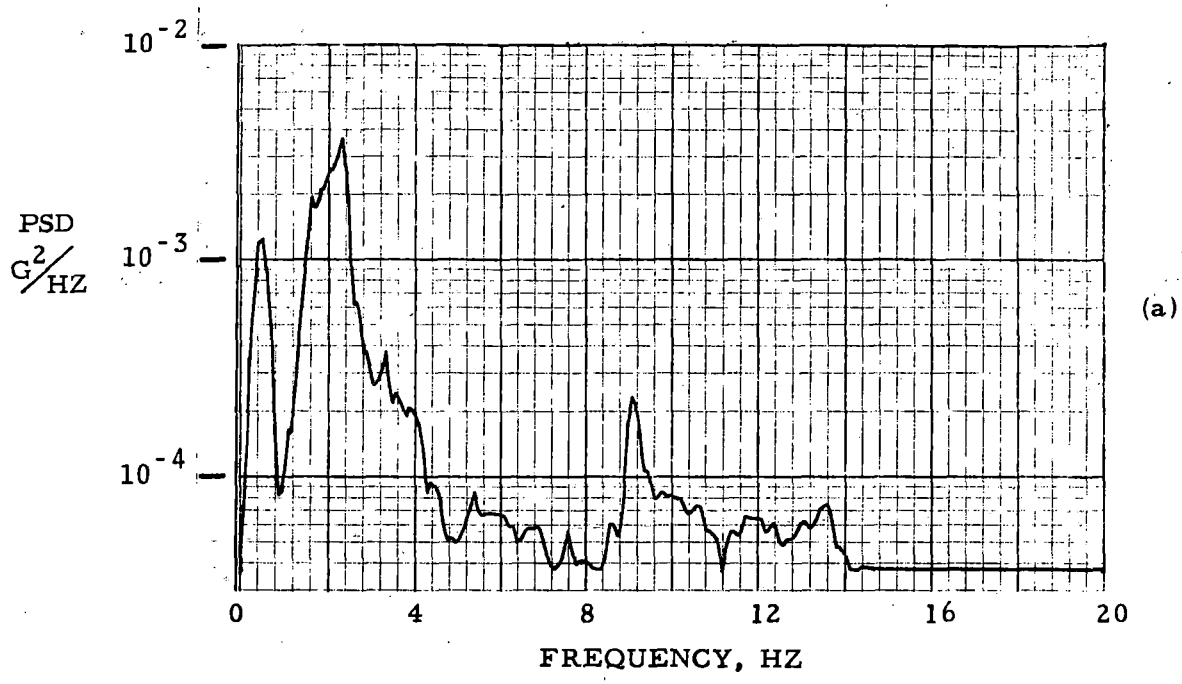

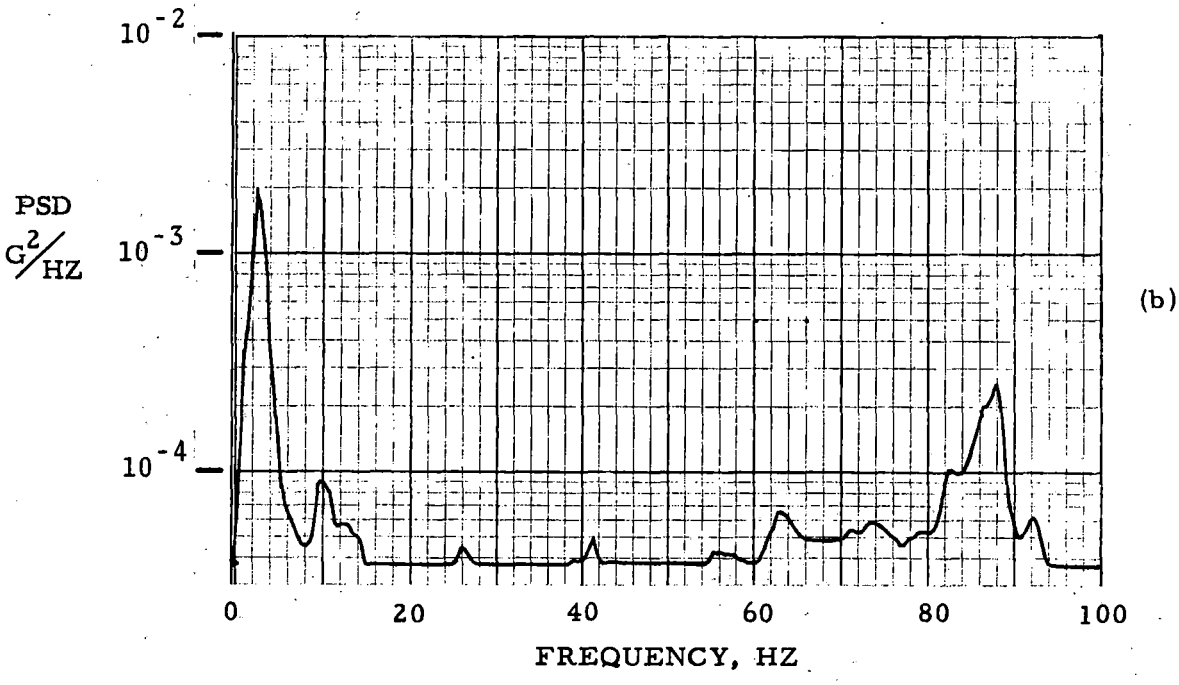

Figure B-10 Acceleration Power Spectral Density, Lateral, 55 MPH, DC Vehicle, Mid-car, Brook Park to Puritas Station, Eastbound

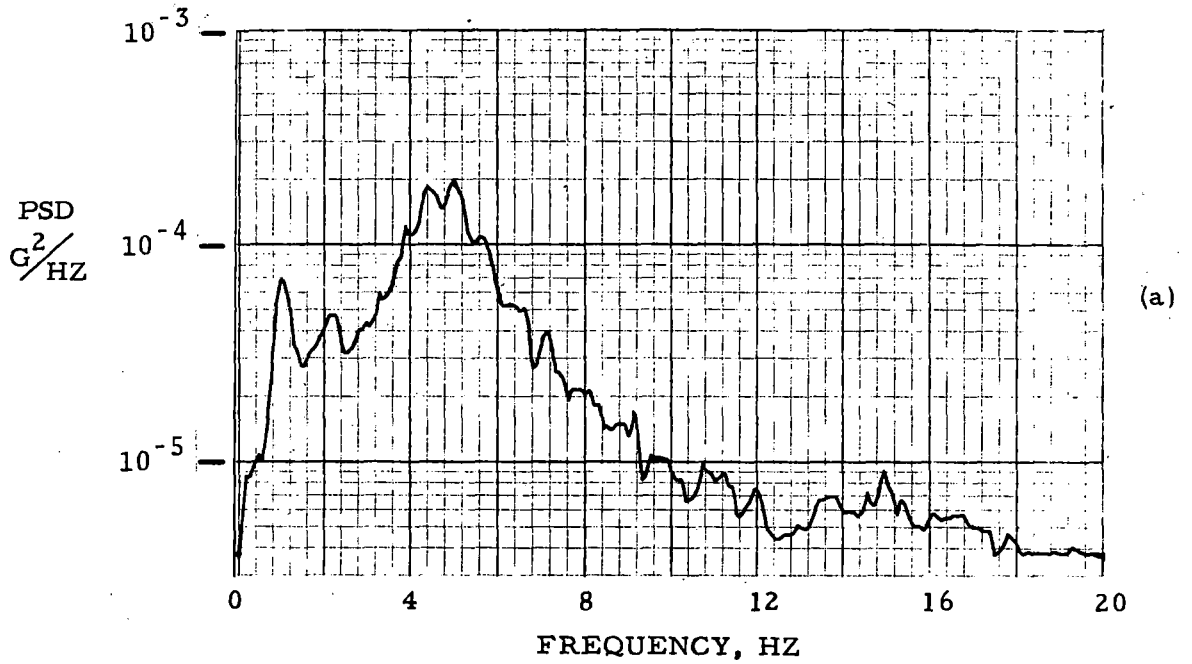

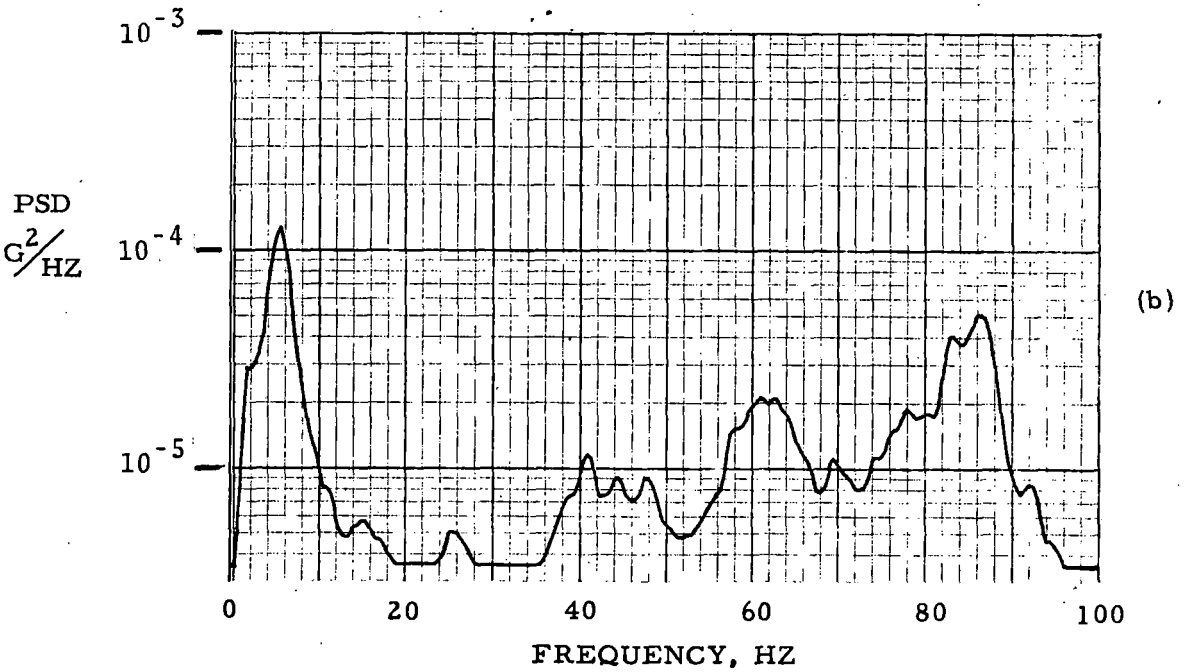

Figure B-11 Acceleration Power Spectral Density, Longitudinal, 55 MPH, DC Vehicle, Mid-car, Brook Park to Puritas Station, Eastbound

APPENDIX C

RIDE ROUGHNESS TESTS

AC VEHICLE WITH CONTROL SYSTEM MALFUNCTION

APPENDIX C

RIDE ROUGHNESS TEST, AC VEHICLE CONTROL SYSTEM MALFUNCTION

Sequence No: 9-73-703

Procedure No: AC-R-5002-CTS

Objective:

To measure vibrations that would be experienced by a passenger near the truck pivot and at mid-car of an AC-propelled transit vehicle.

Status:

A malfunction in the vehicle control system was experienced during the braking cycle. As a result, the collected data were not typical of normal operation. Representative data are presented in this appendix in the form of distance- and time-based stripcharts of the roughness signals.

Test Description:

The test configuration, instrumentation, and procedures used on this AC test vehicle were identical to those described in Appendix A. Car 154 was outfitted with the instrumentation and two round trip runs were completed on Tuesday, September 11, 1973. A malfunction in the vehicle control system caused severe deceleration transients during the approach to several stations. These transients occurred with a repetition rate of about 0.75 hertz. Because of these abnormal transients, the test results were not valid for comparison to other vehicle tests. The AC vehicle was repaired and the test repeated the following week.

Data:

Representative samples of data from this test are shown in Figures C-1 and C-2. Figure C-1 is a distance-based chart with the sensor located near the truck pivot on a westbound run. Control system malfunctions occurred at E79, E55, Downtown, W98, and W117 Stations on this run, as observed on the longitudinal ride roughness plot. Figure C-2 shows the deceleration/acceleration sequence as a function of time at E55 station westbound. The control system malfunction was most severe at this station during this run. The 0.75 hertz component is evident in the longitudinal data.

TEST SEQUENCE: 9-73- 703

DATE: SEPTEMBER 11 , 1973

SITE: CLEVELAND TRANSIT SYSTEM

TIME: 6:47 AM to 7:32 AM

DIRECTION: Westbound

VEHICLE: AC. No. 154

SENSOR LOCATION: Truck Pivot

SIGNAL PROCESSING: Accelerometer signals weighted (filtered) to approximate the human body response to vibration. The resulting signal is processed by a true root-mean-square (RMS) analyzer with a three second RC averaging time constant.

CHART ABSCISSA: Distance

NOTE 1. Ride roughness signals do not always reach zero when the vehicle stops. The movement of passengers and the vibrations of vehicle sub-systems may continue to excite the acceleration sensor.

NOTE 2: At the instant the vehicle wheels lock following deceleration, a large longitudinal acceleration transient is generated.

NOTE 3: The length of the event marks at stations is not significant. These marks were manually activated by the forward observer during the test run.

NOTE 4: The longitudinal scale factor on this chart differs from that on corresponding charts in Appendices A and B.

NOTE 5: The acceleration (RMS, weighted) signal caused by the control system malfunction.

NOTE 6: The deceleration/acceleration sequence at E55 Station westbound is also shown on a time-based chart in Figure C-2.

Figure C-1 Ride Roughness Data

Figure C-1. Ride Roughness Data, AC Vehicle, Truck Pivot, Westbound, Brake Control Malfunction
(See facing page for detailed information)

TEST SEQUENCE: 9-73- 703

DATE: SEPTEMBER 11, 1973

SITE: CLEVELAND TRANSIT SYSTEM, E55 STATION

TIME: 7:00 AM

DIRECTION: Westbound

VEHICLE: AC, No. 154

SENSOR LOCATION: Truck Pivot

SIGNAL PROCESSING: Accelerometer signals weighted (filtered) to approximate the human body response to vibration. The resulting signal is processed by a true root-mean-square (RMS) analyzer with a three second RC averaging time constant.

CHART ABSCISSA: Time

NOTE 1. Ride roughness signals do not always reach zero when the vehicle stops. The movement of passengers and the vibrations of vehicle sub-systems may continue to excite the acceleration sensor.

NOTE 2: The control system malfunction caused the severe accelerations in the longitudinal axis data.

NOTE 3: The bandwidth of the vertical ride roughness weighting filter is wider than the horizontal filter bandwidth. The resulting vertical signal trace displays higher frequency components.

NOTE 4: The acceleration components (approximately 0.05g in magnitude) caused by the normal braking and accelerating of the vehicle are lower in frequency than the low frequency cut-off of the horizontal ride roughness filters. These components, therefore, are attenuated by the filter and do not appear on the data plot.

Figure C-2 Ride Roughness Data

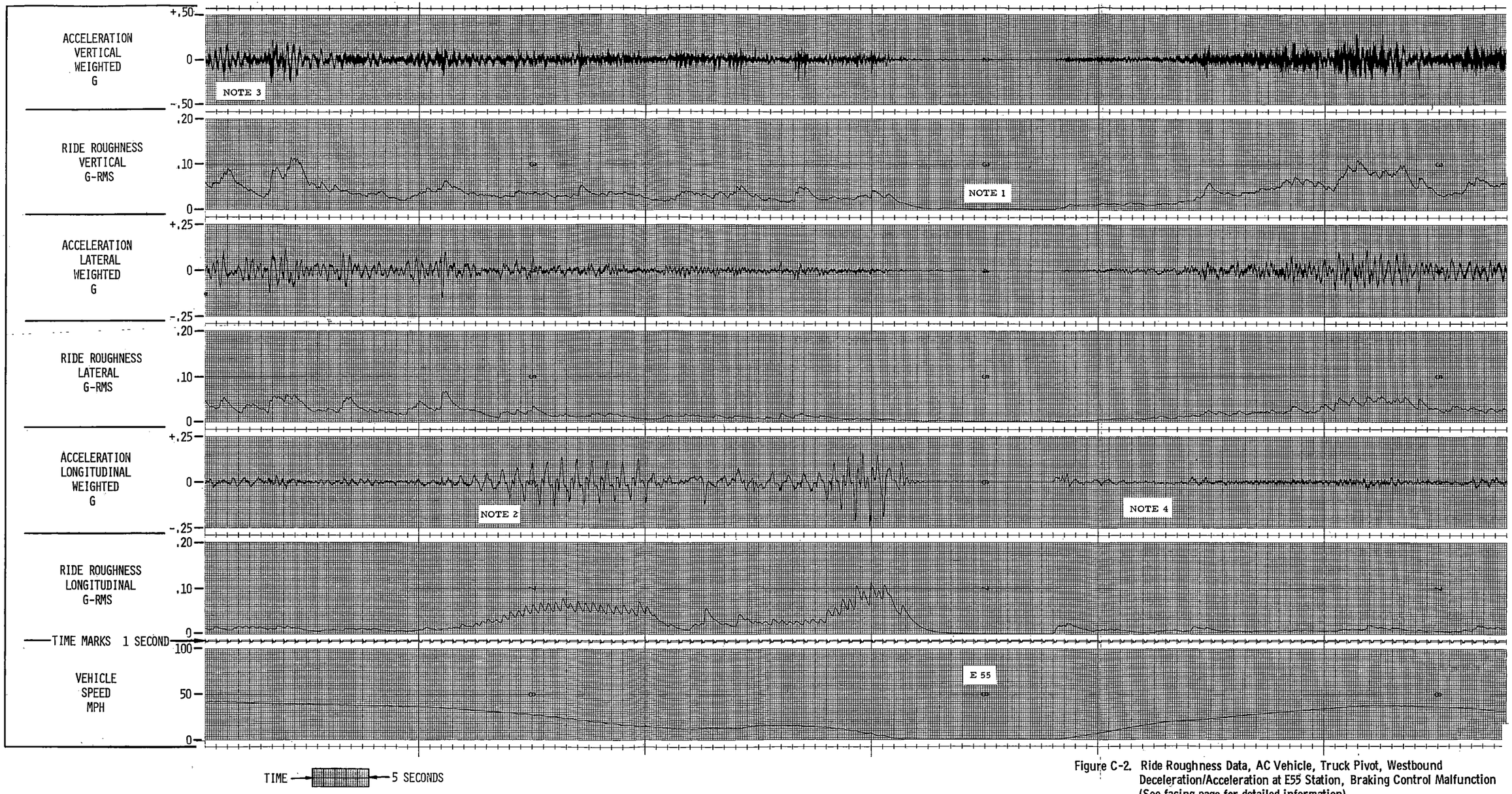

Figure C-2. Ride Roughness Data, AC Vehicle, Truck Pivot, Westbound Deceleration/Acceleration at E55 Station, Braking Control Malfunction (See facing page for detailed information)

APPENDIX D

SYSTEM CALIBRATION

APPENDIX D

SYSTEM CALIBRATION

To maximize the accuracy of the displayed data, the system scale factor for each accelerometer signal was determined. The gain of the chart recorder was then adjusted to compensate for any errors. The system included the sensor, calibration and control unit, tape recorder, tape speed compensation circuits, ride roughness filters (individually calibrated due to AC coupling) and the RMS processors. The largest source of error was in the scaling and buffering operational amplifiers. The input and feedback resistors were not individually matched and linear errors did result. However, by calibrating the chart recorder to the system scale factor, the overall system error was reduced. As a result of this technique, the system error was less than $\pm$ 1.5 per cent.

The calibration procedures for major system components are listed below:

Accelerometer

The two units (prime and back-up) were recently purchased items and had been calibrated by the manufacturer. This calibration was verified by rotating the devices in the earth's field of gravity and noting the sensor output. Small zero-bias errors were disregarded since ride roughness data does not include DC components. The accelerometers contained the optional self-test feature which allows acceleration inputs to be simulated by standard current torquing techniques. The calibration and control unit contains the necessary electronics to simulate a constant acceleration. This calibration signal was recorded on magnetic tape.

Prior to data processing, the data tapes with the calibration signals were monitored. (The constraints of revenue vehicle operation did not always allow calibration). The signals on all tapes agreed to within $\pm$0.8 per cent. This close agreement assures the validity of the data comparisons.

The manufacturers calibration data for the test sensor is given in Figure D-1. In addition, the experimental frequency

PARAMETER	AXIS		
	LONGITUDINAL(x)	LATERAL (y)	VERTICAL (z)
RANGE	± 1 G	± 1 G	± 1 G
+ ONE G OUTPUT	5.000 VDC	5.001 VDC	5.0085 VDC
- ONE G OUTPUT	-5.001 VDC	-5.002 VDC	-4.9745 VDC
VOLTAGE SCALE FACTOR	5.005 V/G	5.0015 V/G	4.9915 V/G
CURRENT SCALE FACTOR	.5379 ma/G	.5566 ma/G	.515 ma/G
ZERO G BIAS	-.0005 VDC	-.0005 VDC	.017 VDC
OUTPUT IMPEDANCE	9.242 K ohms	9.244 K ohms	9.715 K ohms
NATURAL FREQUENCY (9)	537 hz	548 hz	530 hz
DAMPING RATIO	.579	.605	.579
OUTPUT NOISE	.002 V RMS	.0035 V RMS	.004 V RMS
AMPLITUDE RESPONSE	DC->100 hz	DC->100 hz	DC->100 hz

Figure D-1 Manufacturer's Calibration Data, Triaxial Accelerometer, Model 4384/5603, S/N 0109 Systron-Donner

response for each axis is given in Figures D-2 through D-4.

Magnetic Tape Recorder

The FM record/reproduce channels were calibrated using standardized laboratory test instrumentation. The channel gain was set up to IRIG specifications with a maximum input/output variation of 1.0 percent within the passband. Again, small zero bias errors were neglected. The analog record/reproduce channels were similarly calibrated to IRIG standards with particular attention paid to the system frequency response.

Speed and Distance Processor

Since the number of pulses per revolution of the axle-encoder is fixed, the actual distance traveled is a function of the wheel circumference. The circumference was measured prior to testing and the processor was programmed to perform the desired pulse divisions

to furnish the distance output for the chart drive. Speed outputs were calibrated by simulating a given vehicle speed with a pulse generator and adjusting the scale factor of the duty cycle pulse integrator to correspond to the simulated speed. The largest source of error in this system is the round-off error which is less than 1.0 percent for both speed and distance.

Spectrum Analyzer

To verify the amplitude and frequency accuracy of the real time, 200-line spectrum analyzer, calibrated sinusoidal signals were entered into the memory. The signal amplitude was set using an RMS processing module with a calibrated laboratory digital voltmeter. The frequency of the calibration signal was verified by measuring the period on a laboratory counter. On the 20 hertz range, calibration signals of 2, 4, 7, 10, 13, 16, and 19 hertz were analyzed. On the 100 hertz range, the calibration signals were 5 hertz and 10 through 90 hertz in 10 hertz increments. The resultant PSD plots are shown in Figure D-5. A constant error of 0.2 hertz and 1.0 hertz occurs on the 20 hertz and 100 hertz plots, respectively. This error is attributed to a small DC voltage bias in the plotting circuitry.

Instrumentation Noise

Prior to testing, the entire system was operated under simulated conditions and the instrumentation noise within the passbands of interest determined. Both RMS and PSD plots were generated and the measured noise levels were well below one percent of the system full scale signal levels.

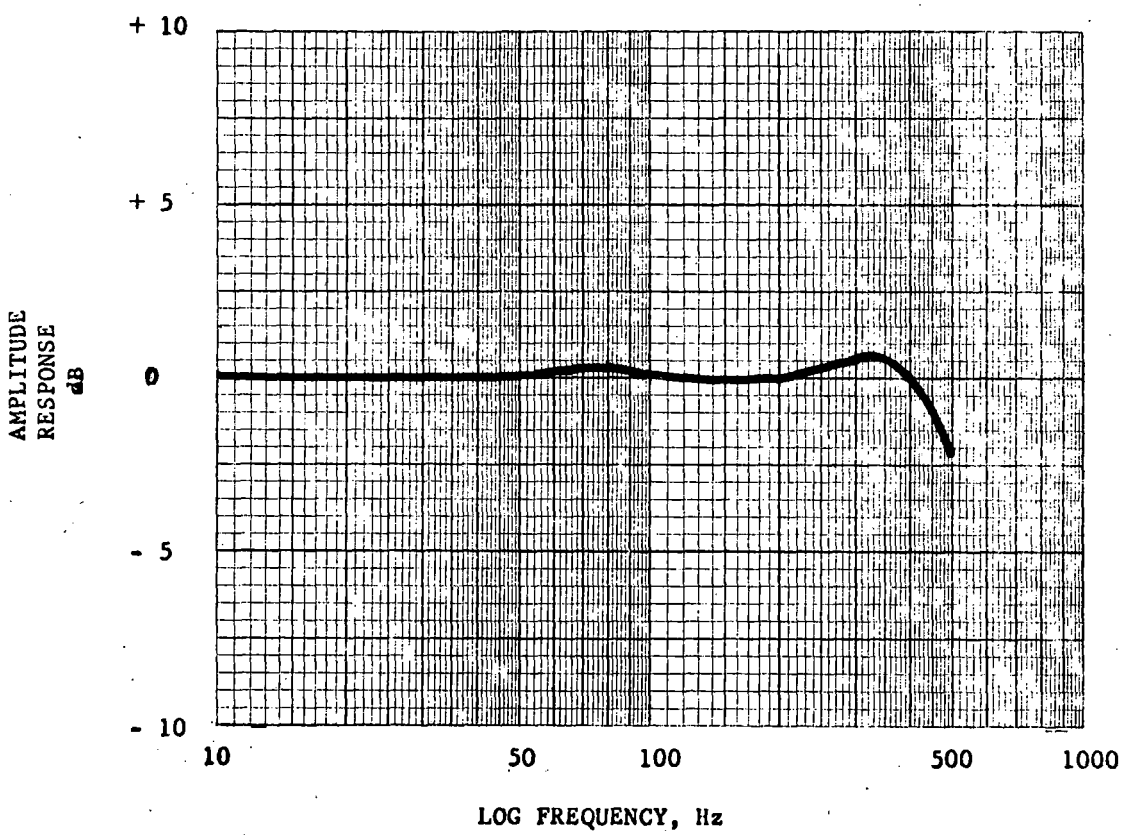

Figure D-2 Accelerometer Amplitude Response, Longitudinal Axis (X)

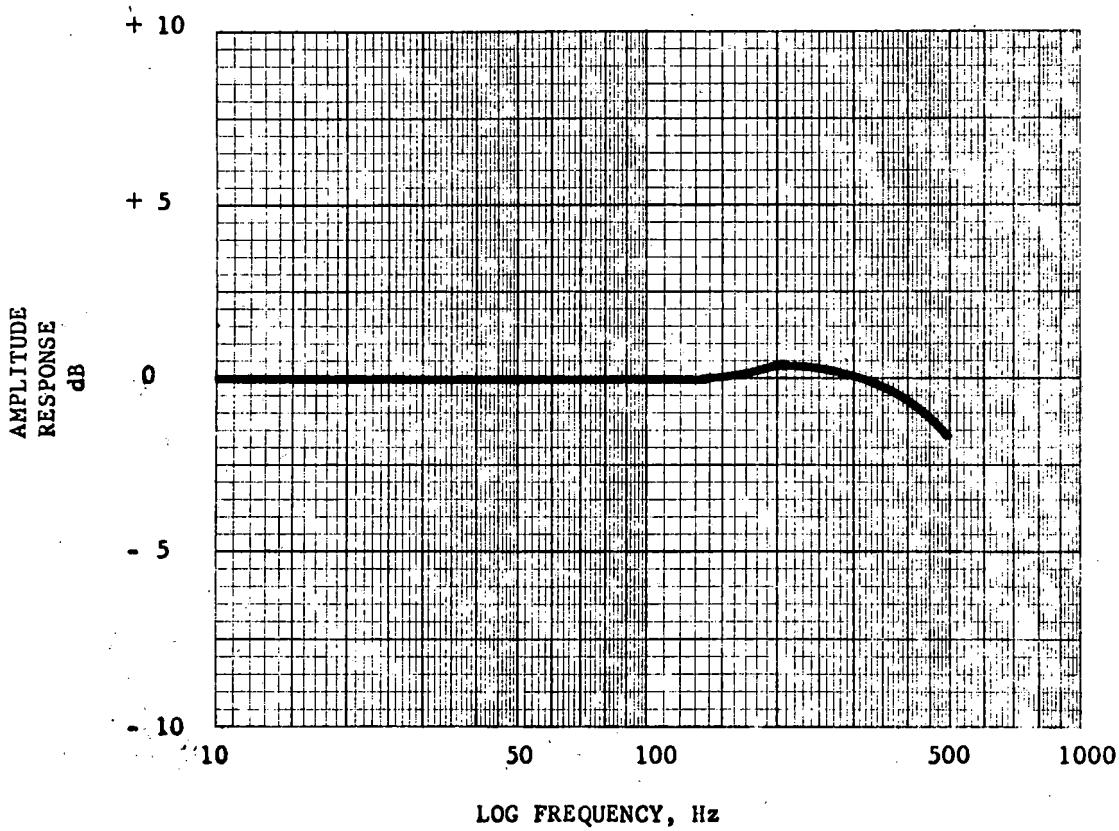

Figure D-3 Accelerometer Amplitude Response, Lateral Axis (Y)

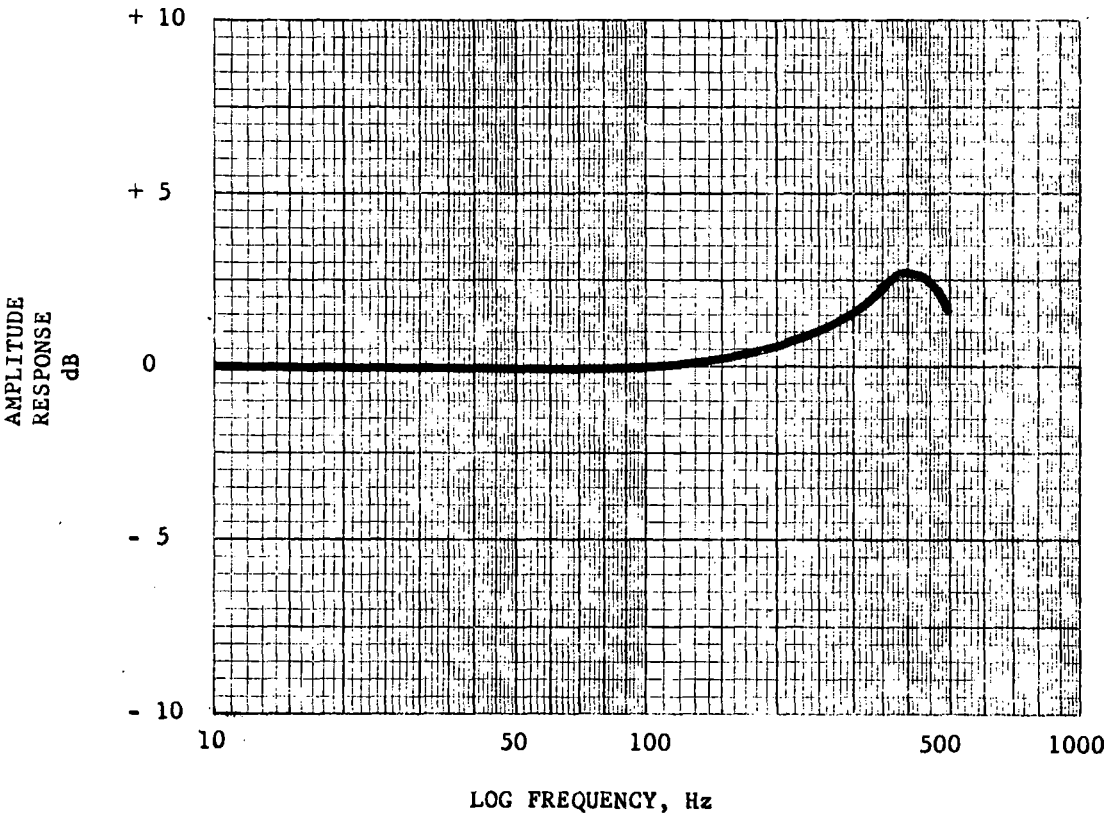

Figure D-4 Accelerometer Amplitude Response, Vertical Axis (Z)

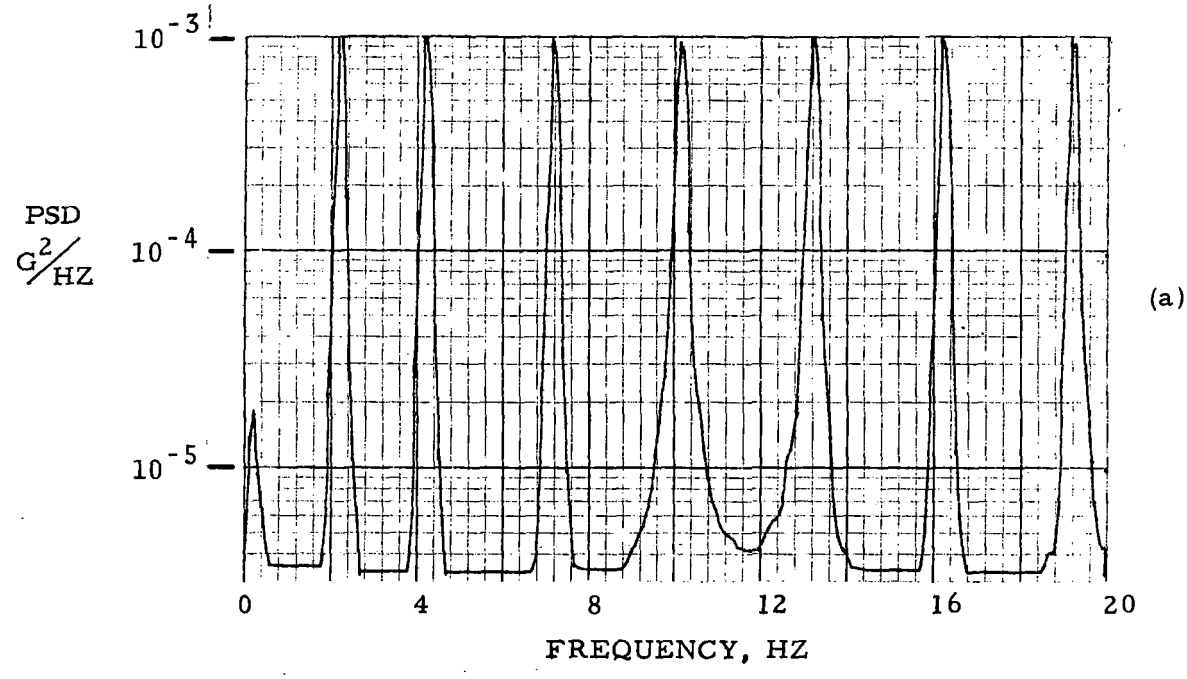

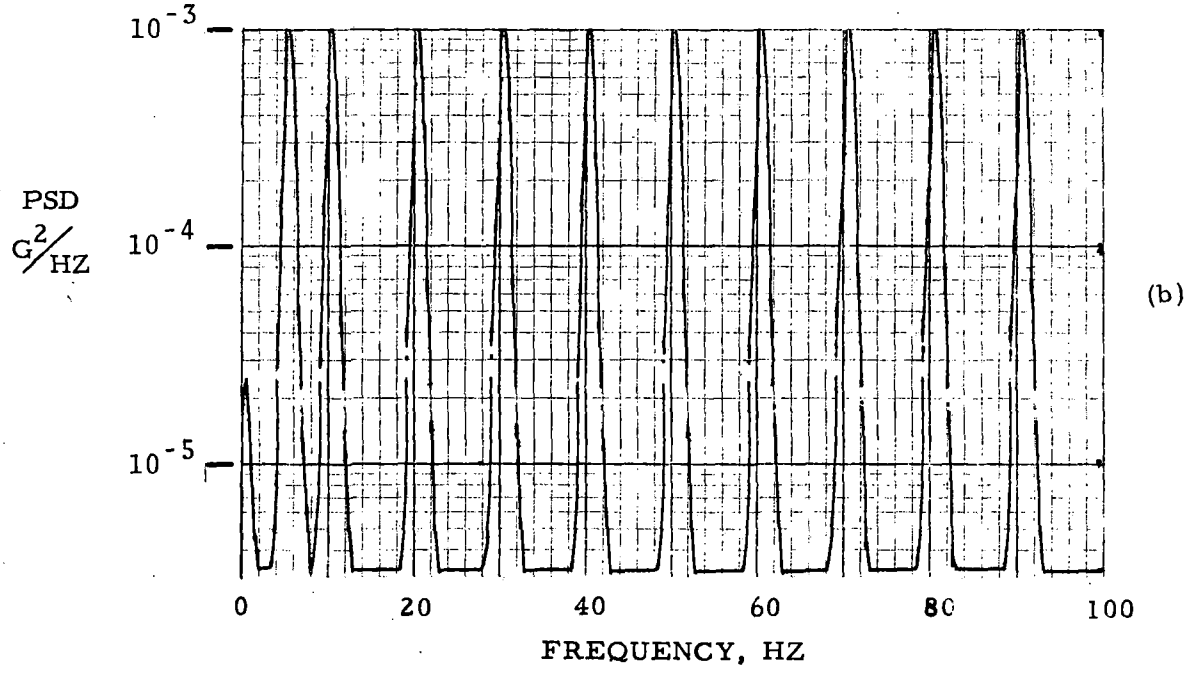

Figure D-5 Spectrum Analyzer Calibration, Simulated Sinusoidal Acceleration, 10^{-3} g^2/hz Full Scale

APPENDIX E

AC PROPULSION SYSTEM DESCRIPTION

APPENDIX E

AC PROPULSION SYSTEM DESCRIPTION

The following technical paper, written by R.T. Bretz of the CTS, was presented at the ATA Rail Transit Meeting, April, 1973. While the paper emphasizes the regenerative characteristics of the AC propulsion system, the total system operation is also described in detail. The paper is reprinted in its entirety with the permission of the author.

CTS EXPERIENCE WITH WABCO REGENERATIVE POWER

Last year at this meeting we described the WABCO PWM DC to AC propulsion system to you and detailed the demonstration program established to prove the viability of this new approach to propulsion in the real world of Cleveland Transit System operations.

The following brief review of the program will serve to refresh your memory:

Six Cleveland Transit System "Airporter" cars are involved in this demonstration.* Three of these are retrofitted with WABCO PWM Propulsion and with the new appearance design. The other three will be treated as a control to assure a valid comparison. Table I shows how each car will be retrofitted.

TABLE I

Car No.	Propulsion	Appearance Design
151	STD	New
152	PWM	New
153	PWM	New
154	PWM	Standard
162	Standard	Standard
163	Standard	Standard

The following major features are being demonstrated:

1. AC Traction Motors - Torque characteristics and reduced maintenance of the three-phase induction motor.
2. Regenerative Brake - General effectiveness, net power reduction, response to line receptivity, blending with friction brake, and reliability. (Preliminary results are the subject of this paper).

*UMTA Demonstration OH-06-006

3. Solid State Continuous Torque Control - Jerk rate limited acceleration and deceleration have been shown. General reliability and maintainability of solid state circuitry are also being demonstrated.

4. Speed Regulation - Precision and smoothness of automatic speed regulated control.

5. Coupled Axle Effect on Wheel Slip - Observations are being made over the demonstration period as to comparative wheel life of PWM-equipped cars and standard Airporters.

6. Compatibility with Communication and Signal Systems - A radio frequency interference test will be performed to establish broad band and discrete frequency emanations from the propulsion system under all modes of operation.

   A signal system interference test will also be performed to determine any possible effects of the Pulse Width Modulated Inverters on the integrity of train protection. Since CTS has both a low frequency (60 HZ) continuous energy signalling system and the more modern audio frequency modulated system, a comprehensive evaluation applicable to all transit systems will be possible.

7. Compatibility with Conventional Cars - Although optimum performance of the PWM Inverter Propulsion System is best demonstrated with a continuous control and the demonstration is presently being operated in this mode, it is recognized that installations requiring some degree of compatibility with present-day cars may be desirable. To this end, the

cars will be modified for compatibility and operated as both lead and trailing cars in trains of standard "Airporters."

8. Improved Passenger Comfort - The continuous envelope control inherent in the WABCO PWM propulsion system will provide a high degree of smoothness which should be registered in improved passenger comfort. To evaluate the significance of this feature, a passenger reaction survey will be made by a professional survey group during the revenue service trial period. Since this survey can also be readily used to evaluate appearance factors in passenger acceptance, the redesigned car interiors will be concurrently evaluated.

Operation

To assist in the understanding of power regeneration as performed by this propulsion system a brief description of the operation is in order.

The WABCO PWM Propulsion System is a torque regulated drive employing AC induction motors in combination with a solid state PWM inverter. Negative torque is provided by regeneration with friction brake backup. The function of the inverter is to convert the 600 volts DC supply voltage to polyphase AC for the motors. All control of speed, traction, and direction is accomplished electronically through the inverter; and without contactors. This combination permits fully proportional control of tractive effort at all speeds during either acceleration or deceleration. During deceleration, part of the kinetic energy of the car can be returned to the power distribution system. This regenerative braking makes possible significant reductions in power consumption and heat rejection which until now have been more matters of conjecture than of fact.

The major devices making up the WABCO PWM Propulsion System are:

- Master Controller
- Logic Unit
- Inverter
- Line Filter
- Reactor
- Auxiliary Control Unit
- AC Traction Motor
- Friction Brake Operating Unit

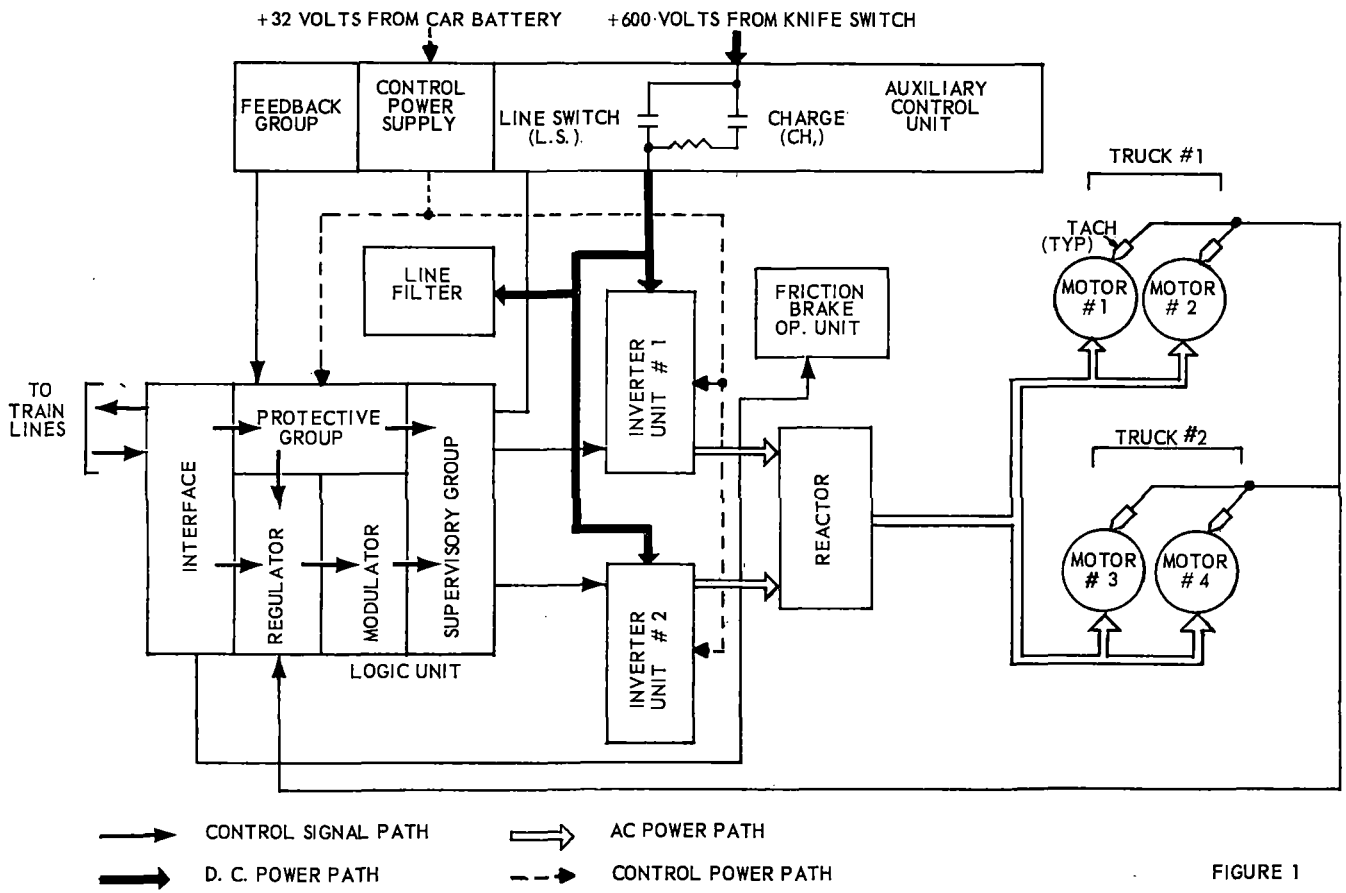
+32 VOLTS FROM CAR BATTERY
+600 VOLTS FROM KNIFE SWITCH
FEEDBACK GROUP
CONTROL POWER SUPPLY
LINE SWITCH (L.S.)
CHARGE (CH,)
AUXILIARY CONTROL UNIT
TRUCK #1
TACH (TYP)
MOTOR #1
MOTOR #2
LINE FILTER
FRICTION BRAKE OP. UNIT
INVERTER UNIT #1
TO TRAIN LINES
PROTECTIVE GROUP
INTERFACE
REGULATOR
MODULATOR
SUPERVISORY GROUP
LOGIC UNIT
REACTOR
TRUCK #2
MOTOR #3
MOTOR #4
INVERTER UNIT #2
CONTROL SIGNAL PATH
AC POWER PATH
D. C. POWER PATH
CONTROL POWER PATH

FIGURE 1

Figure 1 is a block diagram of the WABCO PWM Propulsion System, showing the relationship of the various major devices.

The motors are three-phase, four-pole induction motors with cast aluminum rotor windings. They are self-ventilated. Each motor contains a pulse-type tachometer in one end-bell. The four motors on the trucks are connected in parallel.

The motors are supplied with AC power by the inverter, which is divided into two units of three phases each. Power from these units is combined by the paralleling reactor, which ensures equal load sharing and removes some unwanted harmonic components from the voltage. The inverter units receive DC power from the power distribution system. Capacitors filter the DC supply preventing ripple currents from the inverter from appearing on the distribution system and providing cushioning to enable the system to absorb line transients.

The auxiliary control unit contains three groups of circuitry with the following functions: a DC control group consisting of two contactors which precharge the capacitors and connect the DC power to the inverter; a control power supply which accepts the 32-volt battery voltage and inverts it to AC for distribution to the control circuits in the inverter units and the logic unit; a feedback group which isolates and transmits to the logic unit signals representing DC line voltage, motor currents and voltage, motor overload, and contactor status.

The control signals for the inverter and the control unit are generated by circuitry located in the logic unit. This circuitry can be divided functionally into five groups: the supervisory group which provides proper sequencing for starting, running, and shutting down; the protective group

which monitors critical variables with both limiting and protective shutdown functions; the modulator group which converts input signals representing frequency and voltage into the correct wave forms to operate the motor; the regulator group which monitors motor speed, current, and voltage, and adjusts the modulator inputs to obtain the desired traction; and the interface group which converts the trainline signals to proper form for the other groups. The interface group also generates outgoing signals to the brakes and trainlines.

In an AC induction motor, torque is proportional to slip where slip is defined as the instantaneous difference in speed between the rotor and the rotating magnetic field. If the inverter is controlled so that its voltage is proportional to frequency, then the maximum torque available (due to inverter current limitations) is independent of speed. This type of operation is referred to as "Constant Torque". However, at some frequency the inverter will reach its voltage limitation; and if the frequency is raised further, the motor flux level will decrease in inverse proportion with the frequency. The torque available at the inverter's maximum current will also decrease inversely with speed. This type of operation is referred to as "Constant Horsepower".

To maintain the motor current as the flux decreases in constant horsepower operation, it is necessary to increase the motor slip. This is possible only to a value of 3%. Once the maximum motor slip is reached, both flux and current will decrease inversely with speed, so that torque decreases inversely with the square of speed. This type of operation is referred to as "Slip Limited".

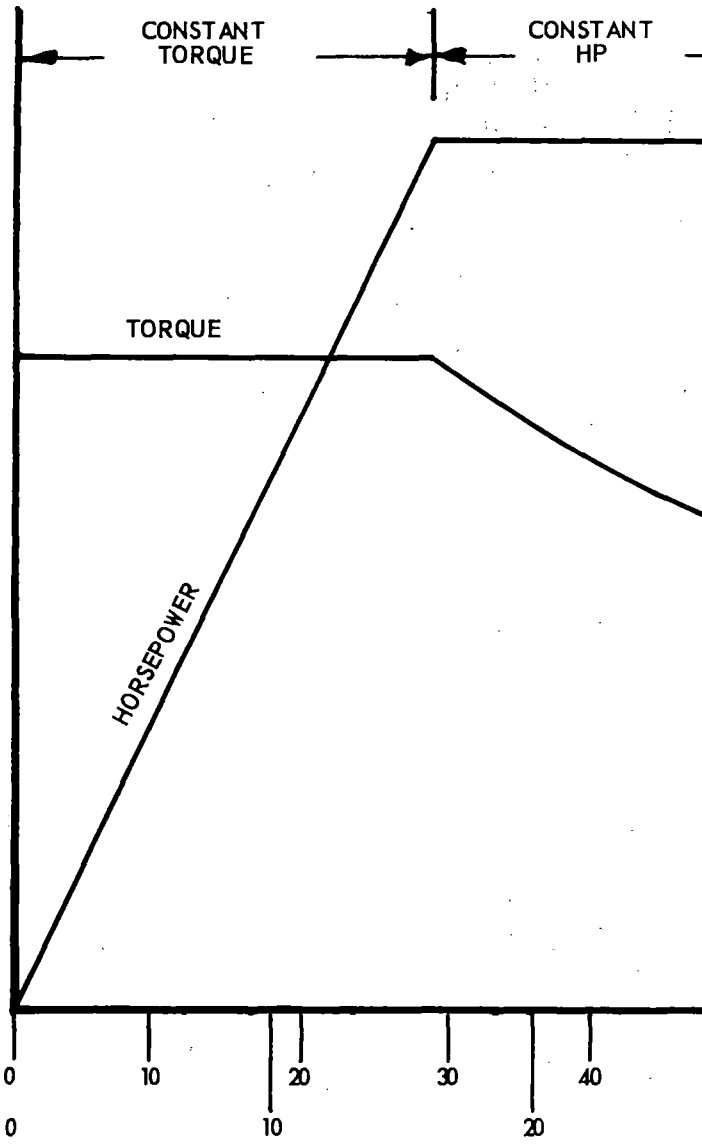
CONSTANT
TORQUE
CONSTANT
HP
TORQUE
HORSEPOWER
0
10
20
30
40
0
10
20

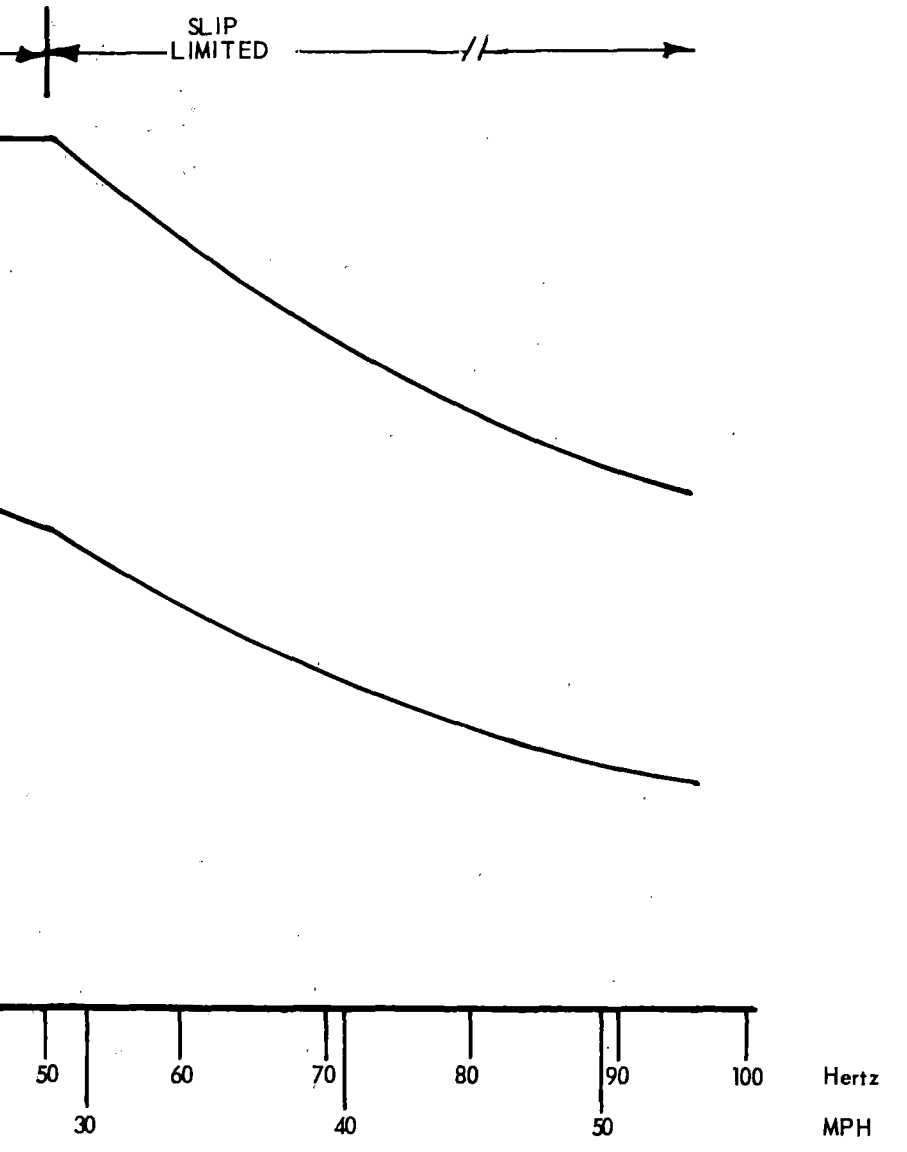

FIGURE 2

Typical range of frequency (speed) in each mode of operation is as follows:

Constant Torque	-	1 to 32 Hz 0 to 18 mph
Constant Horsepower	-	32 to 50 Hz 18 to 28 mph
Slip Limited	-	Above 50 Hz Above 28 mph

These characteristics are illustrated in Figure 2.

To provide positive tractive effort (motoring) the logic adjusts frequency so that motor slip is positive. That is, speed of the rotating field is slightly greater than that of the rotor. To provide negative tractive effort (regenerative brake) the logic adjusts frequency so that slip is negative or lagging. The motor now acts as an induction generator. Since the negative torque produced by an induction generator is a function of slip, as opposed to terminal voltage, it is possible to provide highly effective regenerative braking to speeds as low as 2 mph. A voltage limiting circuit prevents regenerative voltage from exceeding power distribution system maximums. This entire operation is effected with static devices; no line contactors are involved.

If line receptivity limits the negative torque which can be produced by regenerative braking, the fully integrated friction brake control senses this difference and applies sufficient friction brake to assure that the negative torque demand is met.

Line Receptivity

Having established the feasibility of the propulsion systems ability to generate power, the effectiveness then

becomes a function of the distribution of the regenerative trains in the system and the total line load. The receptivity of the line is affected by the parameters of the present substations, but is primarily a function of the actual energy load of the catenary. Present power distribution system design philosophy locates the substations at points along the right-of-way where the trains accelerate, i.e., at the stations. This is fine for non-regenerating systems but is less than optimum for the case of the rolling substation presented by trains which regenerate.

With known regeneration available, spacing of the substations can be adjusted because regenerating points will be statistically scattered to help support the load with a longer separation between substations. Another intriguing possibility is a substation capable of absorbing energy; this would lift a basic restriction of regeneration. Once the load on a line is surpassed, regeneration can no longer produce power savings and energy can be absorbed only in dynamic braking. It is entirely possible to simplify transit car equipment by moving the dynamic brake grids to the substations. Certainly less total resistance will be required and the heat generated will be rejected outside the subway tunnel, thus reducing tunnel ventilation load. A further refinement would be an inverting substation capable of returning energy to the AC feeder lines. This is technically possible at present and increasing power costs may make it economically feasible in the near future. In this instance the load available for regeneration becomes almost infinite being limited only by line impedence. In any case, good power system planning must be used to make full use of regeneration.

Regenerative Capabilities

After considering the line load or receptivity, some discussion of the regenerative characteristics of the PWM Inverter is in order.

Regeneration can become the design criteria for a system inasmuch as braking horsepower usually far exceeds propulsion horsepower. The inverter itself is current and voltage limited. As installed on the CTS Airporters it will provide a peak regenerative current of around 1200 amps per car and an upper voltage limit of 720 VDC. This upper voltage limit is the same as that of the substation. To elevate the voltage any more runs the risk of damaging other equipment on board. There are refinements of this design which might allow higher utilization but at the expense of simplicity.

At any given location on the CTS line, only a fixed level of energy can be absorbed at any given time. If more than one regenerative car is operating in a train, that train can only return to the line the level of energy that the line is capable of absorbing at that point.

To place total system regenerative capability in perspective, it is obvious that vehicles will regenerate only when braking. It is therefore very important to consider the actual time ratio in which the vehicle is braking. For this reason, you will note in the slides which follow that the date summary lists the times for each operating mode. A high ratio of brake to acceleration and running time will always provide the best power savings.

The regeneration being demonstrated on CTS is not speed dependent and can deliver effective retardation down to two mph. There are no extended line gaps on CTS, however, tests have

shown the system to be capable of sustaining the vehicles auxiliaries without being in contact with the catenary down to a speed of two mph.

Blending

With the limitations imposed on regeneration outlined above, it is necessary to blend dynamic braking and pneumatic braking to insure smooth control of the vehicle. Summing methods similar to those used in electronic brake control are used for this purpose. During the brake mode, a continuous feedback of negative motor torque is provided to the blending system which balances it against the brake demand. As long as the demand is satisfied by regeneration, as evidenced by the torque feedback, no other form of braking is applied. If the demand is not satisfied, however, the deficit is immediately made up by friction brake, and if the friction brake level reaches a predetermined value (30 psi) the dynamic brake grid is inserted in series with the 600 volt line. This creates a local load on the line and motor torque can now increase again. This, in turn, permits friction brake to be reduced. Experience in Cleveland has shown that even in three-car train service there is little need for the resistor grid; and, in many applications, it could probably be omitted without a serious increase in brake shoe or wheel wear.

Reliability

The reliability for this type of regeneration is equal to that of the propulsion system. This is due to the fact that regeneration is inherent to this system. Under this condition, so long as the propulsion package is functional, so is regeneration.

Regeneration Performance on Cleveland Transit System

While the final proof of performance is always the car itself, it is possible, using real data inputs to generate a computer simulation of car performance virtually duplicating the actual car. The advantage of this approach is a high level of flexibility through the full control of the independent variables with a consequent major savings in time over trying to run all of these conditions on the line. Figure 3 is a data summary print-out of an actual test run as recorded by the On-Car data acquisition center and reduced by the WABCO Data Center. Figure 4 is a print-out of a computer simulation of a CTS Airporter. The simulation includes such parameters as size and weight, rolling resistance, system efficiency, characteristics, and the specific line profile. Each line represents the precise performance of the car at a particular point in the simulated run. At the bottom of the print-out, a summary of pertinent results appears indicating time in power and brake, total power consumption, regenerated power, net power consumption, and KWHR/car mile. To run a simulation like this consumes about 20 minutes including the time required to punch in the variables.

Figure 5 is shown as verification of the simulation. The solid lines are speed and power as a function of distance generated by the simulation. The plotted points are actual data for a duplicate run performed by CTS Car 154. From this, it is apparent that the simulation is valid for the cars in question.

The PWM powered cars out-perform the standard car by a measurable amount. To provide a valid comparison of the two, it is therefore necessary to degrade the PWM performance until both are equal. While this will be done to the actual cars

SUMMARY OF RUN FROM 16.24 TO 0.16 (16.08 MILES)

POWER SUMMARY

KWHRS/MILE CAR WEIGHT= 72800.

USED	5.42
REGEN	1.97
NET	3.46

PCT REG=36.3

AVERAGE P-WIRE(POS,NEG)= 2.86,-1.48 AVERAGE RATE(POS,NEG)= 1.27,-1.03

TIME SUMMARY

MODE	TIME(MIN)	PERCENT
POWER	15.121	45.5
REGEN	8.131	24.5
COAST	9.964	30.0
TOTAL	33.215	

TOTAL ELAPSED TIME= 41.0

SPEED SUMMARY

SPEED	TIME(MIN)	PERCENT
0	2.853	8.6
0-10	4.660	14.0
10-20	5.014	15.1
20-30	2.975	9.0
30-40	5.047	15.2
40-50	7.053	21.2
50-60	5.611	16.9
60-70	0.000	0.0

AVERAGE HP/MOTOR (AT MOTOR SHAFT)= 72. RMS HP=105.
AVERAGE INVERTER CURRENT= 363. RMS CURRENT= 535.
AVERAGE INVERTER EHP= 288. RMS EHP= 416.

AVERAGE SPEED(ACTIVE)= 31.7 AVERAGE SPEED(OVERALL)= 29.0

PWM TRANSIT CAR SIMULATION

WHEEL DIA(IN),CAR WT(LBS),EQ WT ROT PARTS,# AXLES?28,72800,0,4

PRINT INTERVALS(3),DWELL TIME?1,1,1.20

NO. OF MOTORS,CAR FRONTAL AREA,NO. OF CARS?4,100,1

GEAR RATIO,GEAR EFF,MAX ACCEL RATE?6.21,.95,2.8

DISTANCE RUN OR MAX SPEED(1 OR 2)?2

MAX SPEED?55.4

NO. OF GRADE CHANGES?0

CONSTANT DECEL. RATE?(1=YES,2=NO)?1

DECEL. VALUE?-3.5

FILE NO.,JERK LIMIT,MIN VOLT.,MAX VOLT.?1,1.5,590,670

CALC TIME INCREMENT?.25

STOP NUMBER 1

TIME SEC	SPEED MPH	ACCEL MPHPS	GRD PCT	DIST FT	MOTOR RPM	RES'T LB/TN	MTORK FTLBS @MS	HP/ MOTOR @MS	TOTAL HP @RAIL	INV AMPS /CAR
1.0	0.7	1.50	0.	0.	56.	4.5	278.	3.	11.	80.
2.0	3.0	2.30	0.	2.	220.	4.7	422.	18.	67.	263.
3.0	5.4	2.59	0.	8.	405.	4.9	475.	37.	139.	382.
4.0	8.1	2.71	0.	18.	601.	5.3	497.	57.	216.	473.
5.0	10.8	2.81	0.	32.	806.	5.7	515.	79.	301.	564.
6.0	13.6	2.83	0.	50.	1016.	6.3	521.	101.	383.	647.
7.0	16.5	2.85	0.	72.	1228.	7.0	526.	123.	467.	737.
8.0	19.3	2.88	0.	98.	1442.	7.8	532.	146.	555.	837.
9.0	22.2	2.89	0.	129.	1657.	8.7	536.	169.	642.	946.
10.0	25.1	2.76	0.	164.	1869.	9.8	515.	183.	696.	1014.
11.0	27.8	2.64	0.	202.	2072.	10.8	495.	195.	742.	1080.
12.0	30.4	2.53	0.	245.	2265.	11.9	476.	205.	781.	1143.
13.0	32.8	2.35	0.	291.	2449.	13.1	447.	208.	792.	1171.
14.0	35.1	2.17	0.	341.	2620.	14.2	416.	207.	788.	1179.
15.0	37.2	1.99	0.	394.	2776.	15.3	386.	204.	775.	1173.
16.0	39.2	1.82	0.	450.	2920.	16.4	358.	199.	755.	1156.
17.0	40.9	1.68	0.	509.	3052.	17.4	334.	194.	737.	1138.
18.0	42.6	1.56	0.	570.	3174.	18.3	313.	189.	719.	1122.
19.0	44.1	1.44	0.	634.	3287.	19.3	295.	184.	700.	1100.
20.0	45.5	1.34	0.	700.	3391.	20.2	277.	179.	680.	1076.
21.0	46.8	1.25	0.	767.	3489.	21.0	262.	174.	662.	1053.
22.0	48.0	1.17	0.	837.	3579.	21.8	249.	170.	645.	1031.
23.0	49.1	1.09	0.	908.	3664.	22.6	237.	165.	628.	1007.
24.0	50.2	1.02	0.	981.	3743.	23.4	226.	161.	611.	982.
25.0	51.2	0.95	0.	1055.	3818.	24.1	215.	156.	593.	957.
26.0	52.1	0.89	0.	1131.	3887.	24.7	205.	152.	577.	933.
27.0	53.0	0.85	0.	1208.	3952.	25.4	199.	149.	568.	919.
28.0	53.8	0.81	0.	1287.	4015.	26.0	192.	147.	558.	904.
29.0	54.6	0.77	0.	1366.	4074.	26.6	186.	144.	549.	889.
30.0	55.4	0.73	0.	1447.	4130.	27.2	180.	142.	539.	874.
30.2	55.6	0.72	0.	1467.	4144.	27.3	179.	141.	537.	870.

* * BRAKING * *

TIME SEC	SPEED MPH	ACCEL MPHPS	GRD PCT	DIST FT	MOTOR RPM	RES'T LB/TN	MTORK LB FT @MS	HP/ MOTOR @MS	TOTAL HP/CAR @RAIL	FRICT HP/CAR @RAIL	INV AMPS /CAR
30.5	55.6	0.35	0.	1467.	4144.	27.3	101.	79.	334.	0.	276.
31.5	55.4	-1.15	0.	1549.	4127.	27.2	-143.	-112.	-474.	-0.	-391.
32.5	53.6	-2.65	0.	1629.	3999.	25.9	-389.	-296.	-1247.	-0.	-1033.
33.5	50.5	-3.50	0.	1706.	3765.	23.6	-530.	-380.	-1600.	-0.	-1334.
34.5	47.0	-3.50	0.	1777.	3504.	21.2	-534.	-356.	-1500.	-0.	-1262.
35.5	43.5	-3.50	0.	1843.	3243.	18.9	-538.	-332.	-1398.	0.	-1187.
36.5	40.0	-3.50	0.	1905.	2982.	16.8	-541.	-307.	-1293.	-0.	-1108.
37.5	36.5	-3.50	0.	1961.	2721.	14.9	-544.	-282.	-1187.	0.	-1024.
38.5	33.0	-3.50	0.	2012.	2460.	13.1	-547.	-256.	-1079.	-0.	-932.
39.5	29.5	-3.50	0.	2058.	2199.	11.5	-550.	-230.	-969.	0.	-832.
40.5	26.0	-3.50	0.	2098.	1938.	10.1	-552.	-204.	-857.	0.	-724.
41.5	22.5	-3.50	0.	2134.	1677.	8.8	-554.	-177.	-745.	0.	-608.
42.5	19.0	-3.50	0.	2164.	1416.	7.7	-556.	-150.	-631.	0.	-486.
43.5	15.5	-3.50	0.	2189.	1155.	6.8	-557.	-123.	-516.	0.	-363.
44.5	12.0	-3.50	0.	2210.	894.	6.0	-559.	-95.	-400.	0.	-244.
45.5	8.5	-3.50	0.	2225.	633.	5.3	-560.	-67.	-284.	0.	-137.
46.5	5.0	-3.50	0.	2235.	372.	4.9	-561.	-40.	-167.	-0.	-53.
47.5	1.5	-3.50	0.	2239.	111.	4.6	-561.	-12.	-50.	0.	-5.

ACCUMULATED DISTANCE= 2240. FT= 0.42 MILES
DISTANCE THIS RUN= 2240.FT= 0.42 MILES
ACCUMULATED TIME= 68.0 SEC = 1.1 MIN
TIME THIS RUN= 48.0 SEC
MAX SPEED ATTAINED=55.57 MPH
AVERAGE SPEED=31.81 MPH

POWER SUMMARY FOR THIS RUN

	KWHRS	KWHRS/MILE
POWER USED	4.39	10.34
REGENERATED	2.17	5.11
NET	2.22	5.23
MECH OUTPUT(ACC)	3.49	8.22
LOSSES	0.90	2.12
MECH INPUT(BRK)	2.96	6.98
LOSSES	0.79	1.87

PCT REGEN=49.4
OVERALL EFF(ACC)=79.5
OVERALL EFF(BRK)=73.2

RMS HORSEPOWER FOR THIS RUN
(CONTINUOUS DUTY

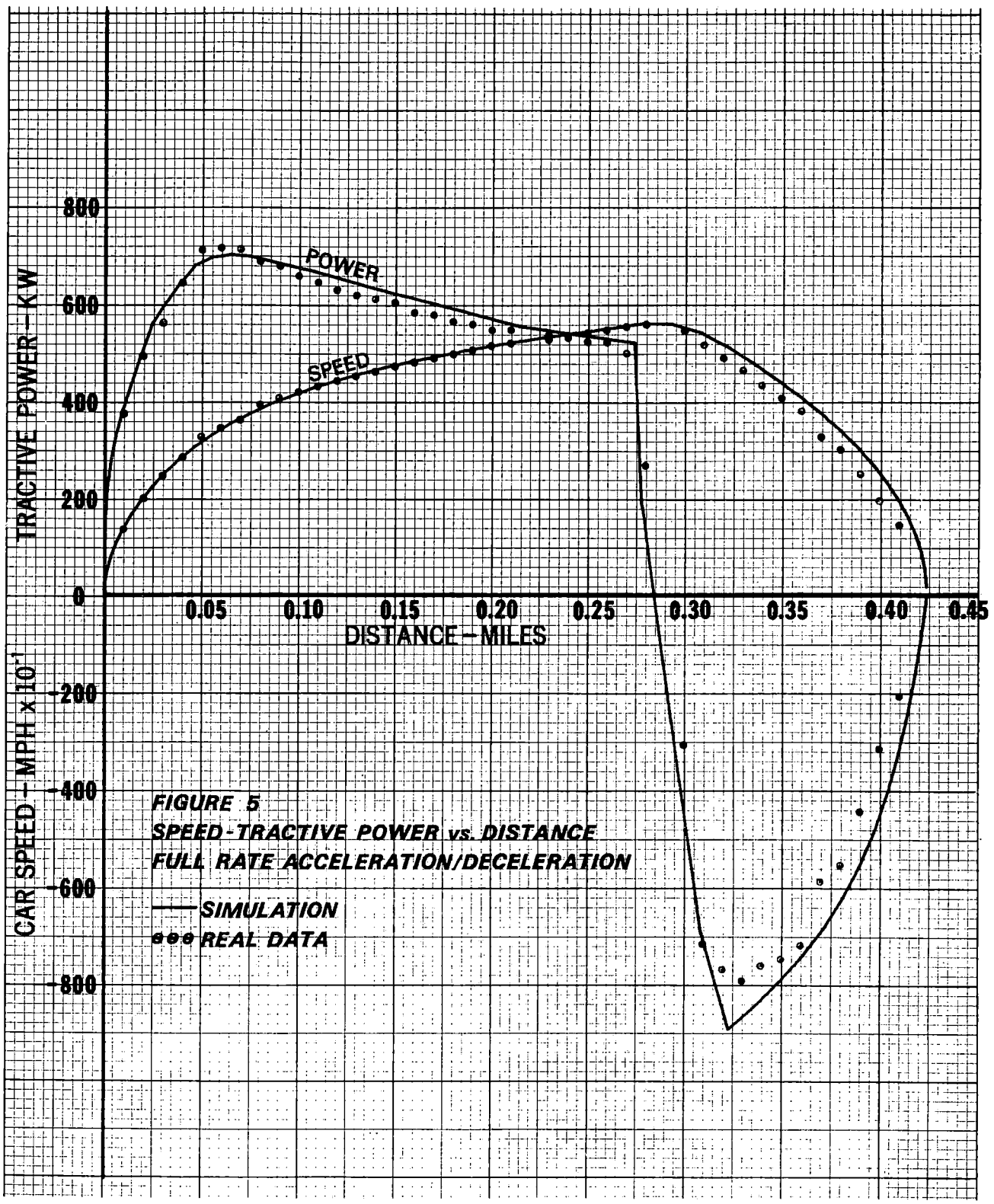

FIGURE 5
SPEED-TRACTIVE POWER vs. DISTANCE
FULL RATE ACCELERATION/DECELERATION

——*SIMULATION*
o o o *REAL DATA*

during the compatibility tests later in the demonstration, the computer simulation provides a quick and accurate method available to us immediately. Figure 6 shows such a simulation for a degraded PWM powered car in direct comparison with actual data from a standard powered car. The solid lines represent the PWM car simulation and the broken lines are actual performance of the cam control car. The net power savings are readily apparent and amount to 49.6% in this particular case.

The preceding curves present the case for a full rate acceleration with an immediate stop representing station spacing of less than half a mile. Similar data for a run between two stations on the CTS Airport line, Triskett to West Park, are shown on Figure 7. The station spacing in this case is slightly more than 0.8 miles. Figure 7 is generated from real car data with full performance available. As can be seen, the power consumed during the period of relatively constant speed operation adds to the acceleration power and so detracts from the regeneration savings.

All that has been shown here is for the single cars since more data are available in this area. The cars are running in multiple unit service, however, and regenerate successfully in this mode as well. When the line will not accept the full regenerative output of the train, the cars share the available load equally. Kilowatt hour per car mile numbers are being continuously generated by the demonstration cars and a statistical evaluation will be available for 12 months of operation in early 1974.

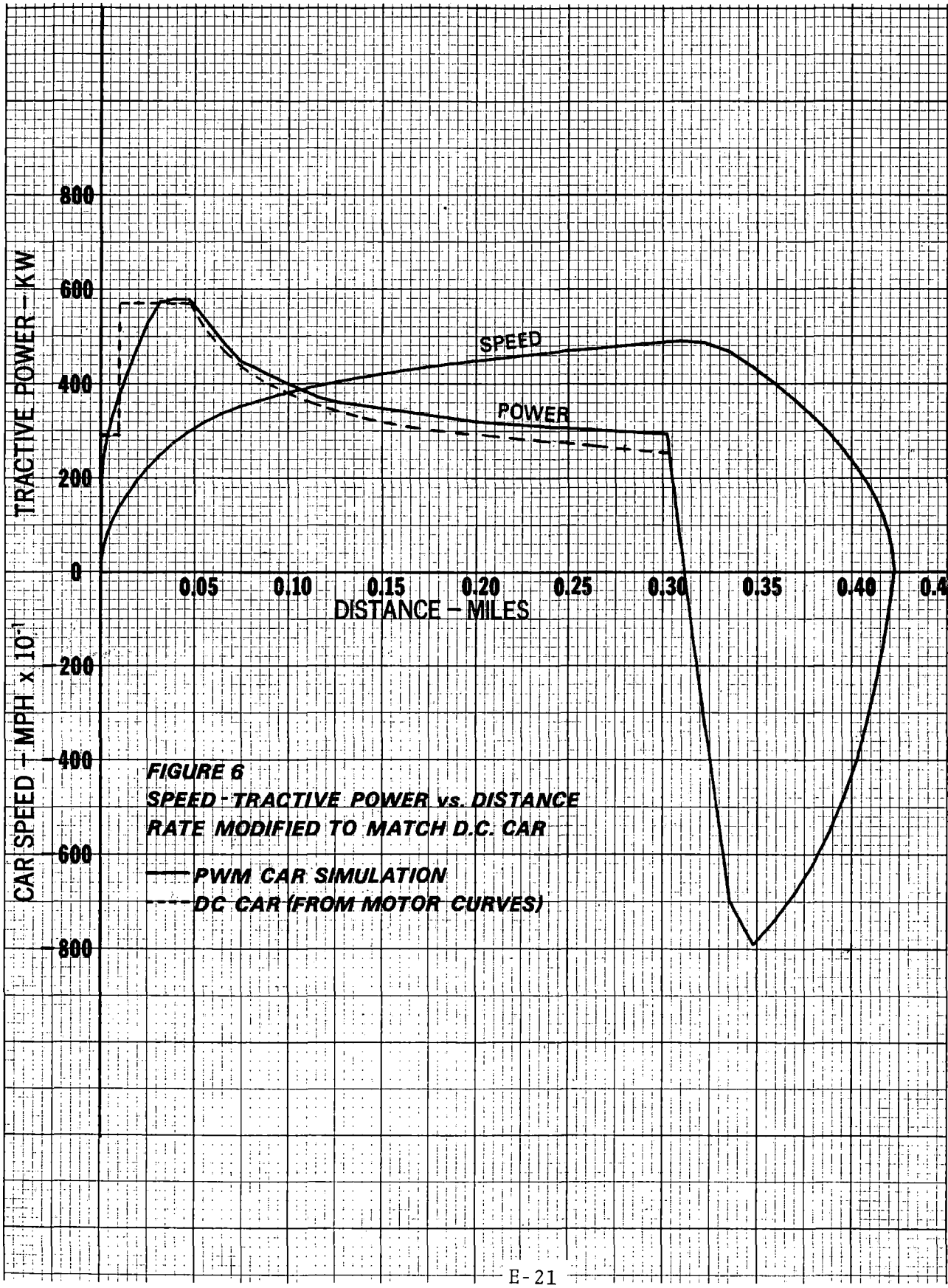

FIGURE 6
SPEED - TRACTIVE POWER vs. DISTANCE
RATE MODIFIED TO MATCH D.C. CAR

——— *PWM CAR SIMULATION*
- - - - *DC CAR (FROM MOTOR CURVES)*

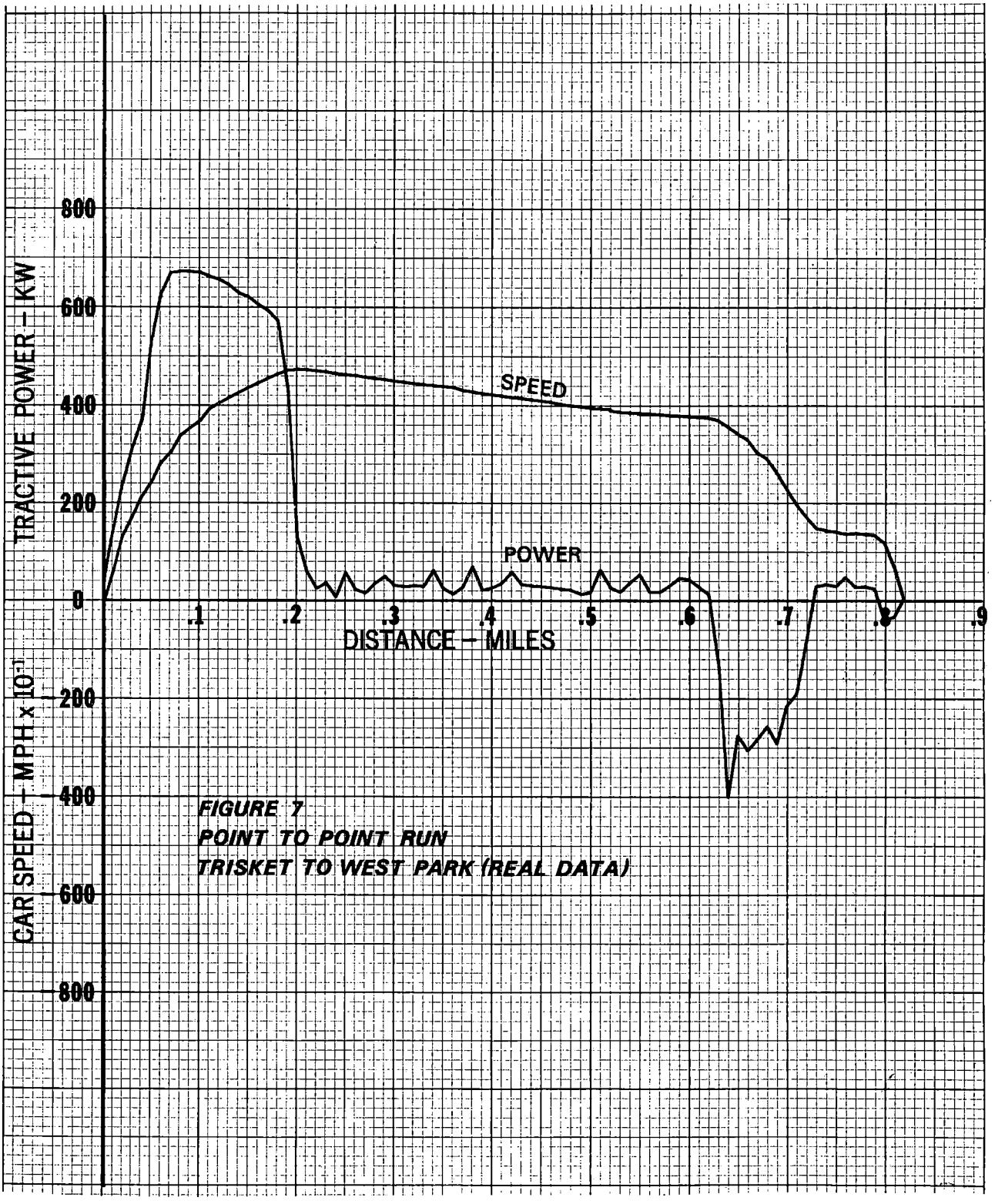

FIGURE 7
POINT TO POINT RUN
TRISKET TO WEST PARK (REAL DATA)

CONCLUSION

Regeneration with PWM Inverter powered cars has been shown to be practical and to offer significant power savings. Short station spacings obviously provide the opportunity for great savings but longer spacings such as those on CTS can also benefit from regeneration. New systems should be designed to make optimum use of regeneration to effect savings in power cost and tunnel heating.

Acknowledgements

The assistance of J. R. Pier, R. D. Smith and Wayne Cymbor of WABCO, Westinghouse Air Brake Division, in the presentation of the data and curves presented in this report is gratefully acknowledged.

APPENDIX F

REFERENCES

APPENDIX F

REFERENCES

1. Nickles, J.E., and Weinstock,H., Preliminary Vibration Measurements on Mark I Vehicle, October, 1971, Report No. DOT-TSC-UMTA-72-2.

2. Weinstock, H., Preliminary Instrumentation Development Test, August, 1971, Report No. PM-P-1.

3. Neat, G.W., Track Geometry System Development Tests, November, 1971, Report No. PM-P-4.

4. Neat, G.W., Checkout of General Vehicle Test Procedures, March, 1972, Report No. PM-P-3.

5. Babb, L., Urban Rail Technology Instrumentation Test, June, 1972, Report No. PM-P-2.

6. Neat, G.W., MBTA Green Line Tests, Riverside Line, December, 1972, Report No. DOT-TSC-UMTA-74-1, I, II, III, IV, V.

7. Bretz, R.T., Cleveland Transit System Experience with WABCO Regenerative Power, ATA Rail Transit Meeting, April, 1973.

8. Sampson, H., Jane's World Railways, McGraw-Hill Book Company, 1972.

9. Lotz, R., and Kasameyer, R., General Vehicle Test Plans for Urban Rapid Transit Cars, DOT Transportation System Center, GSP 064, April, 1972.

10. International Organization for Standardization, Guide for the Evaluation of Human Exposure to Whole - Body Vibration, Document No. ISO/TC 108, June, 1970.